Scientific report; 98 - 02

KNMI

The ASGAMAGE workshop
September 22-25, 1997

Editor ***W.A. Oost***

De Bilt, 1998

Scientific report = wetenschappelijk rapport; WR 98 - 02

De Bilt, 1997

PO Box 201
3730 AE De Bilt
Wilhelminalaan 10
De Bilt
The Netherlands
Telephone + 31(0)30-220 69 11
Telefax + 31 (0)30-221 04 07

Editor: W.A. Oost

UDC: 551.461 551.506.24
546.26 (063)
551.526.63

ISSN: 0169-1651

ISBN: 90-369-2135-x

● ● ● ●

The ASGAMAGE workshop
September 22-25, 1997

Ed. W.A.Oost

KNMI, de Bilt, the Netherlands

January 1998

Report of the ASGAMAGE workshop

Royal Netherlands Meteorological Institute (KNMI)
September 22-25, 1997

Contents:

Course of the workshop

The programme of the workshop is given in Annex 1.
The workshop was opened by Dr.G.J.Komen, Head of the Oceanography Division of KNMI (KS/OO), who welcomed the participants on behalf of KNMI and gave a short survey of past and present KNMI activities in the field of air-sea interaction. After him Prof. B.Huebert, Chairman of MAGE, presented a lecture about another MAGE activity, the ACE-1 project. In the course of a short introduction to the programme of the workshop the Project Leader (PL) told the meeting that Dr.R.Dissly of the NOAA Climate Monitoring and Diagnostics Laboratory had taken up a different job and would not be present at the meeting. Dr.Dissly has written an overview of his results, as well as a manuscript for a journal paper (together with Drs.J.Smith and P.Tans), copies of which he sent to the PL with the remark that secondary copies could be distributed to workshop participants. A number of participants, at their request, received these copies.

Session 1, on the data obtained during both ASGAMAGE phases and the results of their analysis so far, then started. The lectures presented here can be found in Annex 3.

The second session was concerned with the extent to which the four objectives of ASGAMAGE, as stated in the Technical Annex to the EU-contract, have been or will be met. These discussions, summarized in Annex 2, involved three issues:

- Achievements so far and further activity needed
- Publications to be prepared for refereed journals
- What (additional) action is necessary in a follow-up experiment

In the course of the second session, the EU officer responsible for ASGAMAGE, Dr.E.Lipiatou, attended the meeting for a day. In an address to the meeting she expressed her strong support for the research course taken by ASGAMAGE, proof of which was the mention of the project in a brochure containing a selection of MAST-III projects. She furthermore stressed the need to improve on the visibility of the project, both on the Internet and in the shape of an ASGAMAGE brochure. She also pointed to the need to make the project data available through the EU to other researchers. Dr.Lipiatou later had a bilateral meeting with the PL.

On a more formal note, the ASGAMAGE Technical Committee was installed during this workshop. The composition of this Committee is as follows:

For the Bedford Institute of Oceanography, Canada:	Mr.R.J.Anderson
For the Royal Netherlands Meteorological Institute, the Netherlands:	Dr.W.A.Oost
For the Max Planck Institut fhr Chemie, Germany:	Dr.S.Rapsomanikis
For the NOAA Environmental Technology Laboratory,USA:	Dr.J.Hare
For the NOAA Climate Monitoring and Diagnostics Laboratory,USA:	
At present no representative has been appointed.The place is temporarily filled by	Dr.J.Hare
For the University of Newcastle upon Tyne, UK:	Dr.R.Upstill-Goddard
For the Plymouth Marine Laboratories, UK:	Dr.P.D.Nightingale
For the Risø National Laboratory, Denmark:	Dr.S.Larsen
For the Southampton Oceanography Centre, UK:	Mr.A.Hall

For Southampton University,	UK: Dr.D.J.Woolf
For the TNO Physics and Electronics Laboratory, the Netherlands:	Dr.G.de Leeuw
For University College Galway, Ireland:	Dr.P.Bowyer
For the University of East Anglia, UK:	Prof.P.Liss

From their midst the Technical Committee chose a Steering Committee, consisting of Mr.R.J.Anderson for the USA and Canada, Dr.D.J.Woolf for the UK and Ireland and Dr.G.de Leeuw for Continental Europe.

The tour of the Mutual Contract along the participating institutes is still not finished; it appears to be stuck at one of the institutes. The PL will try to find out where the set of copies to be signed is and urge for fast progress.

The last item on the agenda of this first meeting of the Technical Committee concerned the second meeting, which, excluding exceptional circumstances, will be at the occasion of the next workshop. The provisional dates for this workshop, December 1-4, 1998, were selected in connection with the need to make timely arrangements for both the Final Report and the planning of another experiment. The PL mentioned the request of Dr.Lipiatou to turn this workshop into a conference with participants from outside the ASGAMAGE community. All participants agreed to look for a suitable conference near the indicated dates to which the workshop - and an ASGAMAGE session - could be attached.

The next item on the Workshop agenda was Data Banking. The PL pointed to the fact that according to the EU-contract the participants need to make all (final) data publicly available (with some restrictions during an interim period). The EU has given out rather detailed instructions for these data which - as it turned out - were not in the posession of all participants. The PL will therefore send copies of these instructions to all participants. Other points concerning data banking were:

- Each participant will decide for himself which data he will make available, taking into account the EU instructions.
- The PL stressed the need to add, wherever half possible, error margins to the data.
- SI-units are to be used all over; the PL will draw up a list of these units for quantities with complex dimensions and distribute this.
- KNMI will make an FTP site available with read/write permission for ASGAMAGE members only. Instructions for its use will follow later. Data for banking (as well as any other data for use within the ASGAMAGE community) are to be put there. After the project a CD-ROM will be produced containing the banked data. Mr.C.van Oort will act as data manager at KNMI.

The ASGAMAGE Internet site at KNMI will be upgraded, both as far as its accessibility (at present it is hidden rather deep in the hierarchy of the KNMI home page) as well as its contents are concerned.
For the present Workshop Report it was agreed that all contributions from participants would be at KNMI, either in electronic form (Word 7.0, WP 6.0, graphs in Excel 7.0 or Quattro 4) or as hardcopy before November 1. Contributions should be 1 or 2 pages of text, excluding figures. The PL was to add this review of the meeting and a summary of the discussions in Session 2. The workshop report will be a KNMI publication.

The discussion of a future experiment or future experiments was short, thanks to the earlier discussions in Session 2 (see Annex 2). It was agreed that the PL would draft a strawman proposal for the new experiment and send it around with the workshop report. All participants are requested - as far as they didn't do so already - to send an overview of their proposed contributions to the PL, preferably together with their contributions to Annex 1 of this report. Provisionally the fall of 1999 and the spring of 2000 were agreed for the experimental periods of the new experiment (indicated so far as "Project '99).

The short time needed for the final discussion about future experiments made it possible to finish the workshop already at noon on September 25.

Participants

Mr.R.J. Anderson (Bob)
Ocean Circulation Section,
Ocean Sciences Division
Bedford Institute of Oceanography,
1 Challenger Drive,
P.O. Box 1006
DARTMOUTH, N.S.
Canada B2Y 4A2
Tel..: + 1 902 426 3584
Fax: + 1 902 426 2256
E-mail: R_Anderson@bionet.bio.dfo.ca

Dr. P. Bowyer (Peter)
Department of Oceanography
University College Galway
Galway
Ireland
Tel..: + 353 91 524411 ext.3202
Fax: + 353 91 525005
E-mail: Peter.Bowyer@ucg.ie

Not present at the workshop, due to a change in affiliation:
Dr.R.Dissly (Richard); person to contact: Dr.P. Tans
NOAA/CMDL,
R/E/CG1,
Carbon Cycle Group,
325 Broadway,
Boulder, Co 80303,
USA
Tel..: + 1 303 497 6259
Fax: + 1 303 497 6975
E-mail: ptans@cmdl.noaa.gov ; rdissly@ball.com

Dr. A.Graham (Angus)
Oceanography Department
Southampton Oceanographic Centre
Empress Dock,
Southampton SO14 3ZH,
United Kingdom
Tel..: + 44 1703 596498
Fax: + 44 1703 596149
E-mail: ag1@mail.soc.soton.ac.uk

Mr.A.Hall (Alan)
George Deacon Division
Southampton Oceanographic Centre
Empress Dock,
Southampton SO14 3ZH,
United Kingdom
Tel..: +44 1703 596463 or 596377
Fax: + 44 1703 596149
E-mail: ah@soc.soton.ac.uk

Dr.J.Hare (Jeffrey)
University of Colorado and NOAA/ETL
(Cooperative Institute for Research in the Environment (CIRES)
- NOAA Environmental Technology Laboratory),
325 Broadway,
Boulder CO 80303,
USA
Tel..: + 1 303 497-5864
Fax: + 1 303 497 6978
E-mail: jhare@etl.noaa.gov

Prof.B.J.Huebert (Barry)
Department of Oceanography,
University of Hawaii,
1000 Pope road,
Honolulu, HI 96822,
USA
Tel..: +-1-808-956-6896 (?)
Fax: +-1-808-956-9225 (?)
E-mail: HUEBERT@INIKI.SOEST.HAWAII.EDU

Dr.C.M.J.Jacobs (Cor)
Royal Netherlands Meteorological Institute (KNMI)
Wilhelminalaan 10
P.O.Box 201
3730 AE De Bilt
The Netherlands
Tel. + 31 30 2206670
Fax. + 31 30 2210407
E-mail: jacobsc@knmi.nl

Dr.W.Kohsiek (Wim)
Royal Netherlands Meteorological Institute (KNMI)
Wilhelminalaan 10
P.O.Box 201
3730 AE De Bilt
The Netherlands
Tel. + 31 30 2206384
Fax. + 31 30 2210407

E-mail: kohsiek@knmi.nl

Dr.G.J.Komen (Gerbrand)
Royal Netherlands Meteorological Institute (KNMI)
Wilhelminalaan 10
P.O.Box 201
3730 AE De Bilt
The Netherlands
Tel. + 31 30 2206676
Fax. + 31 30 2210407
E-mail: komen@knmi.nl

Ir.G.J.Kunz (Gerard)
TNO Physics and Electronics Laboratory
P.O. Box 96864
2509 JG Den Haag
The Netherlands
Tel..: + 31 70 3740460
Fax: + 31 70 3740654
E-mail: Kunz@fel.tno.nl

Dr.S.Larsen (Søren)
Risø National Laboratory,
Postboks 49,
DK 4000 Roskilde,
Danmark
Tel..: + 45 4237 1212
Fax: + 45 4675 5619
E-mail: metsol@risoe.dk

Dr. G.de Leeuw (Gerrit)
TNO Physics and Electronics Laboratory
P.O. Box 96864
2509 JG Den Haag
The Netherlands
Tel..: + 31 70 3740462
Fax: + 31 70 3740654
E-mail: deLeeuw@fel.tno.nl

Dr.E.Lipiatou (Elisabeth)
CEC, DG XII/D-3,
SDME 7/84,
200 Rue de la Loi,
B-1049 Bruxelles
Belgium
Tel..: + 32 2 296.62.86
Fax: + 32 2 296.30.24
E-mail: Elisabeth.Lipiatou@dg12.cec.be

Dr.P.D.Nightingale (Phil)
Plymouth Marine Laboratory
Prospect Place
West Hoe
Plymouth PL1 3DH
UK
Tel..: + 44 1752 633439
Fax: + 44 1752 633101
E-mail: P.Nightingale@pml.ac.uk

Mr.C.van Oort (Cor)
Royal Netherlands Meteorological Institute (KNMI)
Wilhelminalaan 10
P.O.Box 201
3730 AE De Bilt
The Netherlands
Tel. + 31 30 2206417
Fax. + 31 30 2210407
E-mail: oortvan@knmi.nl

Dr.W.A.Oost (Wiebe)
Royal Netherlands Meteorological Institute (KNMI)
Wilhelminalaan 10
P.O.Box 201
3730 AE De Bilt
The Netherlands
Tel. + 31 30 2206670
Fax. + 31 30 2210407
E-mail: oost@knmi.nl

Mr.D.Sprung (Detlev)
Max Planck Institut für Chemie,
Abteilung Biochemie,
Joh.J.Becherweg 27 (Universitätscampus),
Postfach 3060,
55020 Mainz, Duitsland
Tel..: + 49 6131 305426
Fax: + 49 6131 305487
E-mail: Sprung@diane.mpch-mainz.mpg.de

dr.M.Stoll (Michel)
NIOZ,
Postbus 59,
1790 AB Den Burg,
Texel
The Netherlands
Tel..: + 31 222 369438
Fax:
E-mail: mstoll@nioz.nl

Dr.R.Upstill-Goddard (Rob)
Department of Marine Sciences and Coastal Management,
University of Newcastle Upon Tyne,
Ridley Building,
Newcastle Upon Tyne, NE1 7RU,
UK
Tel..: + 44 191 222 5065
Fax: + 44 191 222 7891
E-mail: Rob.Goddard@ncl.ac.uk

Dr. D.K. Woolf (David)
Department of Oceanography,
the University,
Highfield,
SOUTHAMPTON S09 5NH,
United Kingdom
Tel..: + 44 1703 593038 (direct)
Fax: + 44 1703 593059 (dep.) 593939 (un.)
E-mail: David.K.Woolf@soc.soton.ac.uk

Mr.E.H.W.Worrell (Ed)
Royal Netherlands Meteorological Institute (KNMI)
Wilhelminalaan 10
P.O.Box 201
3730 AE De Bilt
The Netherlands
Tel. + 31 30 2206431
Fax. + 31 30 2210407
E-mail: worrell@knmi.nl

Annex 1

WORKSHOP ASGAMAGE

Buys-Ballot room, KNMI, de Bilt,
September 22-25, 1997

Programme

Monday, September 22

09.30 Welcome, coffee and/or tea

10.00 Opening of the workshop
Speakers:
Dr.G.J.Komen on behalf of KNMI
Prof. B.Huebert on behalf of MAGE

Session 1: Data obtained and analysis so far

Time	*Institute*	*Speaker(s)*
10.30	KNMI	Wim Kohsiek
11.15	KNMI	Cor Jacobs
12.00	lunch	
13.30	TNO-FEL	Gerard Kunz
14.15	Risø	Søren Larsen
15.00	coffee/tea	
15.30	SUDO	David Woolf,
16.15	SOC	Angus Graham
17.00	UCG	Peter Bowyer
17.45	end of today's meeting	

Tuesday, September 23

Session 1: Data obtained and analysis so far (cont.)

Time	*Institute*	*Speaker(s)*
09.00	MPIC	Detlev Sprung
09.45	BIO	Bob Anderson
10.30	coffee/tea	
11.00	NOAA/ETL	Jeffrey Hare
	NOAA/CMDL	Jeffrey Hare for Richard Dissly
12.00	lunch	
13.00	PML/NUT	Phil D.Nightingale, Rob Upstill-Goddard
14.00	Selection of intensive analysis periods.	
15.00	end of session 1	
	coffee/tea	

Session 2: How are we progressing toward our objectives?

For each objective we will discuss, after an introduction,

- what we have achieved so far,
- what publications we will prepare and
- what additional action we will take.

15.30 *Objective 1: To find relationships between the transport coefficients for the gas fluxes and any relevant geophysical parameters.*

17.00 end of today's meeting

Wednesday, September 24

Session 2: How are we progressing toward our objectives? (cont.)

09.00 *Objective 2: To intercompare different methods and systems to measure the transfer velocity of trace gases over the sea.*

10.30 coffee/tea

11.00 *Objective 3: To find out whether and, if at all, under what conditions there can be a significant vertical change in the carbon dioxide concentration in the upper meters of the water column.*

11.30 *Objective 4: To test new methods and new equipment for the measurement of air-sea fluxes of CO_2, N_2O, CH_4 and DMS.*

12.30 end of today's meeting

Thursday, September 25

Session 2: How are we progressing toward our objectives? (cont.)

09.00 Summary of our position.

10.00 end of session 2
coffee/tea

10.30 **Meeting of the Technical Committee**
Installation of the Technical Committee
Composition Steering Committee
Mutual Contract
Future Meetings

11.00 **Data banking**

12.00 lunch

13.30 **Arrangements Workshop report**

Contents
Authors
Time frame

14.30 **Discussion future experiment(s)**

17.00 End of workshop

How are we progressing toward our objectives?

Achievements so far and further activity needed

Objective 1: To find relationships between the transport coefficients for the gas fluxes and any relevant geophysical parameters.

All data have been converted now into physical quantities and have been corrected and screened for their quality and the data analysis is at a stage that the question contained in this objective can be adequately addressed. A number of participants already studied the relationship between the transport coefficients and the main parameter, the wind speed. A more in depth analysis requires combining data from several institutes. As a first step in this activity KNMI will distribute a list of periods during which a number of parameters all had values within a range that is considered to be of interest. From this list a selection of periods for intensive analysis will be made. The parameters of the list are:

*	wind speed	4 - 18 m/s
*	wind direction	200°-330°
	wave length	flag $\lambda > 75$m
		only cases without swell
*		1D spectrum (results dir.waverider on request)
*	wave height	1D spectrum (results dir.waverider on request)
*	temperature	
*	rain	no rain
*	atm.stability	z/L, approximate calculation.
*	boom position	
*	relative humidity	resolve RWS riddle

*= values to be provided with the list of favourable periods.

The file should be ready and distributed before November 1.

Objective 2: To intercompare different methods and systems to measure the transfer velocity of trace gases over the sea.

The values that have been found during ASGAMAGE for the transfer coefficient for CO_2, measured with the eddy-correlation (EC) technique, are still something like a factor two higher than those found with the differential tracer (DT) technique, even though both types of measurements have been done in the most careful way, applying all techniques, precautions and corrections presently known. Both techniques are furthermore to be considered as in principle sound with only minor uncertainties, at least compared to the ratio of the resultant values.
A factor which has so far been neglected in the comparison of the values resulting from both techniques is the difference in the times needed: whereas the EC technique needs 20 to 45 minutes, DT measurements require a time span of 24hrs or longer. From a first order analysis of the effect of fluctuations in the flux and in the concentration difference across the surface, the conclusion can be drawn that for time scales long compared with the time in which e.g. the

wind changes, a correction factor applies that is proportional to the average value of the correlation of the fluctuations in the flux and in the concentration difference. The measured data show that both the flux and the concentration difference are correlated with the wind, so they are of necessity also correlated to each other. Based on this conclusion an attempt was made to estimate the correction factor, which turned out to be of the order of 0.06 and so could not explain the difference in the measured values for k. A somewhat more detailed report is given in the contribution of the PL to Annex 3.
Other factors that may be important for the intercomparison of the techniques is the effect of the reactivity of CO_2 in water and the horizontal homogeneity of the measurement site. More information in these respects will become available as the modeling work progresses.

Objective 3: To find out whether and, if at all, under what conditions there can be a significant vertical change in the carbon dioxide concentration in the upper meters of the water column.

From information obtained later it turned out that the extremely strong CO_2 concentration fluctuations, measured at a depth of 5m below MSL during the 1993 ASGASEX experiment, which were the basis for this research objective, must be considered as incidental. They have to all probability been caused by an episode of extremely high CO_2 concentrations in the waters of the river Scheldt. These concentrations have been measured by Dr.M.Frankignoulle of the University of Liège (e.g. Frankignoulle, M., I.Bourge, C.Canon and P.Dauby: Distribution of surface seawater partial CO_2 pressure in the English Channel and in the Southern Bight of the North Sea, *Cont.Shelf Res.* 16, (1996), 381-395). The vertical CO_2 profile measurements at the platform, during the A as well as during the B phase, do not show significant vertical gradients, except in one case at the very end of the B-phase, when the flux measurements already had been halted. Even this gradient was only a fraction of those measured during ASGASEX. All of these profiles were measured during slack tide. However, vertical CO_2 profiles have also been measured from RRS "Challenger" during periods that a tide was running and these data suggested that under those circumstances significant vertical gradients could be present. Another factor in this discussion is the modelling effort that at present is being made at KNMI and Risø. To account for the fluxes that have been measured the KNMI model at least requires a significant concentration gradient, concentrated near the surface i.e. in the upper meter of the water column. Further efforts to find and quantify these gradients should therefore be concentrated on this area.

Objective 4: To test new methods and new equipment for the measurement of air-sea fluxes of CO_2, N_2O, CH_4 and DMS.
New methods that have been applied during ASGAMAGE are
- The differential tracer method using non-volatile tracers and a large overdetermination of the system through the use of five different tracers;
- The eddy correlation technique for DMS and O_3
- The relaxed eddy accumulation technique for DMS
- The inertial dissipation method
- The simultaneous use of two CO_2 fluctuation sensors to reduce experimental noise.

New equipment:
- The closed NOAA/CMDL ultrasensitive CO_2 detection system, used for eddy correlation, relaxed eddy accumulation and gradient measurements of the CO_2 flux.
- The latest version KNMI Infrared Fluctuation Meter (for eddy correlation measurements)

- The equipment needed for the new techniques described above.

The large majority of these new methods and equipment have yielded results that so far appear to be useful. Only the eddy correlation and relaxed eddy accumulation measurements with the NOAA/CMDL instrument have only yielded upper limits, due to the long inlet tube, an insufficient flow speed in that tube and an unexpected difference in the effective flow speeds of water vapor and CO_2 in the tube.

Publications to be prepared for refereed journals

Objective 1: To find relationships between the transport coefficients for the gas fluxes and any relevant geophysical parameters.

Authors from (bold = lead author)	*Subject*
KNMI, TNO, Risø, NIOZ:	Micrometeoflux CO_2, k-CO_2 (after consensus has been reached about the dPCO2 values to be used)
NUT/UEA:	Differential tracer fluxes
KNMI, BIO, NOAA:	Cross-talk in the KNMI/IFM and the Oakridge CO_2 sensor
SUDO/SOC, UCG, TNO-FEL:	Bubble populations
SUDO/SOC, UCG, TNO-FEL, KNMI, Risø, NUT/UEA:	Bubbles and fluxes, waves etc.
KNMI and all other participants:	Overview paper

Objective 2: To intercompare different methods and systems to measure the transfer velocity of trace gases over the sea.

Authors from (bold = lead author)	*Subject*
KNMI, UEA/NUT, Risø/FEL-TNO, (BIO/NOAA)	A possible explanation for the difference in the results of chemical and micrometeorological methods to measure CO_2 fluxes
NOAA/CMDL (Dissly, Smith and Tans)	Possible Evidence of Greatly Enhanced CO_2 Air-Sea Exchange at High Wind Speeds from Vertical Gradient Measurements over the North Sea

See further Objective 4.

Objective 3: To find out whether and, if at all, under what conditions there can be a significant vertical change in the carbon dioxide concentration in the upper meters of the water column.

Authors from (bold = lead author)	*Subject*
1a. **Risø**, KNMI	Gradients near the surface measured at MPN
1b. **PML/NUT/UEA**	Gradients near the surface measured on board RRS "Challenger"

A third paper combining the results of both sets of data is under consideration

Objective 4: To test new methods and new equipment for the measurement of air-sea fluxes of CO_2, N_2O, CH_4 and DMS.

Authors from (bold = lead author)	*Subject*
Risø, TNO- FEL, BIO:	Inertial dissipation versus eddy correlation; Inertial dissipation versus gradient
TNO-FEL, Richard Dissly (NOAA/CMDL)	Eddy correlation versus gradient
MPIC	REA versus EC for DMS (Provisionally)

At the moment it is not possible or even sensible to impose deadlines per paper. A general deadline, though, is that the papers have to be submitted before the end of the project (March 1, 1999). Lead authors are responsible to achieve this.

What (additional) action is necessary in a follow-up experiment

General remark #1: To be able to convince people who have to evaluate it of the importance of a proposed new project, the objectives have to be stated with the utmost clarity.

General remark #2: During ASGAMAGE Meetpost Noordwijk was at the limit of its capacity. Additional measurement activities, as proposed below, require a different logistic approach from the one used so far.

Objective 1: To find relationships between the transport coefficients for the gas fluxes and any relevant geophysical parameters.

Parameters/instruments, additional to what was used in ASGAMAGE, for which the need was felt:

- Turbulence in the water
- Surface renewal (δT, skin temperature, gene probing)
- Slicks, surface tension (rotating drum, cryogenic micro layer sampler)
- Free drifting buoys with ARGOS transmitters to mark the movement of water masses

More attention should be paid to
- Biogeochemistry
- Study of regional oceanography (the "PROFILES" project)
- (CO_2 profiles in the atmospheric boundary layer, balloons, planes)

More regular data than in ASGAMAGE are needed from
- CTD
- ADCP

There is a definite need for the participation of
- a ship

Objective 2: To intercompare different methods and systems to measure the transfer velocity of trace gases over the sea.

Parameters/instruments, additional to what was used in ASGAMAGE, for which the need was felt:
- CO_2 gradient measurements (vertical and horizontal, flux gradients): use ship or aircraft (contact, e.g.: NOPEX, DLR).

More attention should be paid to
- Continuous CO_2 measurements in air and water

There is a definite need for
- more eddy accumulation
- more eddy correlation + inertial dissipation (DMS!)
- more levels

There is a definite need for the participation of
- buoys (PML)

Objective 3: To find out whether and, if at all, under what conditions there can be a significant vertical change in the carbon dioxide concentration in the upper meters of the water column.

Parameters/instruments, additional to what was used in ASGAMAGE, for which the need was felt:
- Gradients CLOSE to the surface: CO_2, DMS, P_H, TCO_2, alkalinity using
  at MPN: float, wave follower
  from a ship: skimmer, cryogenic micro layer sampler (also for SF_6 and ^3He)

Objective 4: To test new methods and new equipment for the measurement of air-sea fluxes of CO_2, N_2O, CH_4 and DMS.

Parameters/instruments, as were used as well as additional to what was used in ASGAMAGE, for which the need was felt:
- Fluxes and concentrations with multiple systems (EC, REA (gradients)), for CO_2, DMS, NH_3, CH_3I.

Papers presented

KNMI analyses of ASGAMAGE data and results: status September 1997

Cor Jacobs, Wim Kohsiek, Wiebe Oost, Cor van Oort, Hendrik Wallbrink and Ed Worrell
Royal Netherlands Meteorological Institute (KNMI), de Bilt, the Netherlands

Introduction

The analyses of ASGAMAGE data performed so far at KNMI concentrated on the direct determination of the air to sea transfer velocity of CO_2, k_{CO2}. Furthermore, some attention was paid to the bulk transfer coefficients for the transport of latent and sensible heat, C_{EN} and C_{HN}, respectively.
The direct determination of k_{CO2} uses the fact that this parameter is defined by:

$$F_{CO2} = k_{CO2}\, D[CO_2] \qquad [1]$$

where F_{CO2} is the CO_2 flux, $D[CO_2]$ is the difference between the CO_2 concentration in the water, C_w, and the equilibrium concentration, C_{eq}. The latter concentration is defined by $C_{eq} = C_a/K_H$, with C_a the CO_2 concentration in the air and K_H is the dimensionless Henry coefficient. This coefficient depends mainly on the solubility of the gas under consideration and is a function of temperature, T, and salinity, S. For CO_2, its value is about 1 at T = 12 °C and S=31°/oo.
During ASGAMAGE, all components needed to compute k_{CO2} from [1] (F_{CO2}, C_w, C_a, T and S) were observed. Below, results for F_{CO2}, C_w, C_a and for the resulting k_{CO2} are discussed. Finally, results for C_{EN} and C_{HN} are given.

CO_2 flux, F_{CO2}

The CO_2 flux was determined using the eddy correlation (ec) method (wind speed: Solent sonic anemometer; CO_2 concentration: IFM, see Kohsiek, 1997). The averaging time was 55 minutes, denoted as one run. Data were accepted only if the wind direction during a run remained greater that 200 degrees, in case of no rain, if the relative humidity was less than 95% and if the optics of the IFM where sufficiently clean. Flow distortion and tilt corrections were applied following Oost *et al* (1994). Runs for which the drag coefficient C_D turned out to be outside the range $0.0005 < C_D < 0.004$ were accompanied by u'w' cospectra of suspect quality (where u' and w' denote horizontal and vertical wind velocity fluctuation, respectively). These runs were also rejected, as were other runs with similar spectral features (Fig. 1).
The Webb correction (Webb *et al*, 1980) and a cross-talk correction (Kohsiek, 1997) where applied to the CO_2 flux data. The effect of the latter corrections is illustrated in Fig. 2 for data from ASGAMAGE B. It can be seen that both corrections have a significant impact on the flux data. However, the Webb correction is by far the largest correction and in many cases turns negative fluxes into positive ones. During the B-period, positive fluxes are to be expected because of the oversaturation of the water with respect to CO_2 (see below).
Fluxes measured during the A and the B period are depicted together in Fig. 3. A consistent picture arises from the combination of data. As expected, the fluxes increase with increasing wind speed. Fluxes are predominantly negative during the A-phase and positive during the B-phase, which is in accordance with the air-to-sea concentration difference (see below).

CO_2 concentration of the water, C_w

To determine C_w, water from depths 0.5, 2, 3.5, 5, 7, 11 or 15 meters was continuously sprayed into an equilibrator. Within 5 to 10 minutes, the air inside the equilibrator will be in equilibrium with the sea water. Then, its CO_2 concentration is C_a^{eq}, from which follows $C_w = C_a^{eq}/K_H$. The value of C_a^{eq} was determined using an Infra Red Gas Analyser (IRGA). The influence of water vapour in the air samples on the resulting CO_2 concentration was avoided by drying the samples (NIOZ) or corrected for by means of the internal software of the instrument used (KNMI, TNO). Data were accepted only if the standard deviation of the signal was less than one ppm (Fig. 4). Furthermore, we required a continuous signal during a significant part of the run (Fig. 5).
Figure 6 shows the observed partial pressure during the B-period, as obtained by different institutes prior to any re-calibration (KNMI, NIOZ, TNO). The data include C_w from all levels. The trend turns out to be similar, but a systematic difference of 10-15 matm may be observed as well.
On some occasions, preferably around slack tide, profile measurements were made by switching the inlet depths along all the available levels. Each level remained connected for 15-30 minutes, to allow the CO_2 measurement system to reach a new equilibrium. Results from the profile measurements are given in Fig. 7. It can be seen that, between depths 0.5 and 15 m, there is hardly any significant stratification of C_w in most cases.

Concentration in air, C_a

The CO_2 concentration of air was determined by sampling air from a height of 2, 12, 20 or 30 m. Air samples where analysed using the same IRGA as for C_w, and selection and correction procedures were similar to those applied for C_w. The partial pressure in air as observed by three different institutes, prior to any re-calibration, is depicted in Fig. 8 for the B-period. Again, trends appear to be similar and a systematic difference shows up. However, the systematic difference in this case does not agree with the difference in case of the C_w measurements.

Transfer velocity k_{CO2}

To obtain k_{CO2} from [1] the partial pressure data were converted to concentrations ignoring any vertical CO_2 stratification within the water column (see above) and averaging results from the different institutes. Further, from a number of CTD casts taken near the measurement platform it was concluded that T and S gradients were also sufficiently small to be ignored for our purpose. The temperature, needed to compute K_H, was taken equal to the near-surface water temperature. This temperature was measured using a PT100 resistance thermometer just below the water surface, at a maximum depth of 30 cm. A typical value of S = $31^{o}/_{oo}$ was derived from the CTD casts and used in all further computations. The values of k_{CO2} resulting from [1], using the observed fluxes and concentration differences averaged per 55 minutes, were normalised to a temperature of 20°C (Wanninkhof, 1992).
The *concentration* difference $D[CO_2]$ observed during ASGAMAGE is depicted in Fig. 9. It is seen that $C_w < C_{eq}$ during the A-period, which must result in a negative CO_2 flux (downward CO_2 transport). For the B-period the reverse is true. The overall trends for C_{eq} as well as for C_w are consistent for the two observation periods.
In Fig. 10 k_{CO2} is plotted as a function of the "neutral wind speed at a height of 10 m", $U_{N,10}$. Although the scatter is large, a relation between $U_{N,10}$ and k_{CO2} can clearly be seen. Data from the A and the B period are consistent. A curve of the type $k_{CO2} = aU_{N,10}^2$ can be fitted through the data with $a = 0.53$ (Fig 10). This is still high as compared to the coefficient suggested by Wanninkhof (1992), which is $a = 0.31$ (Fig. 10). However, the difference of less than a factor

of 2 is much closer than the results from previous experiments using a micrometeorological (ec) technique to determine the CO_2 flux (Smith and Jones, 1979).

Bulk transfer coefficients C_{EN} and C_{HN}

Data on the water vapour flux and the heat flux were obtained using the ec method (wind speed: Solent sonic anemometer; H_2O concentration: IFM; temperature: thermocouple). Selection criteria and applied corrections were as described for the CO_2 flux measurements. The Webb correction to the water vapour flux was found to hardly affect the results for the B-period and was ignored further on. Wind speed (sonic anemometer) as well as air temperature and humidity (Väisälä aspirated thermo-hygrometer) were adjusted to a height of 10 m and neutral stratification. Appropriate corrections to account for the sea water flow near the platform were made. Surface temperature was taken equal to the near surface water temperature. The surface specific humidity was computed as the saturation specific humidity for sea water at the observed surface temperature and atmospheric pressure.
Results for C_{EN} are given in Figs 11 and 12. A statistical screening (Chauvenet criterion) has been applied to the data shown here. C_{EN} can be computed as the mean of the values from Fig. 11, or from the linear regression shown in Fig. 12, giving a value of $C_{EN}=1.12\text{x}10^{-3}$ in both cases. This is equal to the value reported by DeCosmo *et al.* (1996). Data from the A and B period are consistent.
In Figs. 13 and 14 results for C_{HN} are depicted. Statistical screening was performed by demanding that the difference between the surface temperature and the temperature adjusted to neutral conditions and to a height of 10 m, Dq, be > 0.5K. Requiring even larger temperature differences reduced the number of data without a significant further reduction of the scatter. Data are distinguished according to stability (data from the A and B period appeared to be consistent again). Our data suggest a large impact of stability on C_{HN}.
For unstable conditions, the scatter is rather large. The mean value for C_{HN} under these conditions is $1.80\text{x}10^{-3}$ with a standard deviation of $0.73\text{x}10^{-3}$. Both values are considerably higher than the values reported by DeCosmo *et al.* (1996; $1.14\text{x}10^{-3}$ and $0.35\text{x}10^{-3}$, respectively) and others. By contrast, the data for stable conditions show much less scatter, and suggest a dependence on wind speed: $C_{HN} = (0.077U_{N,10} - 0.44)\text{x}10^{-3}$ ($r^2 = 0.5012$). This relation leads to values of C_{HN} that are comparable to those reported by Large and Pond (1982) for stable conditions ($C_{HN} = 0.66\text{x}10^{-3}$). A stable regime was not reported by DeCosmo *et al.* (1996). There appears to be a third regime characterised by a positive air-sea temperature difference under unstable conditions. The reason for this apparent inconsistency is probably the existence of a considerable latent heat flux in combination with the small sensible heat flux. Data within this regime behave more like the stable data, and lead to negative values of C_{HN} in many cases.
In Fig. 14 C_{HN} can be obtained from linear regression analysis. It then becomes $1.57\text{x}10^{-3}$ under unstable conditions. It seems not to be realistic to analyse the data for stable conditions by means of a single fit.

Conclusions

ASGAMAGE data from the A and the B period were found to be consistent. The direct measurement of the air-sea transfer velocity of CO_2 has been applied with reasonable success. The results are within a factor of two from those of the more traditional methods. The bulk transfer coefficient for latent heat agreed very well with values reported previously. However, for sensible heat exchange the transfer coefficient showed a strong stability dependence, the unstable value being rather large and with high standard deviation, while the data for stable conditions suggest a wind speed dependence.

References

DeCosmo, J., *et al.*, 1996: *J. Geophys. Res.*, **101**, 12001-12016.
Kohsiek, W., 1997: *This volume.*
Oost, W.A., *et al.*, 1994: *J. Atmos. Oceanic Technol.*, **11**, 357-365.
Smith, S.D. and E.P. Jones, 1979: *Boundary-Layer Meteorol.*, **17**, 375-379.
Wanninkhof, R., 1992: *J. Geophys. Res.*, **97**, 7373-7382.
Webb *et al.*, 1980: *Q. J. R. Meteorol. Soc.*, **106**, 85-100.

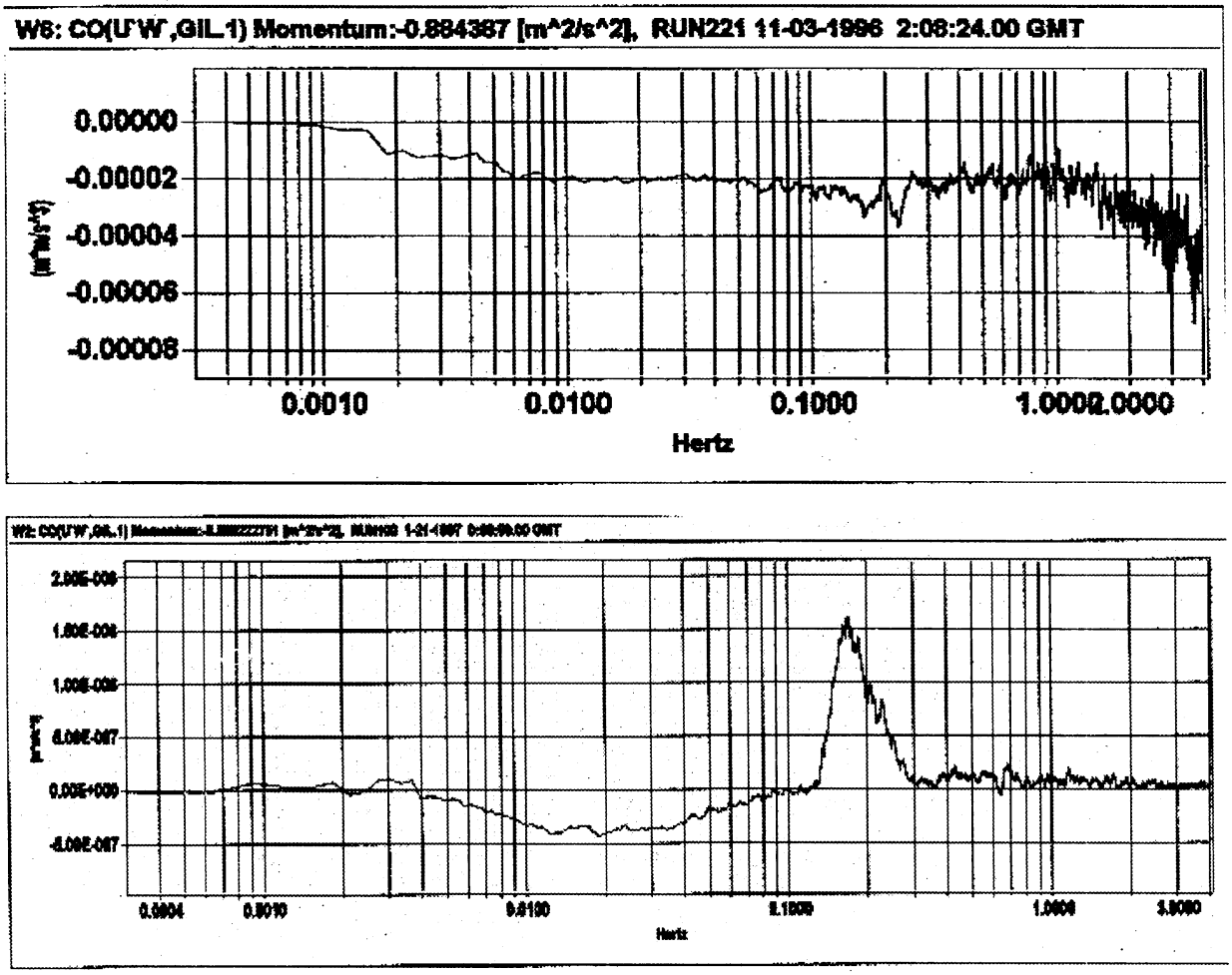

Figure 1. *Examples of w'u' cospectra leading to rejected runs. Upper panel: continuously increasing contribution of high frequencies to momentum flux; lower panel: abnormal high positive contribution to momentum flux of frequencies in the range 0.15-0.3 Hz.*

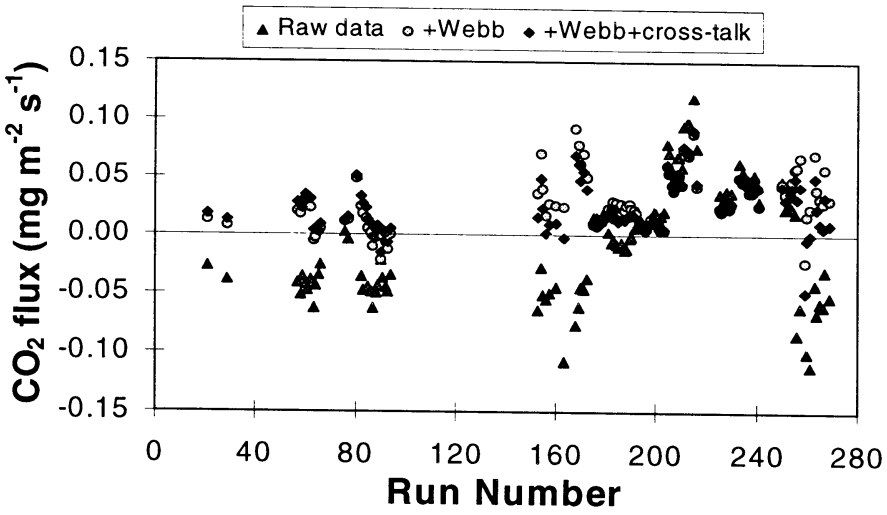

Figure 2. *Illustration of the impact of the Webb-corrections (Webb* et al., *1980) and of the cross-talk correction (Kohsiek, 1997) on the CO_2 fluxes measured during ASGAMAGE-B. The correction for cross-talk was applied after application of the Webb correction.*

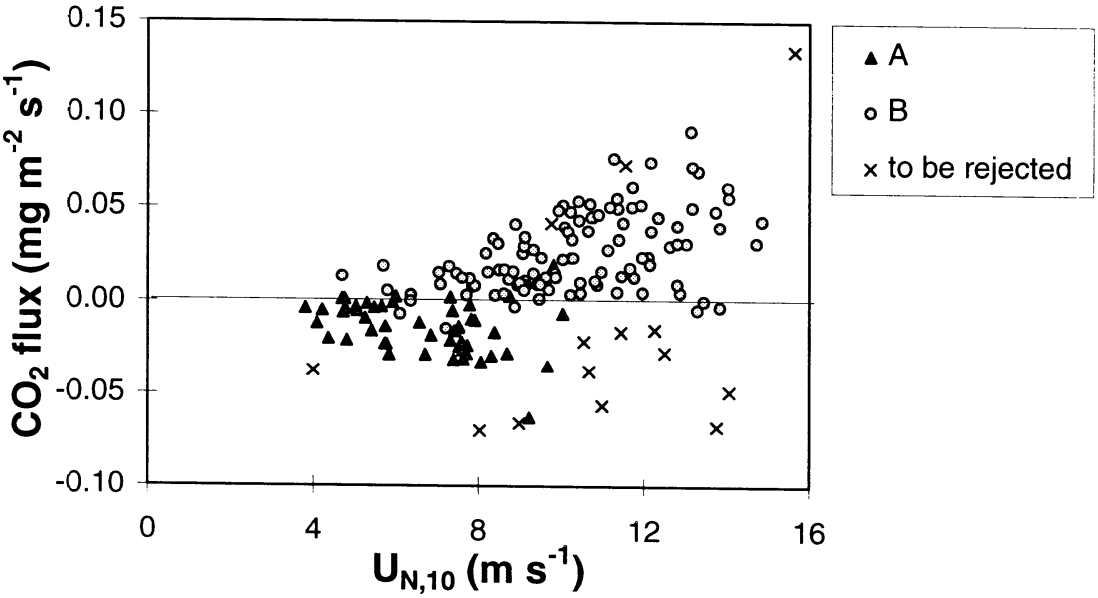

Figure 3. *CO_2 flux versus the neutral wind speed at a height of 10 m ($U_{N,10}$) for ASGAMAGE A (triangles) and B (circles). Crosses refer to data that led to statistical outliers for k_{CO2} as determined using the Chauvenet criterion. These ouliers were due either to an abnormal flux or to an abnormal air-sea CO_2 concentration difference.*

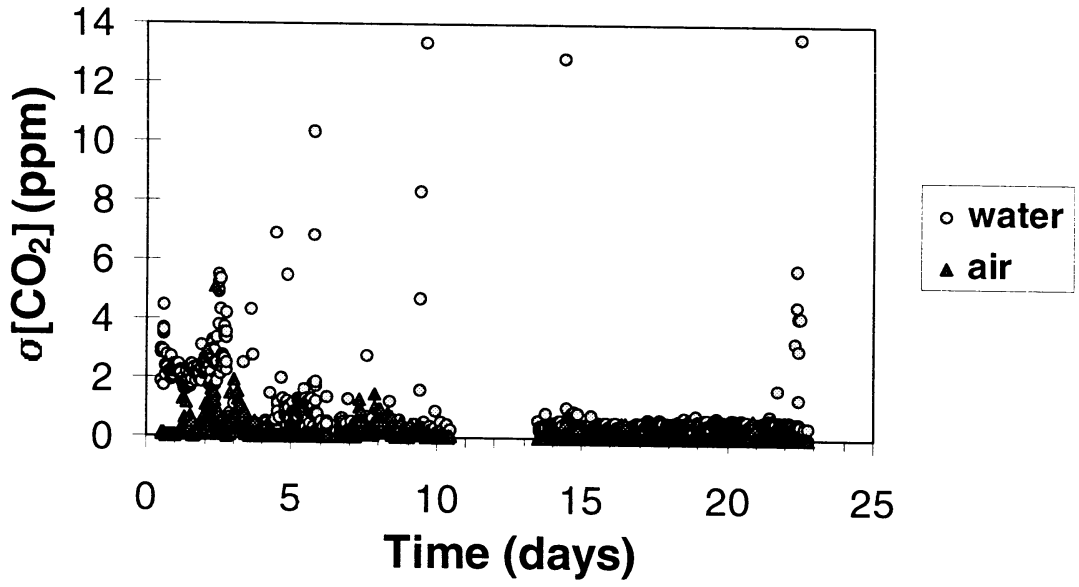

Figure 4. *Illustration of selection of air and water CO_2 concentration data by means of the standard deviation of the sample signal (data provided by FEL-TNO). The standard deviation, $s[CO_2]$, is plotted versus time. Data with $s[CO_2] > 1$ ppm were rejected.*

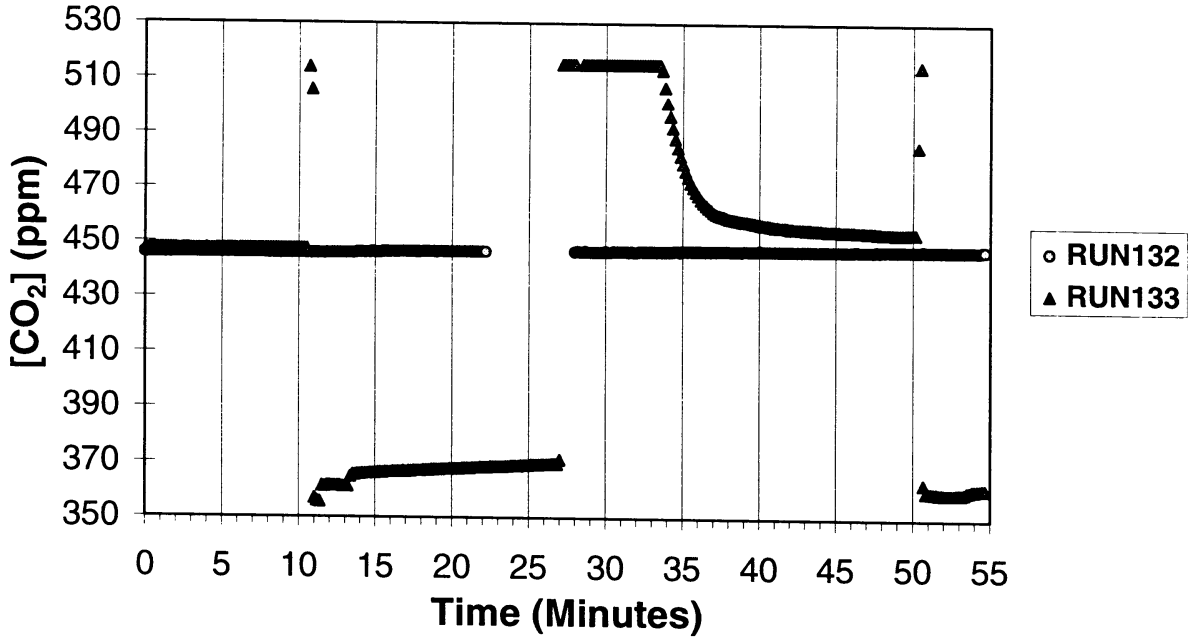

Figure 5. *Example of run marked as "continuous" (RUN132) or "discontinuous" (RUN133) with respect to $[CO_2]$. Discontinuous runs were not used to compute k_{CO2}.*

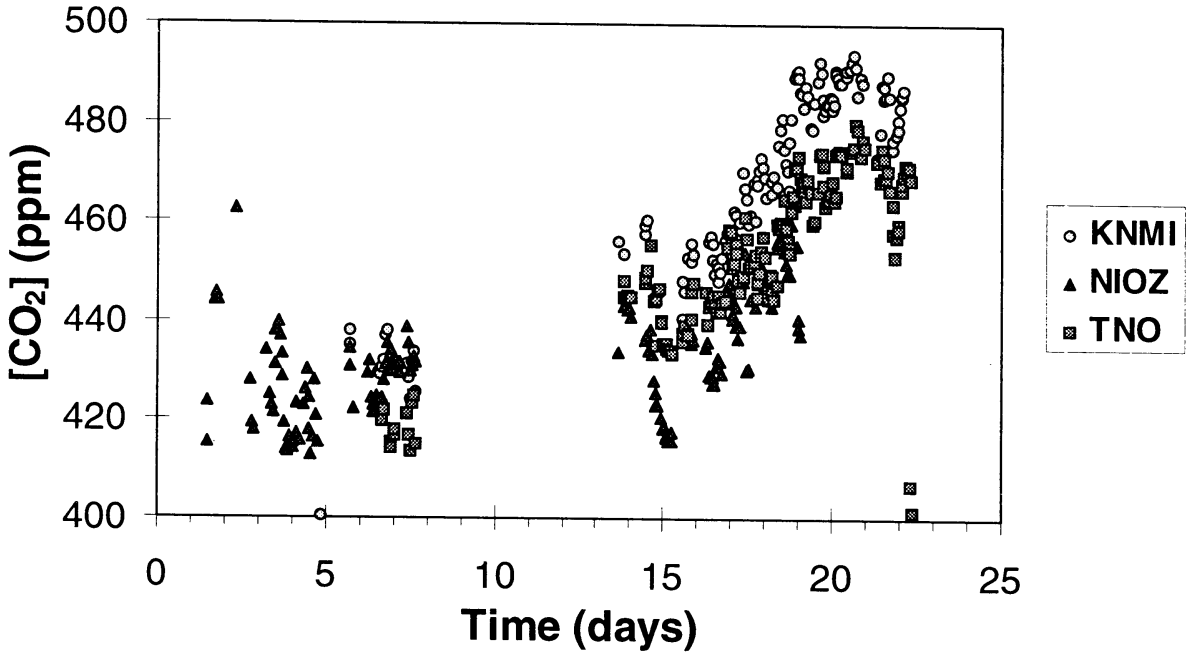

Figure 6. *Comparison of CO2 content of the water as obtained by three different institutes, prior to any re-calibration (ASGAMAGE-B). The CO_2 content is expressed as the observed molar fraction in the equilibrator air. Day zero denotes the start of the measurement campaign. The drop in $[CO_2]$ at the end of the period is due to malfunctioning of a submerged pump used to sample sea water and these particular data were not used to compute k_{CO2}.*

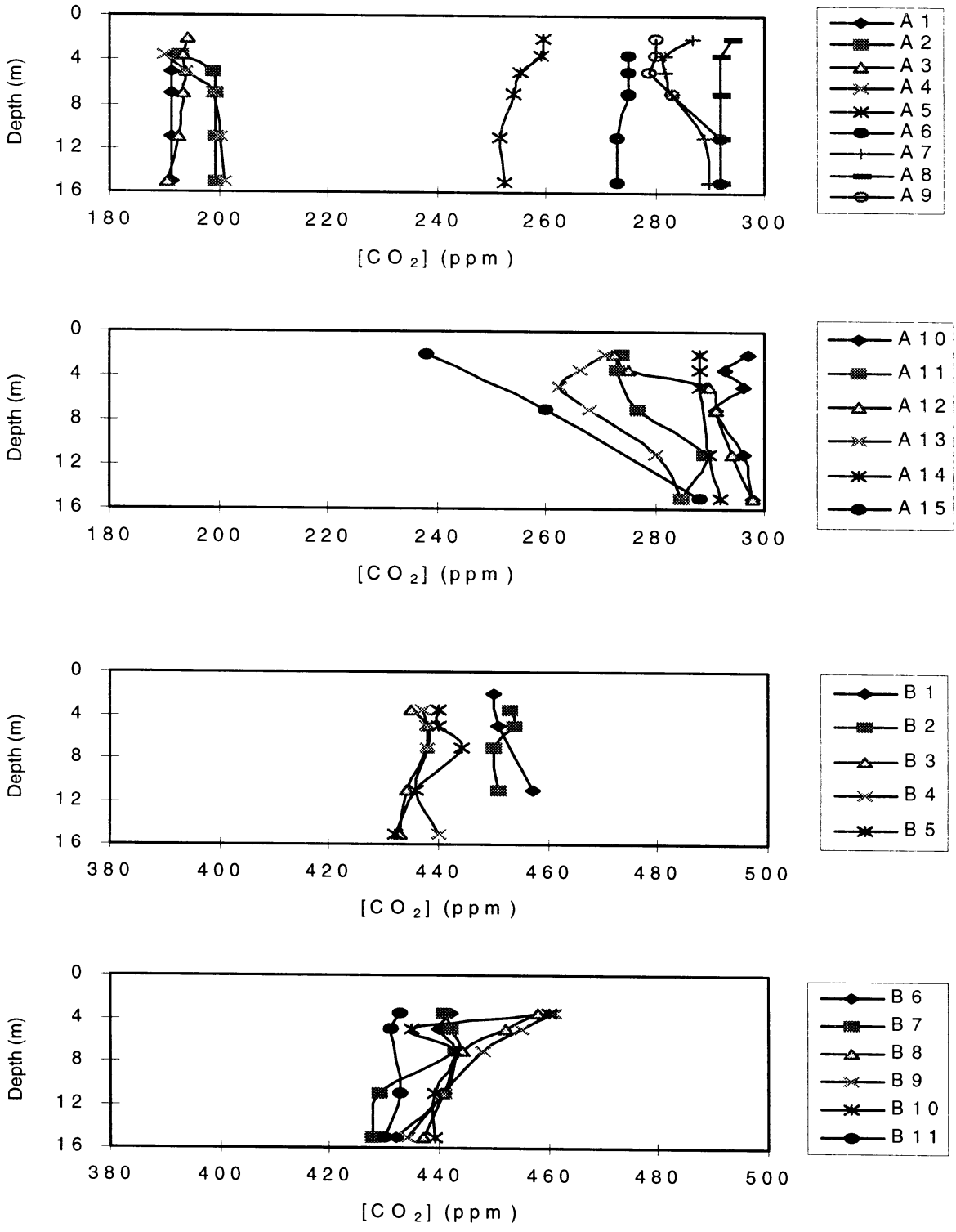

Figure 7. *Profiles of CO_2 content of the water during ASGAMAGE (KNMI-data). The profiles are marked according to the measurement period (A or B) and numbered chronologically. CO_2 content is given as the molar fraction in the equilibrator air. Note the shift in the scale for the lower two panels (B-period).*

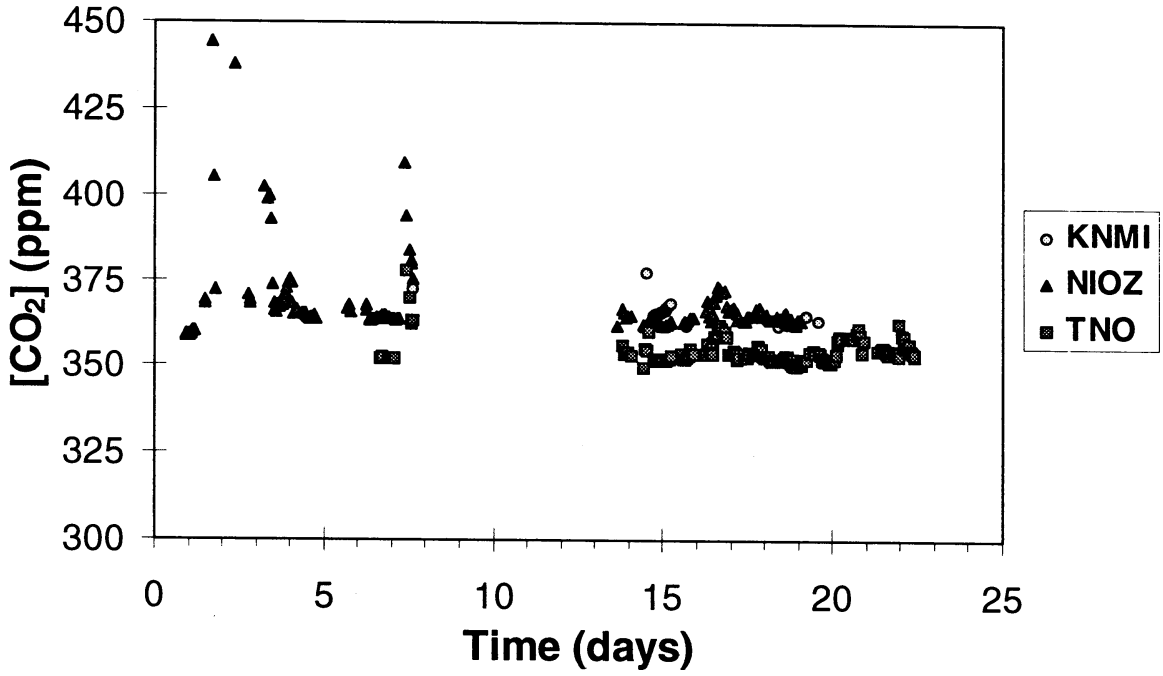

Figure 8. *Comparison of the molar fraction of CO2 in air as obtained by three different institutes and prior to any re-calibration (ASGAMAGE-B data). Day zero denotes the start of the measurement campaign.*

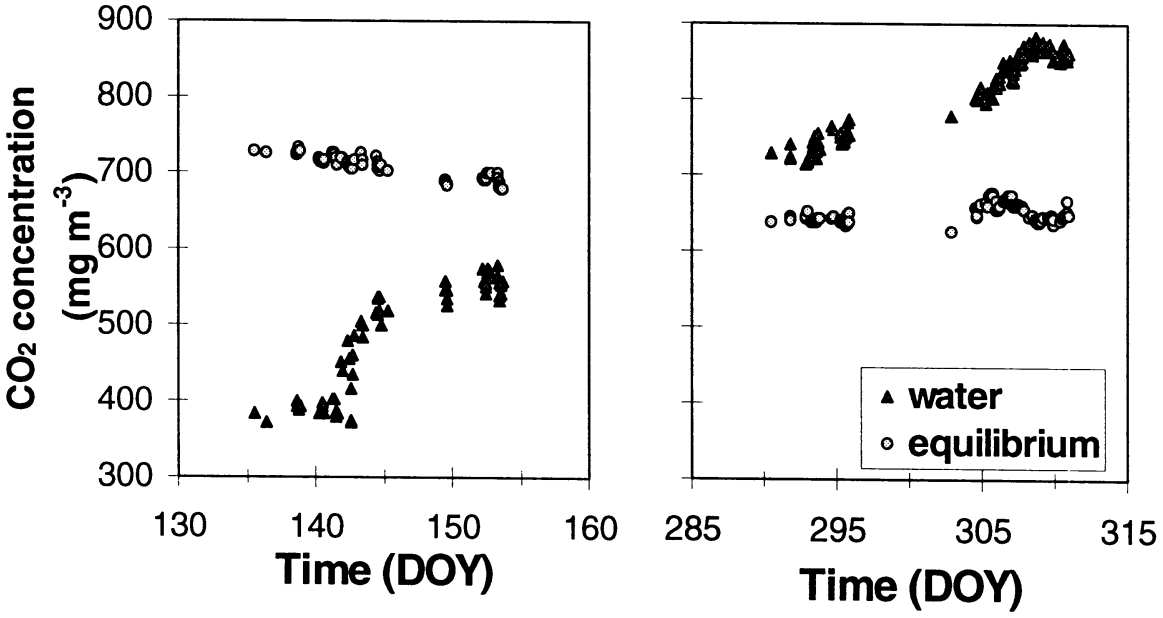

Figure 9. *Observed CO_2 concentration in water (c_w, triangles) and equilibrium concentration (c_{eq}; circles) for ASGAMAGE-A (left) and ASGAMAGE-B (right). Time is in Day Of Year (DOY). The concentration difference shown in this figure is the difference actually used to compute k_{CO2} ($D[CO_2]$ in [1]).*

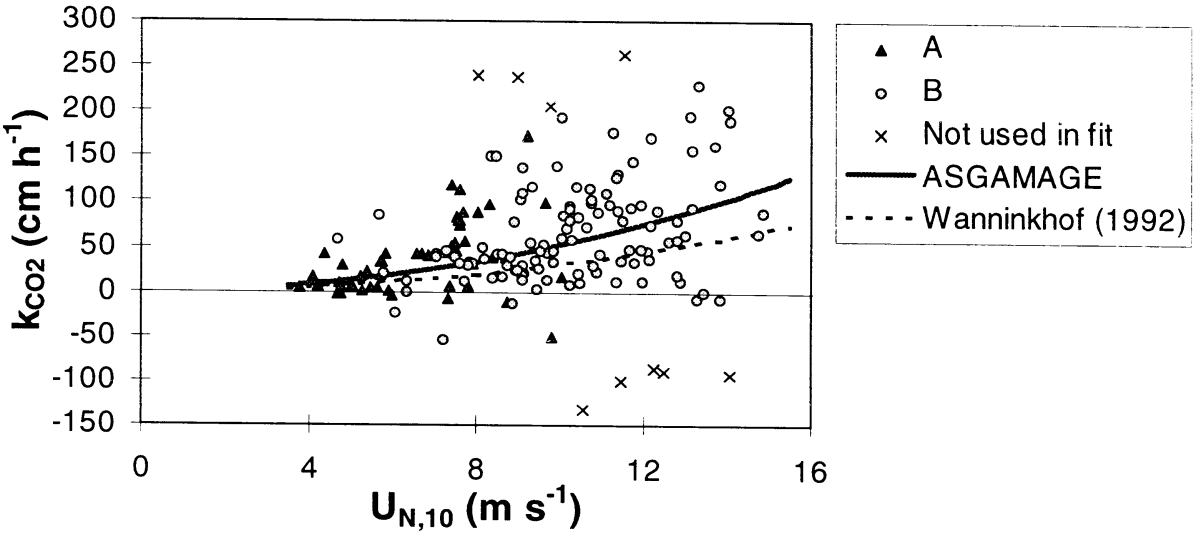

Figure 10. *Computed k_{CO2} normalised to 20 °C versus the neutral wind speed at a height of 10 m, $U_{N.10}$, for the ASGAMAGE data set. Triangles: ASGAMAGE-A; Circles: ASGAMAGE-B; Crosses: outliers according to the Chauvenet criterion with reference to the fit, and subsequently removed fromthe fit. (not shown: four outliers with k_w < -150 cm h^{-1} and one with k_w > 300 cm h^{-1}). A quadratic fit through the data, $k_w = 0.53\ U^2_{N,10}$ is also shown (solid line), along with the Wanninkhof (1992) fit, $k_w = 0.31U^2_{N,10}$ (dashed line). The ASGAMAGE fit optimises for CO_2 flux. Note: $D[CO_2]$ used to compute k_{CO2} is the average from three institutes, prior to any re-calibration of pCO_2 data. Furthermore, at the time of this analysis $U_{N.10}$ was not yet corrected for sea water current.*

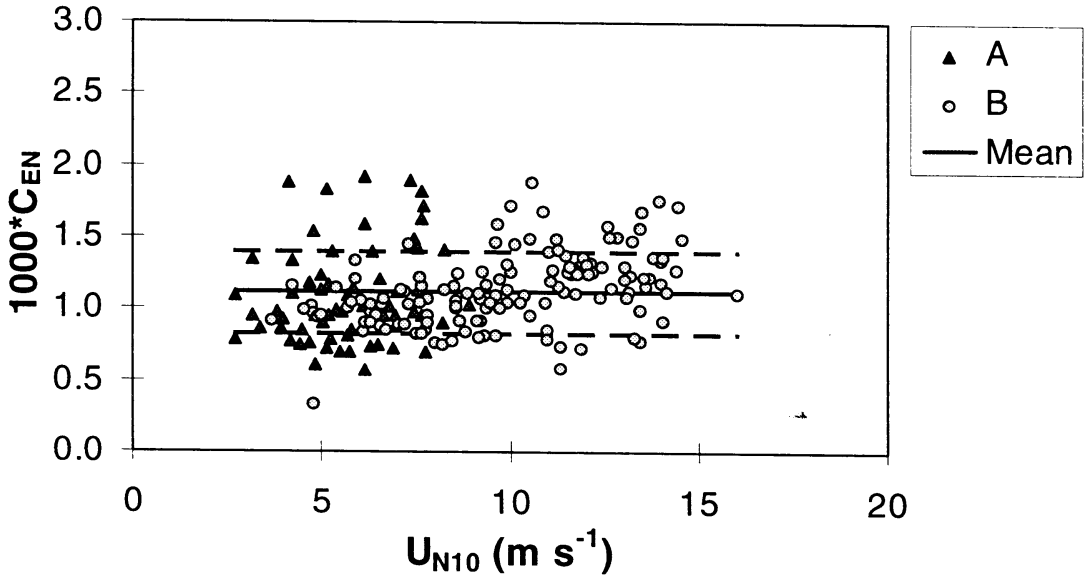

Figure 11. *Latent heat flux bulk transfer coefficient, C_{EN}, adjusted to a height of 10 m and neutral stability conditions versus neutral wind speed at a height of 10 m, $U_{N.10}$. The mean (solid line) is for the combined A (triangles) and B (circles) data set: $C_{EN} = 1.12x10^{-3}$. The dashed lines are the mean plus or minus one standard deviation ($s = 0.29x10^{-3}$). Data include observations where the difference of the specific humidity at the surface (q_s) and the neutral specific humidity at a height of 10 m, $q_{N.10}$, is positive, that is, $q_s - q_{N.10} > 0$. Outliers have been removed according to the Chauvenet criterion applied with reference to the mean.*

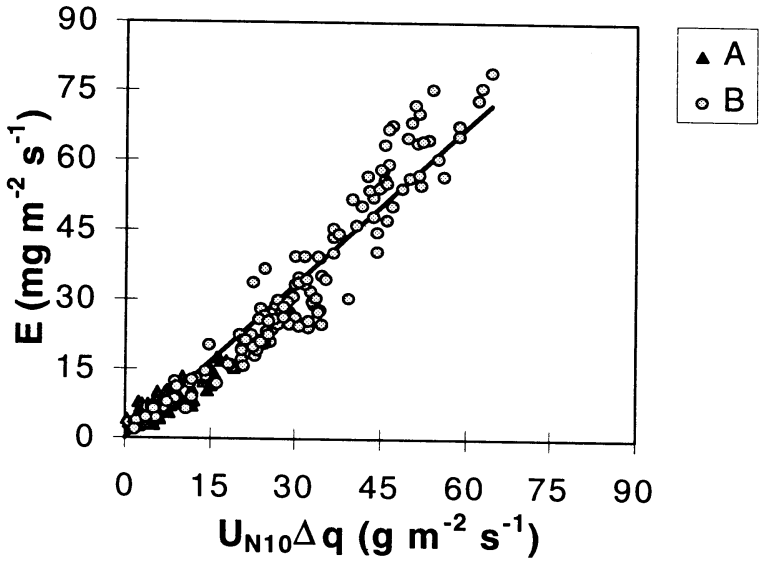

Figure 12. *Measured evaporation rate, E, versus $U_{N,10}Dq$, with $U_{N,10}$ the neutral wind speed at a height of 10 m and $Dq = q_s - q_{N,10}$ is the difference between the specific humidity at the surface, q_s, and the neutral specific humidity at a height of 10 m, $q_{N,10}$. The solid line is the fit of E versus $U_{N,10}Dq$ through the origin, with slope 1.12. Only data with $Dq > 0$ where used and outliers where removed according the Chauvenet criterion applied with reference to the fit.*

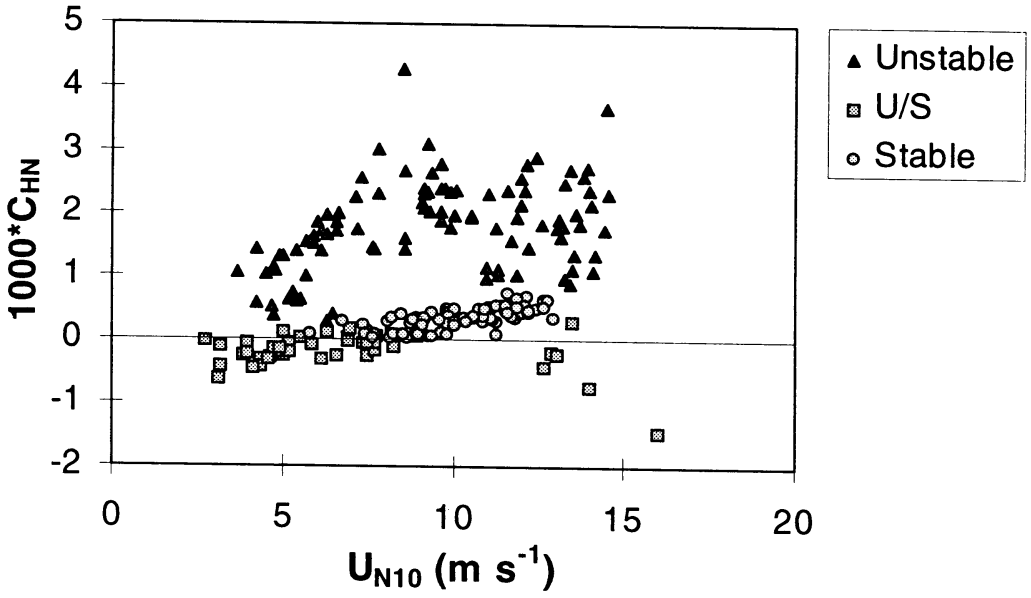

Figure 13. *Sensible heat flux bulk transfer coefficient, C_{HN}, adjusted to a height of 10 m and neutral stability conditions versus neutral wind speed at a height of 10 m, $U_{N,10}$. Data from ASGAMAGE A and B are treated as one set, but a distinction has been made according to stability regime. The U/S regime denotes conditions with a negative Monin-Obukhov length (unstable), but with a positive air-sea temperature difference (consistent with stable conditions). The mean for unstable conditions is $C_{HN} = 1.80x10^{-3}$ a standard deviation of $0.73x10^{-3}$. For stable conditions, data suggest a dependence on wind speed, viz. $C_{HN} = (0.077U_{N,10} - 0.44)x10^{-3}$.*

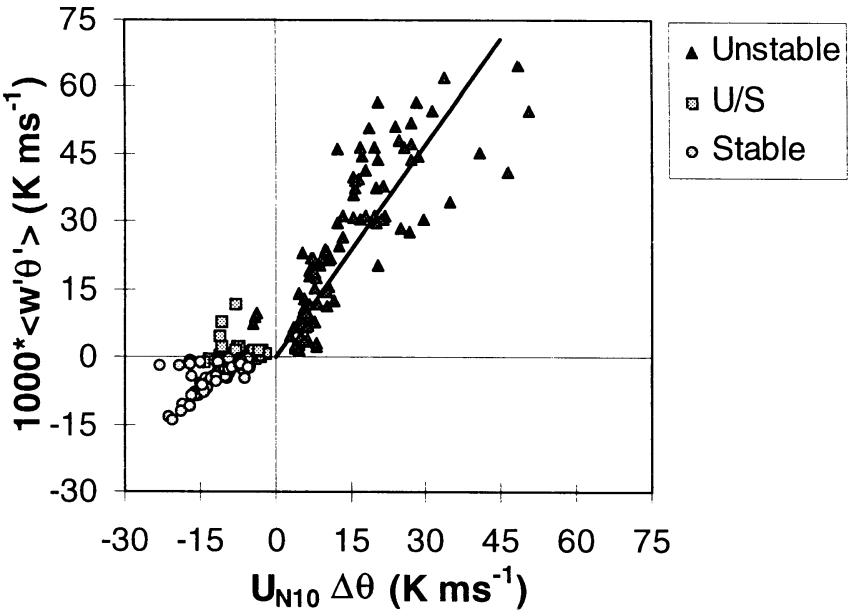

Figure 14. Measured kinematic sensible heat flux, <w'q'>, versus $U_{N,10}Dq$, with $U_{N,10}$ the neutral wind speed at a height of 10 m and $Dq = q_s - q_{N,10}$ is the difference between the sea water temperature and, q_s, and the neutral potential temperature at a height of 10 m, $q_{N,10}$. The solid line is the fit for unstable conditions of $1000<w'q'>$ versus $U_{N,10}Dq$ through the origin, with slope 1.57. Only data with $|Dq| > 0.5$ K where used.

Measurement of CO_2 fluxes with the IFM during ASGAMAGE

W. Kohsiek
Royal Netherlands Meteorological Institute (KNMI), de Bilt, the Netherlands

1. IFM configuration

The IFM is an infrared sensor for the in-situ measurement of turbulent water vapour and carbon dioxide concentrations. The sensor has three parts: a cylindrical body (lenght 25 cm, diameter 17 cm) that houses the lamp, detector, chopper/filter wheel and some electronics, two optical fiber cables, and the sensing head. In the case of ASGAMAGE the cables were 1.6 m long each. The sensing head, which offers an open absorption path of 2 times 22 cm (folded) was enclosed by a perspex to enable measurements during rain. On one side of the cover an electrical fan was mounted. The other side had an intake opening that was directed downwind. This configuration proved to work quite well, we could take virtually uninterrupted measurements also during rain. A slight disadvantage of the protecting cover is that it suppresses the fast fluctuations. From comparison with an unprotected sensor it was found that the cover degraded the fluctuations above about 1 Hz. From the relevant cospectra it was observed that very little is contributed to the flux at frequencies above 1 Hz, so the damping effect of the cover can be neglected.

Inside the cylindrical body of the IFM a spinning filter wheel enables the measurement in four optical wavelength intervals. Normally, the pair of 4.2 μm and 3.9 μm are chosen for the measurement of CO_2, and the combination of 2.6 μm and 2.3 μm for H_2O. The latter wavelength of each pair serves as a reference where no absorption is assumed to occur. By means of software setting of the IFM one can switch from 3.9 μm to 2.3 μm as the acting CO_2 reference. This option was used during the ASGAMAGE-B only. During ASGAMAGE-A the 2.3 μm filter was used as the CO_2 reference at all times.

About halfway ASGAMAGE-B the 2.3 μm filter was replaced by a 4.2 μm filter that had a broader passband than the already mounted 4.2 μm filter. The purpose of this action was to minimize the cross-talk from water vapor to CO_2. By choosing the 'reference' actually around the absorption filter a better cross-talk rejection was anticipated than in case the reference and absorption filters are centered at different wavelengths. The trade-off of this solution is that one sacrifices sensitivity. Another trade-off is that now the (broad) 4.2 μm filter also acts as the reference for H_2O, thus introducing cross-talk from CO_2 to H_2O. Because the CO_2 fluctuations are very small as compared to the H_2O fluctuations, this effect is negligibly small.

During a limited period of time, still another configuration was used: CO_2 was simultaneously measured with the combination of 4.2 μm (small passband) and 4.2 μm (broad passband), and with the combination 4.2 (small) and 3.9 μm. The H_2O channel had to be given up in this situation. Summarizing, four different configurations were used during ASGAMAGE-B:

a. 4.2 (small) and 2.3 (ref.); 2.6 and 2.3 (ref.)
b. 4.2 (small) and 3.9 (ref.); 2.6 and 2.3 (ref.)
c. 4.2 (small) and 4.2 (broad); 2.6 and 4.2 (broad)
d. 4.2 (small) and 4.2 (broad); 4.2 (small) and 3.9 (ref.)

During ASGAMAGE-A the following configuration was used:

e. 4.2 (broad) and 2.3 (ref.); 2.6 and 2.3 (ref.).

Below some results of these various settings will be discussed, but first we will turn to the subject of cross-talk.

2. Cross-talk

In earlier experiments with the IFM at the Meetpost an unprotected open path sensing head had been employed. It was then noted that during periods of rain there was a considerable CO_2 signal, sometimes correlated, at other times anti-correlated with the H_2O signal. In fact the CO_2 signal was so large that it could not be from gaseous absorption by CO_2. A second effect was noted when calibrating the sensor in the laboratory. If the relative humidity was over 70%, there was a signal decrease in all four optical channals. The effect disappeared if the optics of the sensing head were heated several degrees above ambient temperature. It was hypothesized that some absorption of liquid water on the surface of the optics occured, acting as an extra absorbing medium. The same would occur if the optics were wetted by rain. In ASGAMAGE the optics were protected from rain and heated as well. The heating was kept at such a level that it could not affect the environmental temperature.

A thin film of liquid water on the optics may easier form if there is a layer of sea aerosol, in particular salt, on the optics. It was found that in the course of some days the four optical signals decreased. The signals were restored by cleaning the optics. So it is important to clean the optics regularly, say once every day. This fact was not recognized at the beginning of the experiment because the rain protection cover was thought to protect against aerosol as well. Up to and including 29 October the optics of the IFM were not cleaned, thereafter they were cleaned on 30 October, 1, 2 and 3 November.

The magnitude of the effect on the individual filter signals is quite considerable. In situations with dirty optics we found that fluctuations of the 2.3, 3.9 and 4.2 μm channels were perfectly correlated with the 2.6 μm channel and as large as half the fluctations in this channel. The true CO_2 signal in the 4.2 μm channels is 50-100 times smaller, thus putting extreem demands on the cross-talk rejection of the system.

Next to the effect of a water layer on the optics, cross-talk occurs by (1) water vapour absorption (lines or continuum) present in the passband of the CO_2 absorption and/or reference filter, and (2) by line broadening. From data of the Infrared Handbook it is found that the first effect is of the order of 10^{-5} gm^{-3}/gm^{-3} and thus negligible. The magnitude af the second effect is somewhat uncertain. The physics behind it is that CO_2 absorption lines are broadened by collisions with other molecules, that is N_2, O_2 and H_2O. The effect of one molecule of H_2O is different from that of one molecule of N_2 or O_2, so the total effect of moist air is dependent on the mixing ratio of water vapor. To quantify this phenomenom commonly an 'effective' pressure is defined, that is the pressure of the dry gas that would give the same absorption as the actual moist gas. The effective pressure thus depends on the mixing ratio and is calculated by a linear combination of the partial pressures. The constants in this expression are not well settled, however. For instance, see the discussion in the LICOR manual for their LI-6262 analyzer. From LICOR's algorithm follows a cross-talk correction of

$1.4*10^{-4}$ in our situation. This is about -1/6 of the dilution correction, that is the effect of CO_2 dilution if water vapor is added at constant pressure to a dry sample of gas.

It was recently attempted to determine the cross-talk of the IFM by laboratory tests. In the set-up N_2 with 375 ppm CO_2 was led though two dew point generators, one being a LICOR LI-610, the other a home-made version. After allowing ample time for the establishment of equilibrium, the gas exiting from the dew point generators was alternatingly fed to the measuring cell of the IFM. To this purpose the sensing head was enclosed by a aluminium cylinder of 3 cm diameter and 22 cm length. The complete IFM was put in a thermostatted climate chamber. Before entering the cylinder, the gas was led through a spiral wound copper tube of approximately 175 cm length and 4 mm inner diameter that was also placed in the climate chamber to allow the gas to reach the chamber's temperature before entering the cylinder. The flow rate was 1 liter per minute. All other tubing was polyethylene, 4 mm inner diameter, of a brand recommended to us for its low interaction with water vapour and CO_2. In the beginning we used teflon tubing but we got badly reproducible results with that. Every 10 minutes the gas flow was switched from one dew point qenerator to the other. The following conditions were chosen:

a. dew points 1.0 and 12.8 °C, chamber temperature 26.45 °C
b. the same dew points, but chamber temperature 14.9 °C

It should further be noted that the optics of the measuring cell were not heated during these experiments. Thus, in case a. the air inside the measuring cell is always at low relative humidity, whereas in case b. the air is close to saturation if the dew point is 12.8 °C.

It was found that all optical channels reacted to the step in dew point temperature, while the reaction at high relative humidity (R.H., case b.) was a multiple of that at low R.H. Furthermore, in case b. the responses of the reference channels were markedly slower than that of the 2.6 water vapour absorption channel. The reaction of the 2.3 µm channel at low R.H. could be due to the nearby 2.6 µm H_2O vapour absorption band, but the other responses can not be explained by optical absorption by water vapour. For the present it is concluded that effect of water absorption on the optics is always present, also at low R.H., and that this effect increases with increasing R.H.

The cross-talk was calculated from the transmission siqnals after correction for the dilution effect. The transmission signals are the ratios of the CO_2 absorption channel(s) and the reference channel(s) In case b. the transmission signals were not block-shaped but showed weird structures due to the different phase shift of the filter signals, and no cross-talk could be calculated with the exception of the ratio of 4.2(small)/4.2(broad) which showed the same response as incase a.

In case a. the following results were found:

	cross-talk (gm^{-3}/gm^{-3})	
4.2(small)4.2(broad)	$4.3*10^{-4}$	ASGAMAGE-B
4.2(small)/3.9	$3.9*10^{-4}$	ASGAMAGE-B
4.2(small)/2.3	$-2.9*10^{-4}$	ASGAMAGE-B
4.2(broad)/2.3	$-2.6*10^{-4}$	ASGAMAGE-A

The minus sign of the two last numbers may be due to cross-talk of the 2.6 µm channel into the 2.3 µm channel. The accuracy of these values is estimated at +/- $1*10^{-4}$ gm^{-3}/gm^{-3}.

These figures are not small if compared with the H_2O dilution correction, $8*10^{-4}$. Because the 4.2(small)/4.2(broad) cross-talk did not depend on the R.H. it seems that this is the 'true' cross-talk, presumably due to pressure broadening. Then, the pressure broadening effect found here is about half the dilution correction and thereby considerably larger than the effect assumed by LICOR.

3. Results

Here results from ASGAMAGE-B only will be discussed. A total of 282 runs of 55 minutes each was collected. Runs were rejected if the wind direction was unfavourable (outside the interval 200-360 degrees), and if the u'w' cospectrum was suspect (resulting in unrealistic drag coefficients). Data of the KNMI Solent sonic anemometer were used for the flux calculations. Wind speed data were from the MPN platform and CO_2 concentration data of the air and of the sea water from various sources (TNO, NIOZ, KNMI).

The effect of dirty optics was clearly visible in the 4.2(small)/3.9 ratio. In Fig.l fluxes from this ratio are plotted against the product of wind speed and dpCO2, and it is seen that there are many unrealistic negative values. All these values refer to the period of time when the optics were not regularly cleaned. During this period, also data from the 4.2(small)/2.3 ratio were taken. Surprisingly, these data did not exhibit such a suspect behaviour. In Figures 2 and 3 the 4.2(small)/3.9 ratio of the non-cleaning period have been removed. The difference between these figures is the application of a cross-talk correction as found in the foregoing section. It is thought that the 'low humidity' correction is applicable because the optics were heated during the experiment. The correction was calculated as the cross-talk times the observed humidty flux. It is seen that the cross-talk correction is generally small. The data have been divided into three groups according to the reference filter applied. By coincidence these groups also roughly represent cases with low, middle and high U*dpCO2 values. No systematic difference between the three groups can be discerned, which makes us believe that there is no systematic effect of water layers on the final data. For the two runs (not shown in the figures) that the H_2O channel was sacrificed in favour of an extra CO_2 channel (configuration d. in section 1), corresponding CO_2 fluxes were found. This also indicates that there is no systematic cross-talk from water layers left. As a reference the fluxes according to the relation of Wanninkhof are indicated in the figures. The corrected ASGAMAGE data seem to substantiate this relation, although there may be a tendency to exceed Wanninkhof at high wind speeds.

4. Conclusion

In a laboratory study the effect of cross-talk from H_2O on CO_2 was investigated. It was found that both water layers on the optics and pressure broadening play a role. The second effect was found to be about -1/2 the dilution correction. Using the laboratory results, the ASGAMAGE data were corrected. The final data were structured in three groups, according to the optical filter pair used for calculating the CO_2 concentration. No systematic difference between the three groups could be discerned, indicating that no systematic effects of cross-talk are left. The final CO_2 flux data show a spread of typically $5*10^{-5}$ $gm^{-2}s^{-1}$ and follow the relation of Wanninkhof rather well.

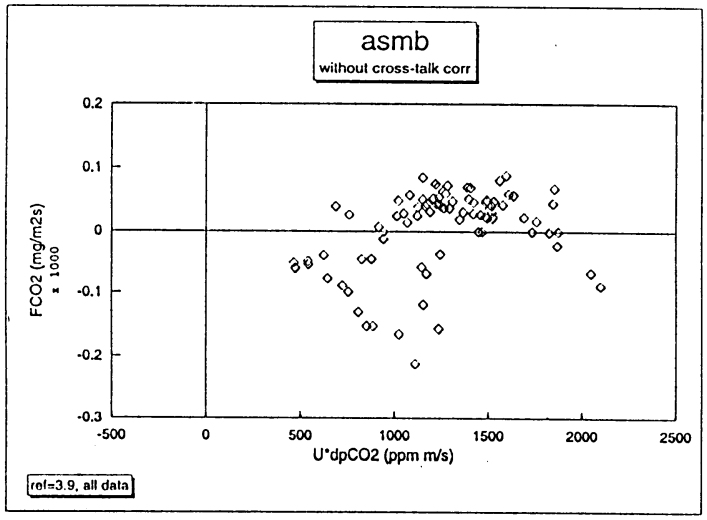

Figure 1

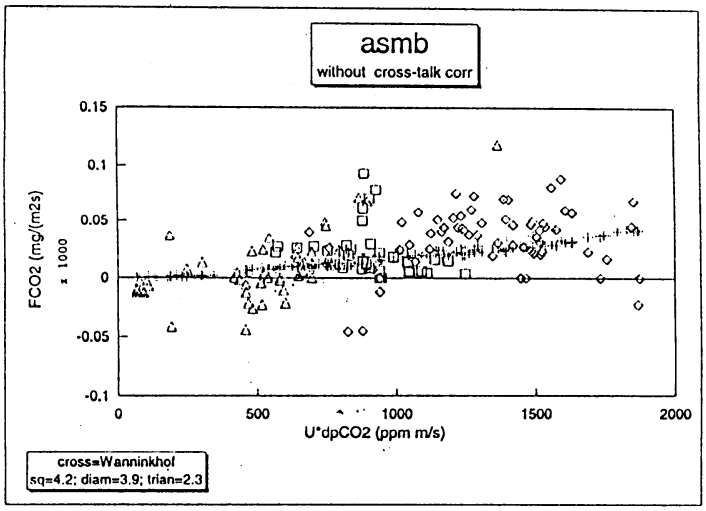

Figure 2

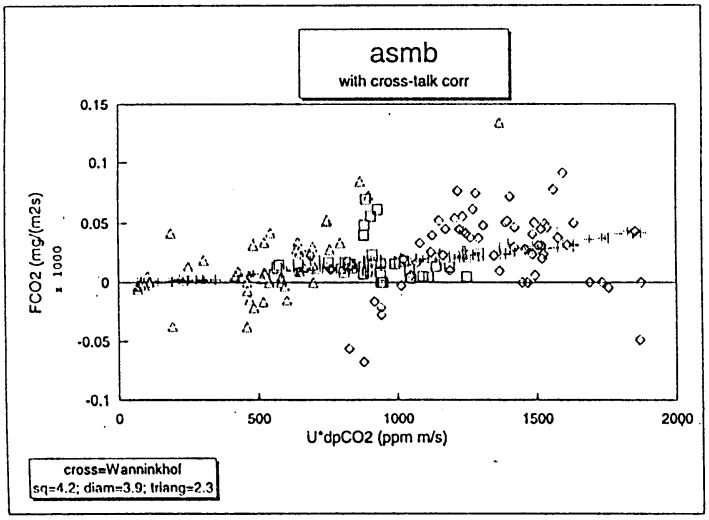

Figure 3

Intermediate report on the contribution of the Max-Planck-Institute for Chemistry Mainz to the ASGAMAGE project

S. Rapsomanikis, D. Sprung, T. Kenntner, M. Baumann
Max-Planck-Institute for Chemie, Mainz, Germany

Our group participated in the measurement campaigns ASGAMAGE A during spring 1996 and ASGAMAGE B during fall 1996. Our main interest was the determination of dimethyl sulphide (DMS) fluxes testing different kinds of micrometeorological techniques. Therefore new devices and new sampling methods for DMS were operated.
We used as reference the bulk method of calculating fluxes:
$F_c = Sc * k_w(u) * c_w$
For this method it is necessary to determine the concentration of DMS in sea-water c_w and the wind velocity u in 10 m height. By the bulk method for trace gases normally the concentration difference between water and air has to be considered. For DMS the air concentration can be neglected. Then the bulk flux is proportional to the Schmidt-number Sc and is calculated as the product of the transfer velocity k_w and the sea-water concentration c_w. For the parameterization of the transfer velocity several models dependent on the wind velocity, exist (Wanninkhof (1992), Liss and Merlivat (1986)). The resulting values differed up to the factor of 2.
Therefore we tried to use direct methods to determine the DMS flux. One possibility is the eddy correlation method:
$F_c = w'c'$
For this technique one has to measure the correlation between the vertical velocity w and the air concentration of DMS c. The primes denote the deviation from the mean. Therefore fast accurate measurements are needed with at least 1 Hz time resolution.
An alternative to this method is the relaxed eddy accumulation:
$F_c = b(z/L)*\sigma_w*(c_{up}-c_{down})$
The advantage of this method is that fast concentration measurements are not necessary. The flux is dependent on the standard deviation of the vertical wind velocity σ_w , a stability dependent (represented by the Monin-Obukhov-stability parameter z/L) factor b and the concentration difference between up- and downward moving air-parcels. A method description is found for example by Businger and Oncley (1990).

Instrumentation:
The needed micrometeorological parameters were measured by a sonic anemometer which was deployed on the North boom of the MPN in about 6.5 m height with 21 Hz. Water vapour fluxes were measured by a LICOR device.
Air concentrations of DMS with a time resolution up to 5 Hz were tried to measure with a new API (atmospheric pressure ionisation) quadrupole mass spectrometer. It was the first time that this device was operated in field campaigns. It was tested for measurements of the DMS flux using the eddy correlation technique.
To determine the sea-water concentration of DMS a GC/FPD system (gas chromatographic system with flame photometric detection) was used (description by Andreae et al. 1994). The probes were taken from two meters depth. These provided the DMS base for the flux estimation by the bulk method.

During ASGAMAGE A additionally air concentrations of DMS were determined by adsorbing on goldwool and using a similar GC/FPD-system like for the water samples after desorbing the DMS (Andreae et al. 1994). Simultaneous samples of 30 minutes were taken of downwards and upwards moving air parcels. The valves for sharing the air-parcels to the right gold wool tube were controlled by the vertical velocity measurements of our sonic anemometer. From these concentration differences it was tried to calculate the flux by the relaxed eddy accumulation method.

Preliminary results from the three used micrometeorological methods:
Bulk method fluxes:
In figures 1) and 2) the time series for the spring and fall campaigns are shown dependent on the Liss/Merlivat-model (Liss and Merlivat 1986). The Schmidt-number dependency is regarded following the parameterization suggested by Turner et al. (1996).
In figure 1) huge fluxes of DMS at the beginning of the campaign are evident. The are driven by DMS concentrations above 10 nmol/l (figure 3)). After a few days the concentration reduced to an average of about 4 nmol/l . During fall the concentrations were below 2 nmol/l (figure 4) all the time decreasing steadily. The fluxes reached values up to 7µmol/m²/day due to the high wind speeds up to 18 m/s.

Eddy correlation technique:
DMS concentration measurements for this method should be done by the mass spectrometer with 5Hz. During campaign A this method failed due to technical problems of the new device. And unfortunately the very high fluxes were only watched at the beginning of the campaign (figure 1). For the second campaign all the time the fluxes and DMS-concentration were very low (figure 3). So no significant crosscorrelation could be found indicating a significant flux. Some tests during the campaign were done regarding the time resolution, which show that for 1 Hz better results could be expected.
The eddy correlation system was verified by considering the measurements of some meteorological parameters. Figure 5) shows the dependency of the neutral drag coefficient on the wind velocity. The results were compared with an empirical curve of the literature. Figure 6) displays the calculated correlation coefficients of the sensible heat flux against the atmospheric stability. The values lie in the expected range.

Relaxed eddy accumulation:
The relaxed eddy accumulation was preferred to the general eddy accumulation, because the paramaterization by the b factor replaces the sampling flow dependence on the magnitude of the vertical velocity. By simulating the eddy correlation data the deadband dependency of the b-factor was simulated. Good agreement with an empirical curve (Businger and Oncley 1990) was found and shown in figure 7). Figure 8) displays the expected differences concentration differences for ASGAMAGE B derived from the calculated bulk fluxes. Figure 9) shows the same for ASGAMAGE A. There a comparison towards some directly measured values is possible. The measured differences show the right magnitude, but the discrepancy is still high due to uncertainties in the sampling method (different locations for sampling and analysing, analysing not immediately after measuring possible and other handling problems). But the calculation of the expected values show that it must be possible to measure the needed concentration differences.

Conclusion and outlook:

Until now the direct measurement methods provide some major problems, resulting from deployment of the new device, and the environment of the sampling platform. As yet we still have to believe in the fluxes calculated by the bulk method.

After these first experiences we think that in the next future measurements with mass spectrometer will either provide some reasonable results by eddy correlation or relaxed eddy accumulation or inertial dissipation. Further investigations are necessary.

This research was carried out in the framework of the ASGAMAGE project. We acknowledge the support from the European Commission's Marine Science and Technology Programm (MAST III) under contract MAS3-CT95-0044.

References

Andreae, T.W., Andreae, M.O., Schebeske, G.: 1994, Biogenic sulfur emissions and aerosols over the tropical South Atlantic: 1. Dimethylsulphide in sea-water and in the atmospheric boundary layer, J.Geoph. Res. Vol.99, No.D11, 22819-22829.

Businger, J.A. and Oncley, S.P.: 1990, Flux measurements with conditional sampling, J. Atm. Ocean. Techn., Vol.7, 349-352.

Garratt, J.R.: 1992, The atmospheric boundary layer, Cambridge University Press, Cambridge, 316 pp.

Liss P.S. and Merlivat, L.: 1986, Air-sea gas exchange rates: introduction and synthesis, in: Buat-Menard, P. (editor), the role of sea-air exchange in geochemical cycling, Reidel, Dordrecht, pp. 113-127.

Turner, S.M., Malin, G., Nightingale, P.D., Liss, P.S.: 1996, Seasonal variation of dimethyl sulphide in the North Sea and an assessment of fluxes to the atmosphere, Mar Chem, 54, 245-262.

Wanninkhof, R.: 1992 Relationship between gas exchange and wind speed over the ocean, J. Geoph. Res., 97, 7373-7381.

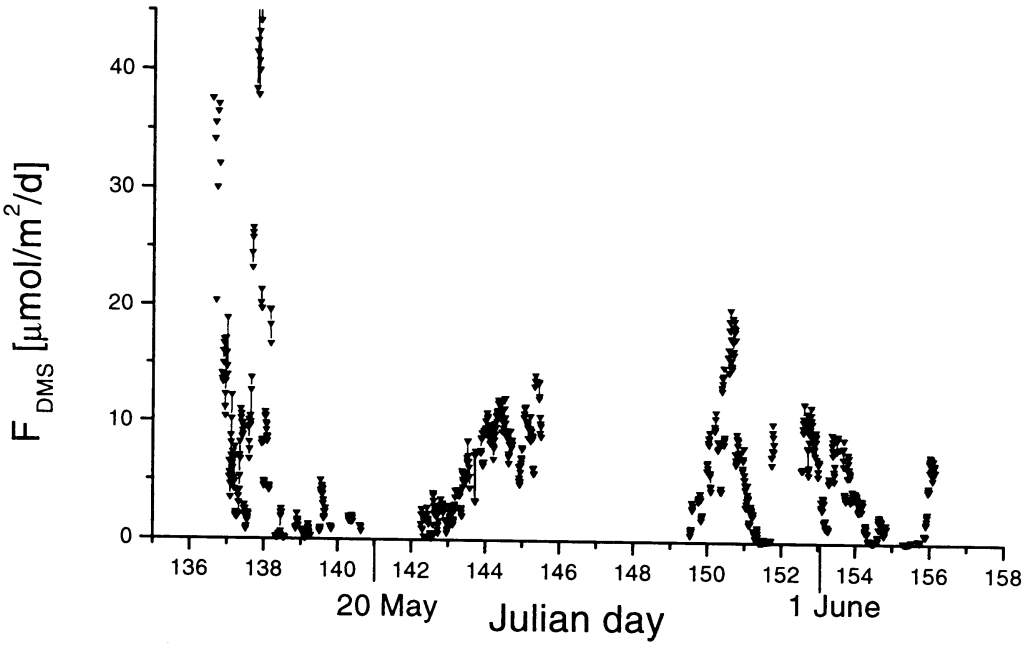

Figure1. DMS flux [µmol/m²/day] of the spring campaign 1996 ASGAMAGE A using the bulk method with the Liss/Merlivat (1986) parameterization

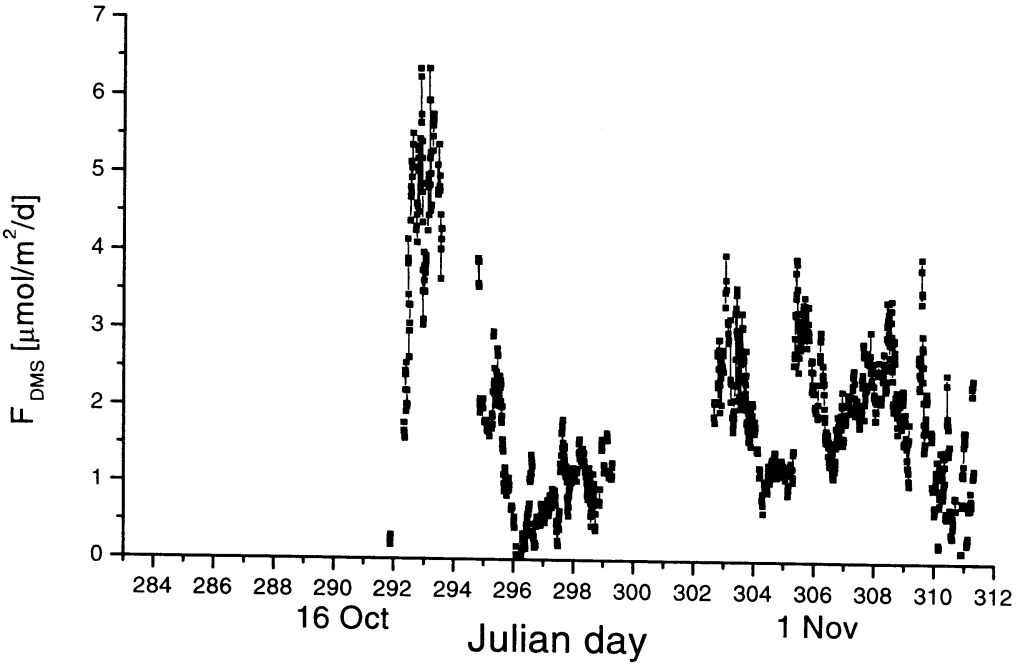

Figure 2. Time series of the DMS flux using the bulk method with the same parameterization as in Fig.1 for the fall campaign (ASGAMAGE B).

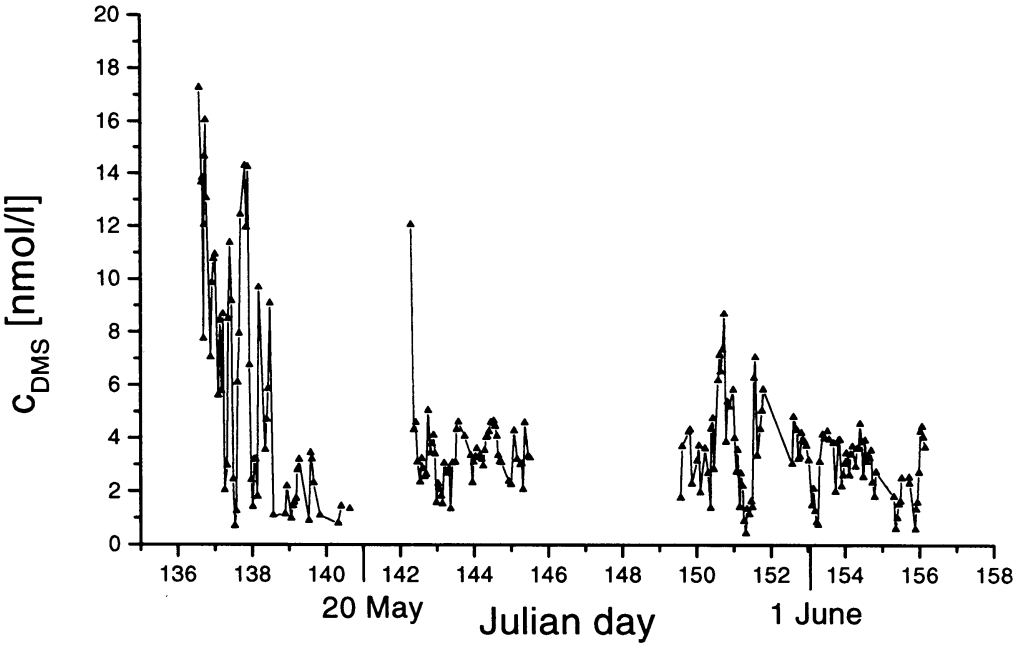

Figure 3. DMS concentration [nmol/l] in seawater during ASGAMAGE A

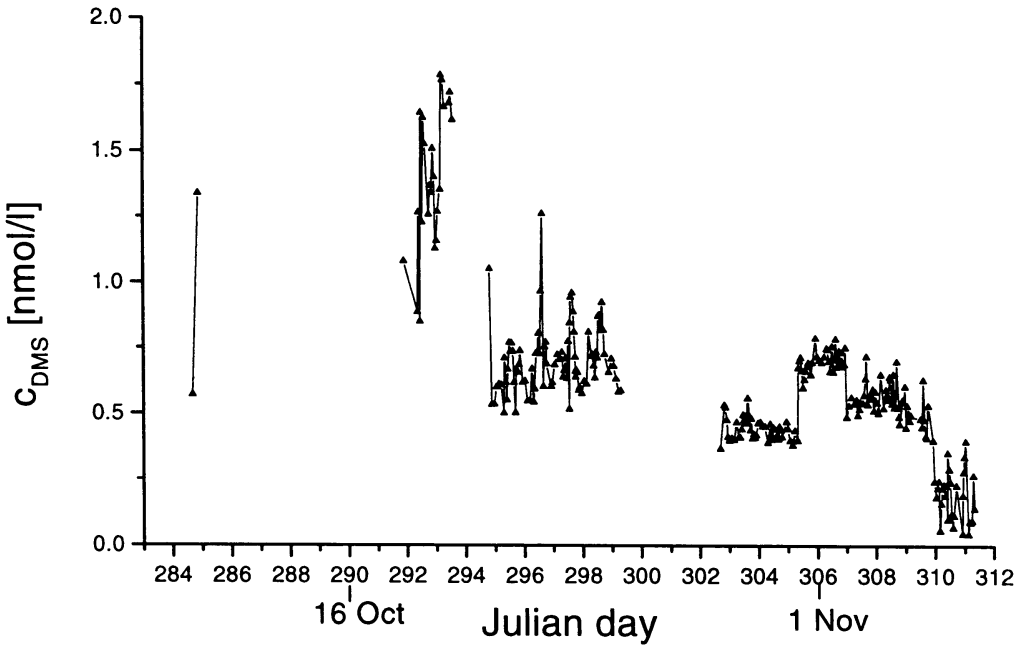

Figure 4. DMS concentration [nmol/l] in sea-water during ASGAMAGE B.

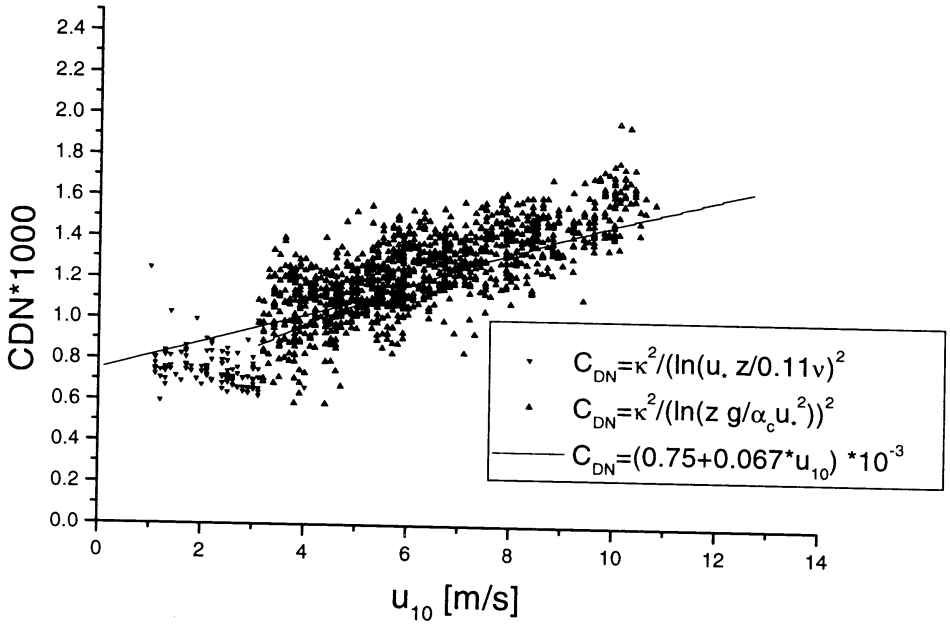

Figure 5. Dragcoefficient vs wind speed. The triangles show the calculated neutral drag coefficients C_{DN} by the eddy correlation method. They are compared to a parameterization due to the wind speed in 10 m height (Garratt, 1992).

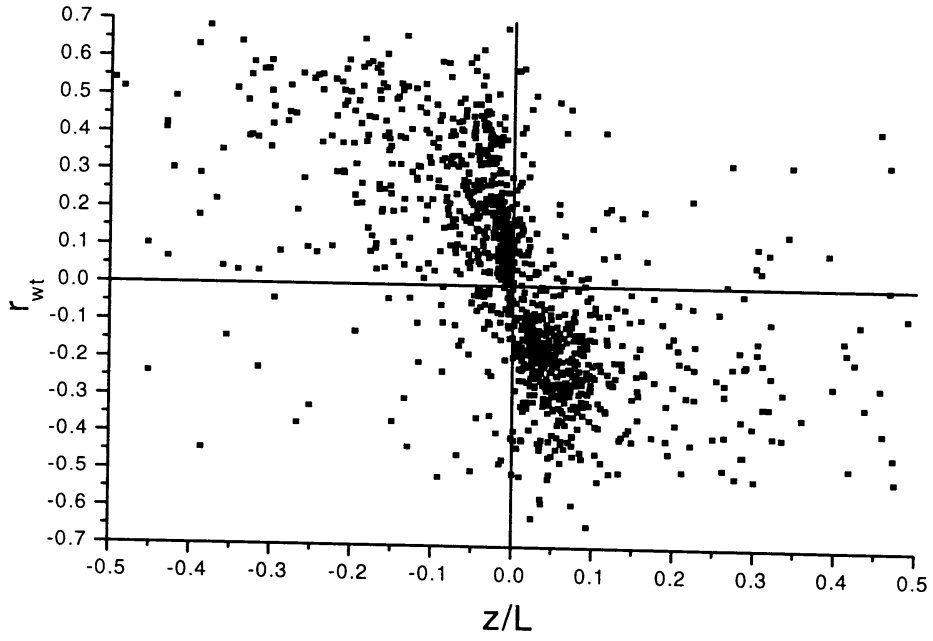

Figure 6. Correlation coefficient for the sensible heat flux against the atmospheric stability for AGAMAGE A.

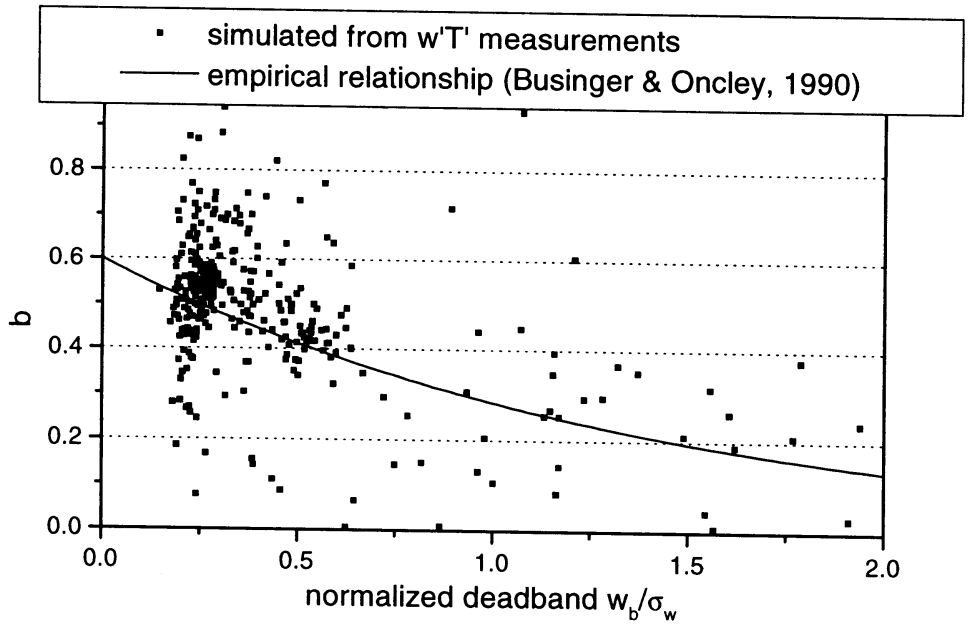

Figure 7. Deadband dependency of the b-factor of the relaxed eddy accumulation method.

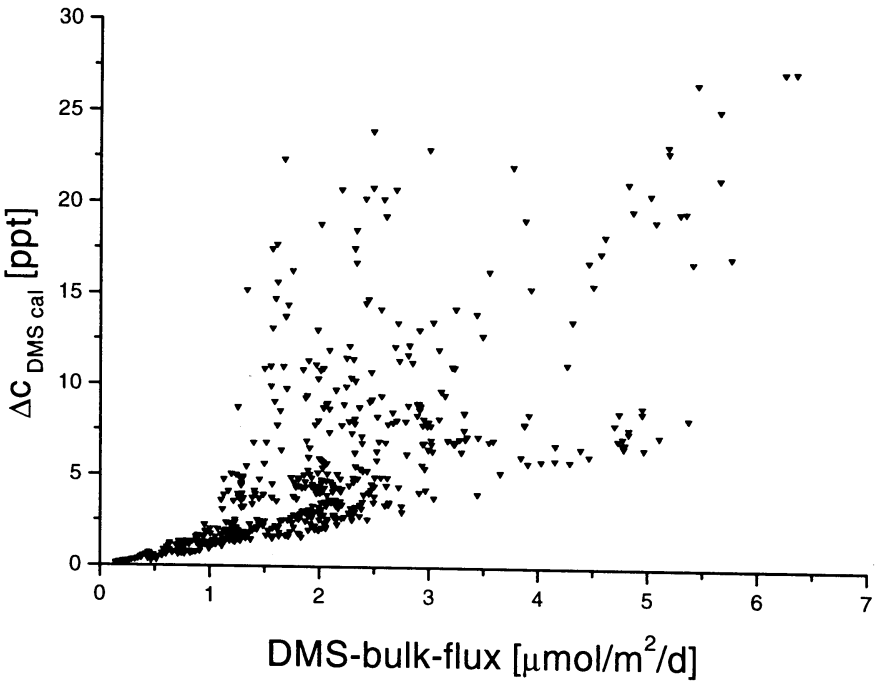

Figure 8. Expected concentration differences of the relaxed eddy accumulation method for ASGAMAGE B .

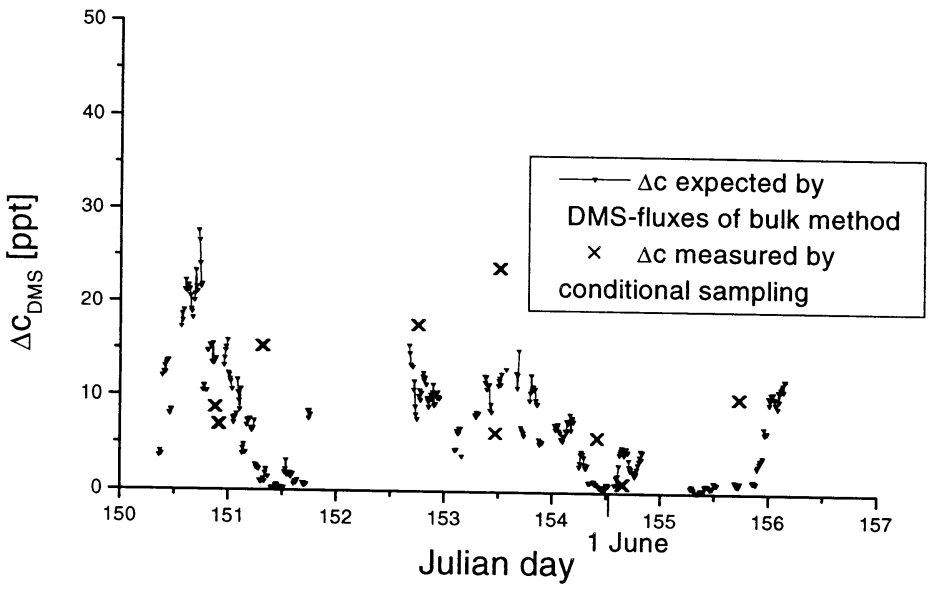

Figure 9. Comparison of the expected and measured concentration differences of the REA for ASGAMAGE A. The flux values of the bulk method are used as reference.

NOAA/ETL Water Vapor Measurements During ASGAMAGE-B

Jeffrey Hare[1), 2)] *and Christopher Fairall*[2)]
[1)] *CIRES, Campus Box 216, University of Colorado, Boulder, 80309 CO*
[2)] *NOAA - Environmental Technology Laboratory*

The NOAA Environmental Technologies Laboratory's (ETL) participation in the ASGAMAGE-B experiment was driven by the need to make direct measurement of the flux of carbon dioxide over the sea. In addition to the data acquisition system used on ASGAMAGE-B, two systems were of interest to ETL: the NOAA Climate Monitoring and Diagnostics Laboratory's (CMDL) closed-path gas analyzer (see the contribution by Dissly, Smith, and Tans) and the NOAA Air Resources Laboratory's (ARL) open-path CO_2/H_2O sensor (hereafter referred to as the Oak Ridge sensor). ETL provided support for the CMDL sensor deployment and analysis and brought the Oak Ridge sensor to the MPN platform for use in the experiment. In addition, ETL mounted an Ophir open-path hygrometer on the west boom of the MPN for comparison with the water vapor channel output of the Oak Ridge sensor.

ETL has taken efforts to determine the proper calibration and utilization of the open-path water vapor sensors. This information is vital to the interpretation of the CO_2 flux measurements due to the Webb effect (Webb, et al., 1980, *Quart. J. Royal Meteor. Soc.*, **v106**, 85-100). In addition, the flux of water vapor over the sea is important to the total heat budget and the turbulence structure in the marine surface layer.

Some characteristics of the Ophir IR-2000 optical hygrometer instrument include: 20 Hz sampling rate, 0.2 ^{B}C dew point temperature resolution, 1.0 ^{B}C dew point temperature accuracy. Measures in the 2.6 :m vapor channel, the 2.5 :m clear channel, and reference (blank).

$$q_v = \left(-\frac{1}{k} * \log_e \left(\frac{C_a}{C_c} * \frac{1}{A_0(1 + A_1 T_{can})} \right) \right)^{1/b}$$

Calibration:
where the units of q_v are g/m^3, C_a and C_c are the absorbing and clear channel counts (referenced), A_0, A_1, k, b are calibration coefficients, and T_{can} is the measured can temperature of the unit.
Note that the absorbing and clear channel counts, as well as the unit temperature, are available from the output of the unit, thereby enabling better diagnostic control by the user.

Characteristics of the Oak Ridge sensor include:
20 Hz sampling rate, measures both CO_2 and H_2O absorption in the infrared. Manufactured at the NOAA/Air Resources Laboratory - Atmospheric Turbulence and Diffusion Division (NOAA/ARL/ATDD) - Oak Ridge, Tennessee - David Auble, Engineer.
Calibration:

$$q_v = 1.145 * V^2 + 1.888 * V + 0.43$$

where q_v has units of g/m^3 and V is the voltage output.

Both sensors are sensitive to rain. However, the Oak Ridge unit appears to be somewhat more sensitive. Furthermore, both sensors are sensitive to window obscurification by sea spray salt. However, conditional sampling for episodes of window contamination is made possible with diagnostic information available from the Ophir. We are currently working on modification to the Oak Ridge sensor to provide more complete information as to drift, sensitivity, and cross-talk (see the contribution by Kohsiek).

The Ophir hygrometer is sensitive to internal temperature and this information is available from the output of the unit and is used in the calibration expression given above. The Oak Ridge sensor temperature sensitivity is unknown at this time.

Figure 1 shows that representative spectra from both units are consistent in shape, but the spectral density is offset. Furthermore , the mean and standard deviation of the computed absolute humidity show systematic bias between the two units as seen in Figures 2 and 3, respectively. These offsets could be attributed to drift of the instruments but is certainly a fundamental calibration issue. Note that in Figure 2, we have included the computed absolute humidity derived from the hand-held psychrometer measurements of the BIO team. This psychrometer provides the most accurate estimate of the mean value of the absolute humidity.

Figure 4 (a)-(b) show the computed covariance humidity flux for the Ophir and Oak Ridge sensors. Also, included are preliminary estimates of the humidity flux provided by KNMI and BIO as well as an estimate of the flux computed using the TOGA/COARE bulk formulation. We see that there is reasonable agreement between most of the estimates in the figure. Both the Ophir and Oak Ridge instruments were physically separated from the sonic anemometer which was supplied by TNO/Risr. It is therefore necessary to correct the computed fluxes for this displacement using the theory according to Kristensen, et.al., (1997) *J. Atmos. Ocean. Technol.*, **v14**, 814-821. Furthermore, a time lag was discovered in the transmission of sonic anemometer information from the TNO/Risr system. An additional correction was therefore included in this analysis wherein an inverse time lag was applied between the sonic vertical velocity and the water vapor signal which was sufficient to maximize the flux.

Because the Webb correction to the trace gas flux is significant, we feel that it is imperative that measurements of the mean humidity and humidity flux be as accurate as possible. Intercomparison of measurements from different instruments is sought from the ASGAMAGE-B participants, especially accurate traceable standard measurements such as those obtained with the psychrometer. This is the first step in verifying the calibration of the Oak Ridge and any other new sensing technology.

Figure 1. Example composite spectra from ASGAMAGE-B for Julian day 360 hours 10-17. Red line (below) is the Ophir spectrum and green line (above) is the Oak Ridge spectrum.

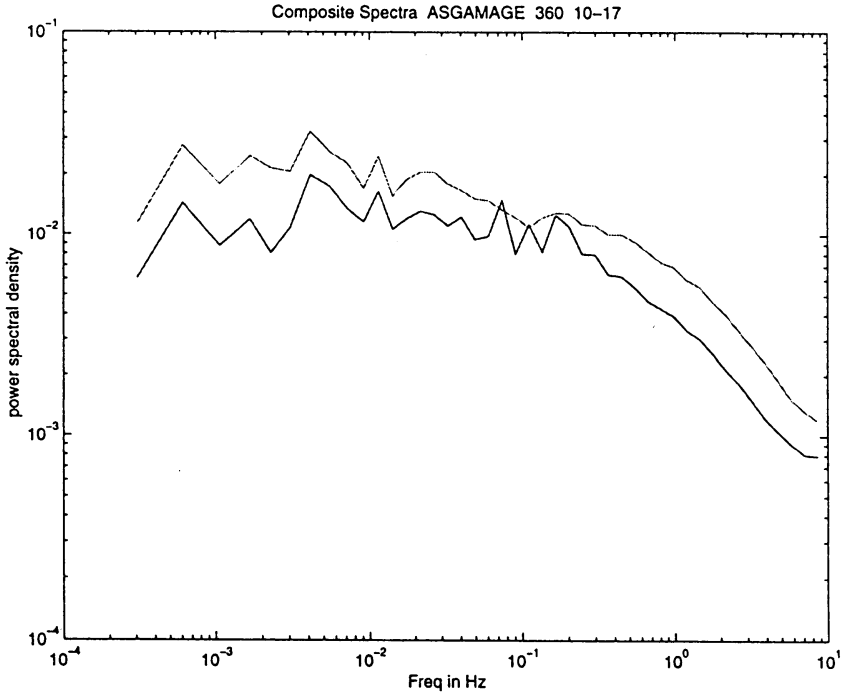

Figure 2. Mean absolute humidity for ASGAMAGE-B from the Ophir [squares], the Oak Ridge sensor [x's], and the hand-held psychrometer of BIO [circles].

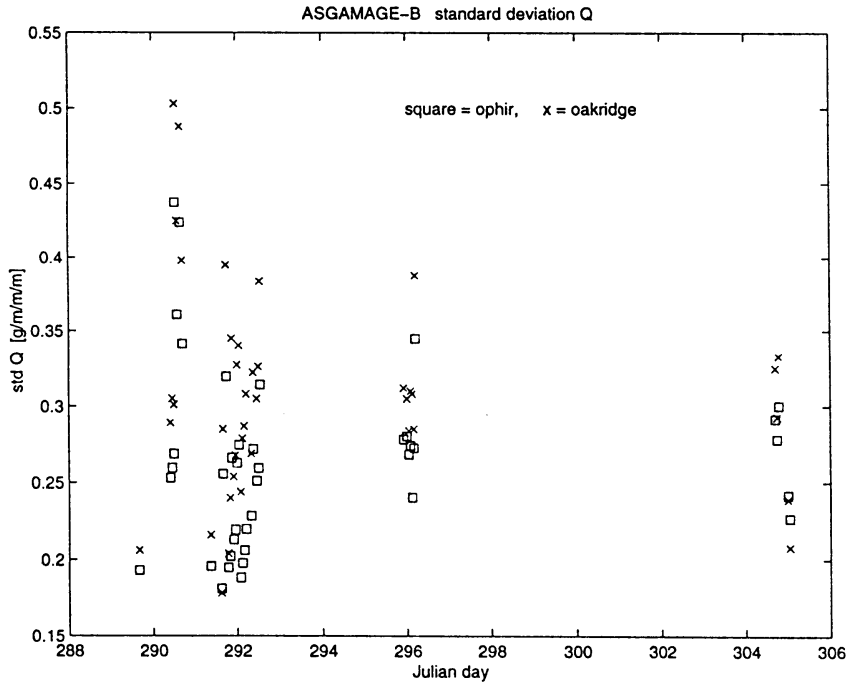

Figure 3. ASGAMAGE-B standard deviation of the absolute humidity from the Ophir [squares] and the Oak Ridge sensor [x's].

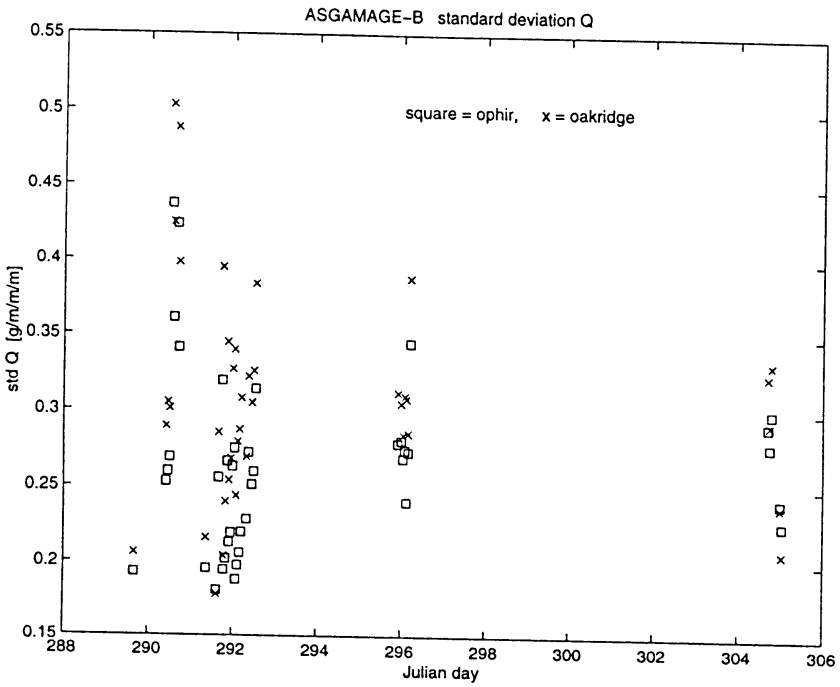

Figure 4(a). Humidity flux from ASGAMAGE-B for Julian days 289-297.Included are estimates from the KNMI system [circles] and BIO system (using the Oak Ridge sensor [pluses]), ETL estimates from the Oak Ridge sensor [x's] and the Ophir [squares], and estimates using the bulk algorithm [solid line].

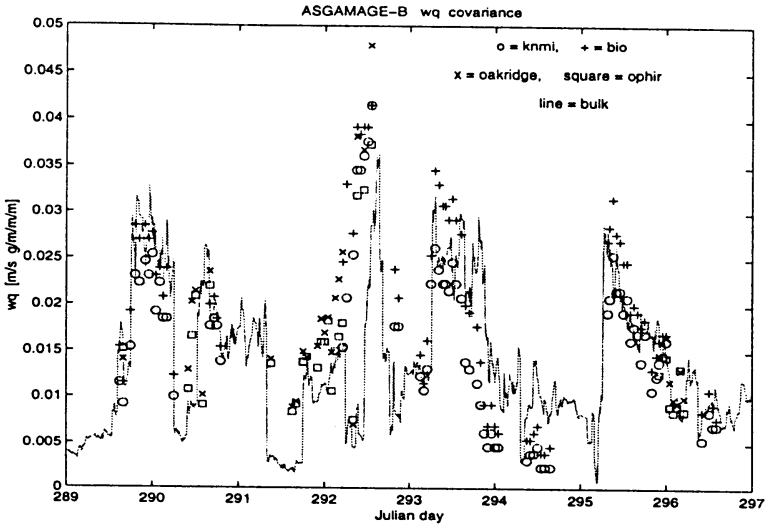

Figure 4(b). Same as (a) for Julian days 302-306.

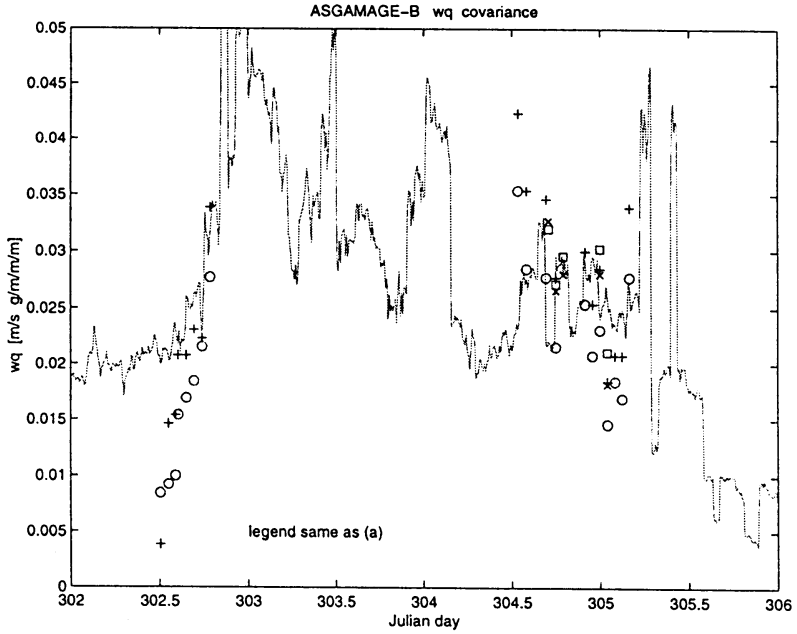

Final Report on the NOAA/CMDL Contribution to ASGAMAGE-B

Richard W. Dissly [1),2)], Jim Smith[3)], and Pieter P. Tans[2)].
[1)] CIRES, Campus Box 216, University of Colorado, Boulder, 80309 CO
[2)] NOAA/CMDL,325 Broadway, Boulder, CO 80303
[3)] Atmospheric Observing Systems, 6372 Niwot Rd., Longmont, CO 80503

The goal of the group from NOAA/CMDL was to utilize a sensitive closed-path analyzer to make direct air-sea flux measurements of CO2. Previous attempts to measure this flux have been either sensitivity limited or have required large corrections for heat and water vapor fluxes. Our intent from the outset was 1) to construct a detection system that had the precision necessary to detect very small differences in CO2 mixing ratio and 2) to dry and thermally equilibrate all air samples to be measured so that no correction factors would be required for heat or water vapor flux. An additional constraint was to maintain rapid flushing through all components of the system to preserve the majority of the turbulent fluctuations responsible for carrying the CO2 flux.

Under the guidelines listed above, a non-dispersive infrared CO2 analyzer with a higher sensitivity than commercially available units was built, under contract with Dr.Jim Smith of Atmospheric Observing Systems, a private company based in Boulder, Colorado. The analyzer makes a differential measurement of the CO2 mixing ratio between two cells. As a rough guide to the level of precision needed to detect a flux of CO2 over the open ocean, we can use the fact that the flux can be approximated by:

$$\text{Flux} \sim \sigma_w * \Delta C$$

where σ_w is the standard deviation in the vertical wind speed and ΔC is the CO2 mixing ratio difference between up and down moving air parcels. If the oceans are a net sink for ~2 Gt yr^{-1} of carbon, and we take 0.2 m s^{-1} as typical vertical wind speed standard deviation, the predicted difference in mole fraction between up and down moving parcels would be ~2 nmol mol^{-1}. Commercial instruments have a sensitivity on the order of a factor of ten worse than this. Fortunately, fluxes during this campaign were much higher than predicted open ocean fluxes, making our task somewhat easier. The delivered instrument demonstrated roughly 5 nmol mol^{-1} precision for integration times of 1000 seconds in the lab, while giving roughly 10 nmol mol^{-1} precision during the ASGAMAGE campaign for similar integration times. The degradation in precision was due to plumbing and flow limitations of intake systems, not electro-optical performance. To beat down the noise over such long integrations, the challenge is to minimize systematic variability in the instrumental response. To accomplish this, the entire instrument as placed in an insulated housing to minimize thermal drifts, and input gas was periodically switched between the two measurement cells to eliminate system bias arising from any differences between the two cells.

To avoid making corrections for a water vapor flux, we attempted to dry the sample air using a Nafion membrane in series with a glass trap cooled to -70 °C in a chilled ethanol bath, but leaks in this system made its use unreliable. Drying was instead maintained with a magnesium perchlorate [$Mg(ClO_4)_2$] trap, a chemical drying agent. Dual drying systems were always used to separately dry the air directed to each of the two measurement cells. While the use of magnesium perchlorate did dry our sample air to typically better than 50 µmol mol^{-1} of water, it required changing at rather short intervals (about every six hours of continuous use),

as the amount of drying agent was kept small to minimize the residence time of sample gas in the dryer.

Three different techniques were used to measure CO2 flux during the ASGAMAGE-B campaign, all implementing the analyzer described above: eddy correlation (EC), relaxed eddy accumulation (REA), and vertical gradient (VG). Our initial goal was to only try the REA method, but as this was the first field test of our full analysis system, we felt that it would be wise to capitalize on the opportunity and learn how our system could be utilized for alternative flux-measuring techniques. Roughly six days of the campaign was spent on EC, eight days on REA, and three days on VG, and the sequence was done in that order. The downside to trying multiple techniques was that a large amount of time was spent in set-up and conversion between the methods. The data we gathered for all techniques are summarized in Table 1, and plotted in Figures 1a and 1b, using different scales. The EC and REA techniques can be best characterized as demonstrating the potential of these methods. We had more success with the interpretation of the vertical gradient measurements. The results of all three techniques are described below. In addition, the results of our gradient measurements are being submitted as a paper to Geophysical Research Letters. A copy of our submission is attached as an appendix to this report.

Eddy Correlation

A schematic outlining our plumbing for eddy correlation measurements is shown in Figure 2. Sample air was acquired from the west platform boom and pumped through 60 m of 3/8" OD Dekabon tubing to our analysis system, at a flow rate of 10 liter min^{-1}. The flow in this line was turbulent (more detail later), and the frequency cutoff of fluctuations in this line was above 1 Hz. The intake line was positioned to be less than a meter away from the sonic anemometer operated by RISØ/TNO, from whom we were acquiring our wind data. This data stream was averaged every second, and a coordinate transform was applied in real time to extract the vertical component. A portion of the air from the intake line was teed off and directed through one drying unit to a measurement cell, and a similar branch was taken from the intake line through the other drying unit to a 10 liter mixing volume. Air samples for the other measurement cell were continuously drawn from this volume. The flushing time for the mixing volume was ~30 min, so that it represented the average concentration of CO2 over this period. The premise was to try to measure the "fast" variability (the line directly from the dryer) against the "slow" baseline (the line from the mixing volume). Air samples were all fully dried and the length of intake line ensured the samples were thermally equilibrated, so no 'Webb" corrections were necessary.

Diagnostic measurements of the frequency filtering performance of various components in our system show some interesting results. While on the platform, we were concerned that poor flow in our 60 m intake line (10 l min^{-1}) might be limiting the frequency response of our system from the start. If the flow in this line were laminar, then slow boundary layer mixing could potentially degrade our signal severely. We had hoped rather to have turbulent flow, which is known to preserve high frequency information in such lines. We placed a Lyman alpha hygrometer on our inlet exhaust, and compared the water vapor fluctuations with a similar hygrometer on the boom. The results suggested that fluctuation coherence was degraded above 0.3 Hz, and that fluctuation amplitude was decreased by an order of magnitude as samples moved through the length of the intake line at a volume flow rate of 10 l min^{-1}. However, we have repeated these experiments in a laboratory setup upon return from the campaign, directly measuring CO2 fluctuations rather than those of water vapor, and find very different results: at the same volume flow rate and for the same length

and diameter of tubing, the frequency response is very strong to 1 Hz, with fluctuation amplitude preserved to better than 90%. Our hypothesis is that water is not a good proxy for CO2 when trying to understand the transmission characteristics of an intake line, probably due to differences in wall interactions. As a result of these tests, we believe the intake line to have no affect on the integrity of our data, as the intake line passes fluctuations faster than our one second signal averaging time.

However, we found that the measurement cells degrade frequencies above 0.1 Hz when flushed at 150 sccm, our operational flow rate for this setup. This cutoff frequency increases with flow rate, making us optimistic about obtaining a higher cutoff in future campaigns, but unfortunately this is a firm limit to our data for the ASGAMAGE program. This poor frequency response yielded only non-detections; integrating the noise down over several hours did not produce a signal. Still, we can place upper limits on the flux from our data. We assume that half of any scalar flux is carried by turbulent frequencies below 0.1 Hz for the typically neutral PBL conditions during the campaign [Panofsky and Mares, 1968]. Therefore, we can approximate the upper limit of the flux as twice the 1σ level of the covariance measurement (w'c') in the neighborhood of the lag introduced by our intake line (9 sec). Three such integration periods are shown in Figure 1a. Note that two of the data points are substantially higher than the parameterized flux predicted by Wanninkhof [1992] for the conditions during the measurement. As these values are only upper limits, their usefulness as a constraint on the flux is rather limited.

Eddy Accumulation

Our plumbing setup was changed for eddy accumulation measurements; a schematic is shown in Figure 3. The 60 m intake line was still directly adjacent to the TNO sonic anemometer, and the intake flow rate was identical, so that all fluctuations slower than ~1 Hz were preserved through the intake line. Most of the intake flow was vented into the room. Samples were obtained through two diaphragm valves connected to the intake line near its end, to partition the air into "up" and "down" moving parcels. To accomplish this, corrected vertical wind data from the sonic was averaged over 1 sec periods, and the valves were fired in accordance to the vertical wind direction. A delay in the valve control was necessary due to the transit time of air samples in the intake line. This delay was on the order of 9 seconds, determined by breathing into the intake inlet on the boom end and measuring the arrival time for this pulse of CO2 enriched air. The partitioning of air samples was also dependent on the magnitude of the averaged vertical wind speed; a "dead band" was inserted in the acquisition valve control software that kept both valves closed when the magnitude was below a set threshold value. In theory, this should maximize the signal to noise in our differential concentration measurements between "up" and "down" air if the dead band magnitude is roughly equal to the standard deviation of the vertical wind speed.

Once the air samples had been separated, they were directed through our chemical dryers and through 1 liter holding volumes. The sampling period is dictated by the length of time required to fully flush these volumes (~10 min). The samples were acquired in two steps: the holding volumes were first actively pumped, so the accumulation was done at subambient pressures (~0.7 atm). The valve to the pump was then closed, and the holding volumes were brought back up to near ambient pressure only through the firing of the acquisition valves. Once near 1 atm, the line near the pump was open to atmosphere. Samples were then drawn from these volumes and measured by our differential analysis system, with no pressure bias between the holding cells, as they were both referenced to atmospheric pressure. The concentration difference between up and down moving samples provides a direct

measurement of the vertical CO2 flux. At least four samples are taken from the holding volume during each run to improve our measurement precision. A long "buffer" length of Dekabon tubing between the opening to the atmosphere and the holding cells allowed us to take multiple sample aliquots at the same pressure without contamination by lab air. For each data point shown in Figure 1, the "up" and "down" acquisition valves were switched for a total of four measurement cycles, to help eliminate bias due to the dryers or the holding cells themselves. After each switch, the holding cells were flushed for 10 min with both acquisition valves left open so that we would start the accumulation process with the same CO2 mixing ratio in both sides.

As stated before, the intake line did not limit our frequency sampling capability below the 1 Hz averaging we used to control our acquisition valves. However, there were other factors that affected our REA measurements. A large uncertainty in the intake delay time arose from the imprecision of our measurement procedure. We used a stopwatch to time the difference between breathing into the intake and seeing the pulse in our analysis system. We then had to subtract the time taken for a sample to move between the acquisition valves and the measurement cells, i.e. through the drying system. This value was variable depending on the age of the drying agent. We measured both delay times several times during the campaign, and had results from 8 to 14 seconds for the delay due to the intake line alone. We made measurements using a range of delay times to cover the uncertainty, but this means that our data are not all uniform. As the implemented delay deviates from the actual one, the precision in our separation of "up" and "down" air samples will be compromised, so that a scaling factor must be multiplied by the measured concentration difference to determine the actual flux.

REA Data Analysis

Several potential problems had to be addressed in the analysis of these data. Each of the problems described below will attenuate our measured concentration differences by degrading the precision to which the air samples are partitioned to the holding volumes. The best solution is of course to eliminate the problem from the outset, but barring that, we have tried to quantify the level of attenuation so that our measured results can be scaled accordingly.

One problem with the EA technique arises from making measurements with a non-symmetric vertical wind speed distribution, or more generally, having any bias in this distribution. We commonly observed two aspects of the w distribution that were a problem. First, the correction angle to isolate the w component from the anemometer data was somewhat variable. We had to make slight changes in this every time the boom was raised and lowered, on the order of 0.5°. Far less predictable was the effect of wind loading on the boom. Under strong wind conditions, we observed that the correction angle needed to be continually updated, perhaps because the position of the boom was not stable. This proved to be a difficulty, as this value often drifted enough during a sampling period to make the data unreliable. We were still able to gather a significant amount of data when this was not an issue. Second, the distribution in w was often not symmetric during a sampling period, even though the mean value of w was nearly zero. Perhaps this was due to a sampling bias over too short a period of time, or some sort of flow distortion set up by the boom and/or platform.

Another problem was that our holding volumes may not have been properly flushed for each sampling period. We tried to eliminate any measurement bias in our analysis system by switching the role of the holding volumes periodically, i.e., switching the "up" for "down" and vice versa. For example, if there were a temperature difference between the volumes, and the samples maintained this difference while being measured, this would cause a bias in our differential concentration measurement. If the flushing time is inadequate, the "up" and

"down" air will contaminate each other, attenuating the difference. Still worse is inadequate flushing after calibration gases have been introduced into the holding cells. Quantifying this attenuation is not straightforward, so we simply eliminated any data taken with a short initial flushing
time.

As stated previously, our uncertainty of the sample transit time through our intake line led us to assume a range of values in the field, so that not all data are uniform. Once in the lab after the campaign, we were able to pin down the transit time with much greater precision (assuming all conditions being equal!). To properly scale our measurements made with incorrect delay values, we simulated the effect of delay error on the simultaneous wind data time series taken from the sonic anemometer. The momentlim flux is defined as the covariance of u and w ($u'w'$). In theory, the momentum flux can also be estimated by partitioning u values in accordance with whether w is positive or negative, with a fixed dead band included. This is just taking u as a proxy for the mixing ratio of CO2. Although CO2 is a passive tracer and momentum flux is not, this should still give us some idea of the coherence of measured flux values in the PBL. An example of this is shown in Figure 4. As can be seen, the coherence falls off rather rapidly. If the assumed and actual delay differ by as little as 1 sec, the momentum flux is attenuated by more than 50%. *This sharp functional dependence stresses the importance of measuring the intake delay time with accuracy.*

These momentum flux simulations were done in the neighborhood (time) of each REA flux measurement we took, propagating the delay error both forward and backwards in time, and trying different data averaging intervals. Once an "average" attenuation was determined for each REA measurement, that measurement was scaled by dividing out the simulated attenuation level. The scaled results are shown in Figures 1a and 1b, to and the procedure is tabulated in Table 2. The wide scatter of our scaled data indicates that making large corrections to the data is not a prudent approach to making accurate REA measurements. The transit time of samples in the intake line really needs to be determined a priori. No quantitative estimation of the error in each measurement is given, as we are uncertain about systematic measurement problems outlined above. However, a large part of the uncertainty in each measurement is due to the size of the correction factor given in Table 2.

Vertical Profiling

We have definitive data using this technique for the period of 4-7 November, and we are submitting these results for publication. A full description of the technique and the corresponding results are given in the appendix to this report.

In summary, we have sparse flux data for the full campaign, from three different techniques. Unfortunately, we could not overlap these methods to intercompare the results. Together the three data sets measured significant limits on the size of the observed CO2 flux. The information obtained during ASGAMAGE-B will provide valuable information for further development of each of these flux measurement techniques in subsequent campaigns.

References

Panofsky, H.A., and E. Mares, Recent measurements of cospectra for heat-flux and stress, *Quart. J. Royal Met. Soc.*, **94**, 581-585, 1968.

Wanninkhof, R., Relationship between wind speed and gas exchange over the ocean, *J. Geophys. Res.*, **97**, 7373-7382, 1992.

Table 1 - Full Measurement Summary

Date	Measurement Period	U_{10} (avg) (m/s)	EC flux (mmol/m^2/hr)
19 Oct. 1996	12:57 - 13:17	8.72	<9.8
20 Oct. 1996	00:00 - 05:00	5.18	<0.9
20 Oct. 1996	18:40 - 20:00	11.0	<13.0

Date	Measurement Period	U_{10} (avg) (m/s)	Corrected REA flux (mmol/m^2/hr)
29 Oct. 1996	00:00-03:00	17.03	129.0
30 Oct. 1996	13:00 - 15:00	9.934	0.2
30 Oct. 1996	17:00 - 19:00	9.531	0.8
30-31 Oct.1996	23:00 - 01:00	9.531	4.3
31 Oct. 1996	08:00 - 11 :00	13.32	-1.9
01 Nov,1996	21:00 - 24:00	10.18	3.2
02 Nov,1996	00:00 - 02:00	11.22	-2.5
02 Nov,1996	16:00 - 19:00	12.92	8.8
03 Nov,1996	00:00 - 03:00	12.11	-5.9
03 Nov,1996	05:00 - 08:00	13	-4.0
04 Nov,1996	00:00 - 02:00	10.34	~.8
05 Nov,1996	00:00 - 02:00	13.56	-3.2

Date	Measurement Period	U_{10} (avg) (m/s)	Gradient (ppb)	Uncertainty (ppb)	Gradient Inferred Flux (mmol/m2/hr)	Uncertainty (mmol/m2/hr)
04 Nov,1996	13:34 - 13:54	14.61	285	12	7.0	0.3
04Nov,1996	21:10-21:30	12.63	49	31	1.0	0.6
06 Nov,1996	16:22 - 16:42	15.42	638	18	16.9	0.5
06 Nov,1996	16:42 - 17:02	14.99	498	37	12.7	0.9
06 Nov,1996	20:32 - 20:52	13.98	206	32	4.7	0.7
06 Nov, 1996	20:52 - 21:12	13.84	81	27	1.8	0.6
06 Nov,1996	21:15 - 21:35	13.6	135	9	3.0	0.2
06 Nov,1996	21:34 - 21:54	13.6	125	14	2.8	0.3
06 Nov,1996	21:53 - 22:13	13.58	106	14	2.3	0.3
06 Nov,1996	22:12 - 22:32	13.64	118	8	2.6	0.2
06 Nov,1996	22:31 - 22:51	13.5	95	11	2.1	0.2
06 Nov,1996	22:50 - 23:10	13.26	84	17	1.8	0.4
06 Nov,1996	23:10 - 23:30	13.34	47	7	1.0	0.2
07 Nov,1996	00:48 - 01:08	13.42	114	11	2.5	0.2
07 Nov,1996	01:07 - 01:27	13.16	84	12	1.8	0.3
07 Nov,1996	01:26 - 01:46	13.16	98	12	2.1	0.3
07 Nov,1996	01:45 - 02:05	13.08	61	11	1.3	0.2
07 Nov,1996	02:04 - 02:24	13.06	63	19	1.3	0.4
07 Nov,1996	02:24 - 02:44	13.02	50	10	1.0	0.2
07 Nov,1996	02:43 - 03:03	13.22	44	11	0.9	0.2
07 Nov,1996	03:02 - 03:22	13.32	42	11	0.9	0.2
07 Nov, 1996	03:21 - 03:41	13.28	43	18	0.9	0.4
07 Nov,1996	03:40 - 04:00	12.69	49	11	1.0	0.2
07 Nov, 1996	03:59 - 04:19	12.29	27	16	0.5	0.3
07 Nov, 1996	04:19 - 04:39	12.8	44	19	0.9	0.4
07 Nov, 1996	04:38 - 04:58	12.72	30	10	0.6	0.2

07 Nov, 1996	04:57 - 05:17	12.21	27	12	0.5	0.2
07Nov,1996	05:16-05:36	11.73	18	10	0.3	0.2
07 Nov, 1996	05:35 - 05:55	11.26	28	14	0.5	0.2
07Nov,1996	05:54-06:14	11.24	-1	12	0.0	0.2
07 Nov, 1996	06:13 - 06:33	10.98	25	18	0.4	0.3
07 Nov,1996	06:33 - 06:53	10.58	54	16	0.8	0.2
07 Nov,1996	06:52 - 07:12	10.46	69	11	1.1	0.2

Table 2 - REA Data Analysis Summary

Date	Measurement Period	U10 (1) (m/s)	ΔC (ppb)	σ_w (2) (m/s)	Raw REA Flux (3) (mmol/m2/hr)	Correction Factor	Corrected RE Flux (4) (mmol/m2/hr)
29 Oct, 1996	00:00 - 03:00	17.0	120	1.03	11.6	11.1	129.0
30 Oct, 1996	13:00 - 15:00	9.9	3	0.47	0.1	1.5	0.2
30 Oct, 1996	17:00 - 19:00	9.5	13	0.42	0.5	1.5	0.8
30-31 Oct, 1996	23:00 - 01:00	9.5	25	0.44	1.0	4.2	4.3
31 Oct, 1996	08:00 - 11:00	13.3	-7	0.77	-0.5	3.8	-1.9
01 Nov,1996	21:00 - 24:00	10.2	34	0.46	1.5	2.2	3.2
02 Nov, 1996	00:00 - 02:00	11.2	-21	0.56	-1.1	2.3	-2.5
02 Nov, 1996	16:00 - 19:00	12.9	65	0.80	4.9	1.8	8.8
03 Nov,1996	00:00 - 03:00	12.1	-35	0.74	-2.4	2.4	-5.9
03 Nov, 1996	05:00 - 08:00	13.0	-26	0.64	-1.6	2.6	-4.0
04 Nov, 1996	00:00 - 02:00	10.3	-31	0.54	-1.6	5.6	-8.8
05 Nov, 1996	00:00 - 02:00	13.6	-5	0.75	-0.4	9.1	-3.2

Notes
(1) Average U_{10} over measurement period, using the corrected MPN data
(2) Standard deviation in vertical wind speed, from 21 Hz data (TNO/RISØ sonic data)
(3) Flux = $(0.6)*(\Delta C)*(\sigma_w)$
(4) Corrected Flux = (Correction factor)*(Raw REA Flux)

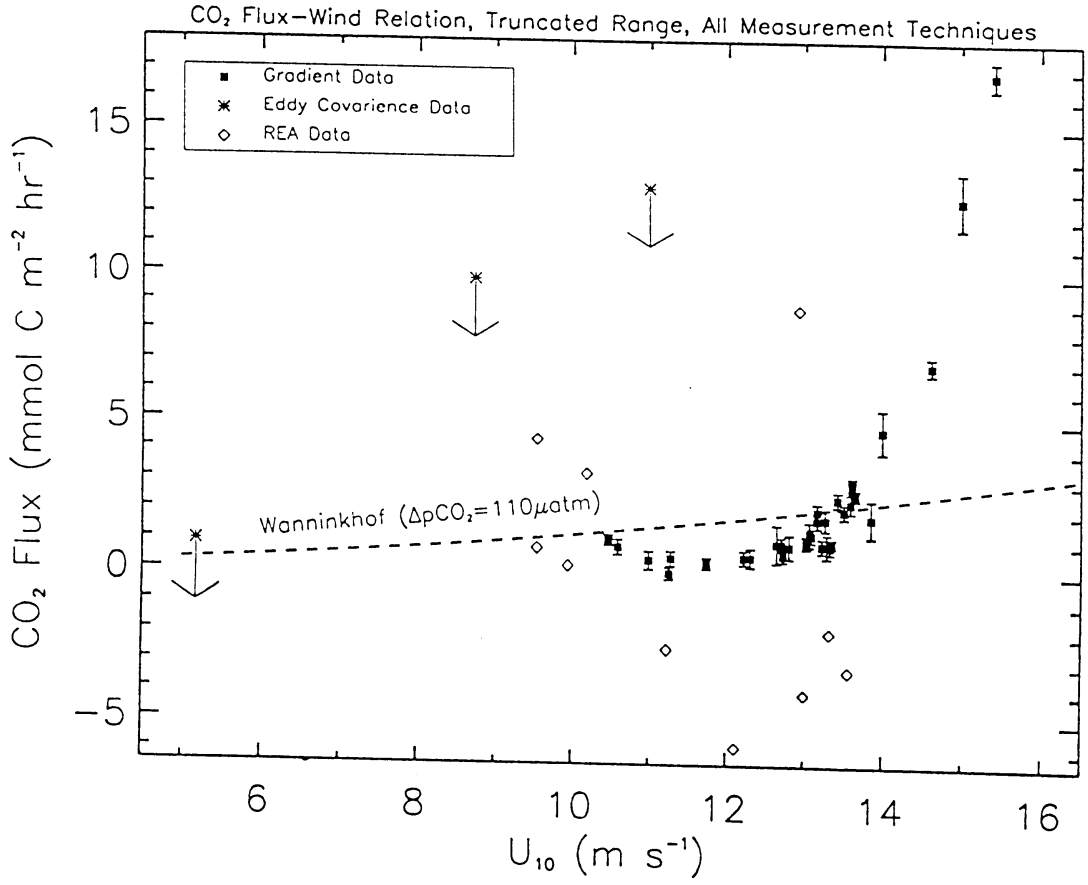
CO₂ Flux–Wind Relation, Truncated Range, All Measurement Techniques
Gradient Data
Eddy Covariance Data
REA Data
Wanninkhof (ΔpCO₂=110μatm)
CO₂ Flux (mmol C m⁻² hr⁻¹)
U₁₀ (m s⁻¹)
15
10
5
0
−5
6
8
10
12
14
16

Fig. 1a

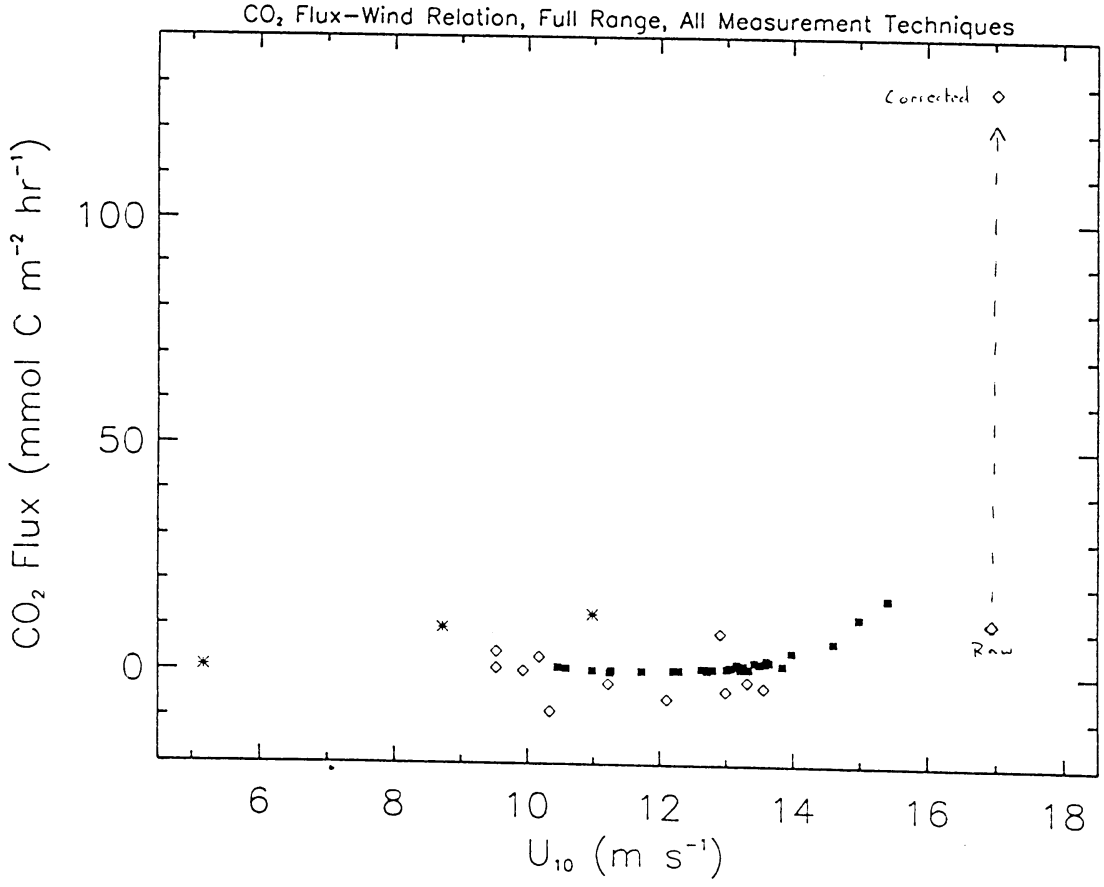
CO₂ Flux–Wind Relation, Full Range, All Measurement Techniques
Corrected
CO₂ Flux (mmol C m⁻² hr⁻¹)
U₁₀ (m s⁻¹)
100
50
0
6
8
10
12
14
16
18

Fig. 1b

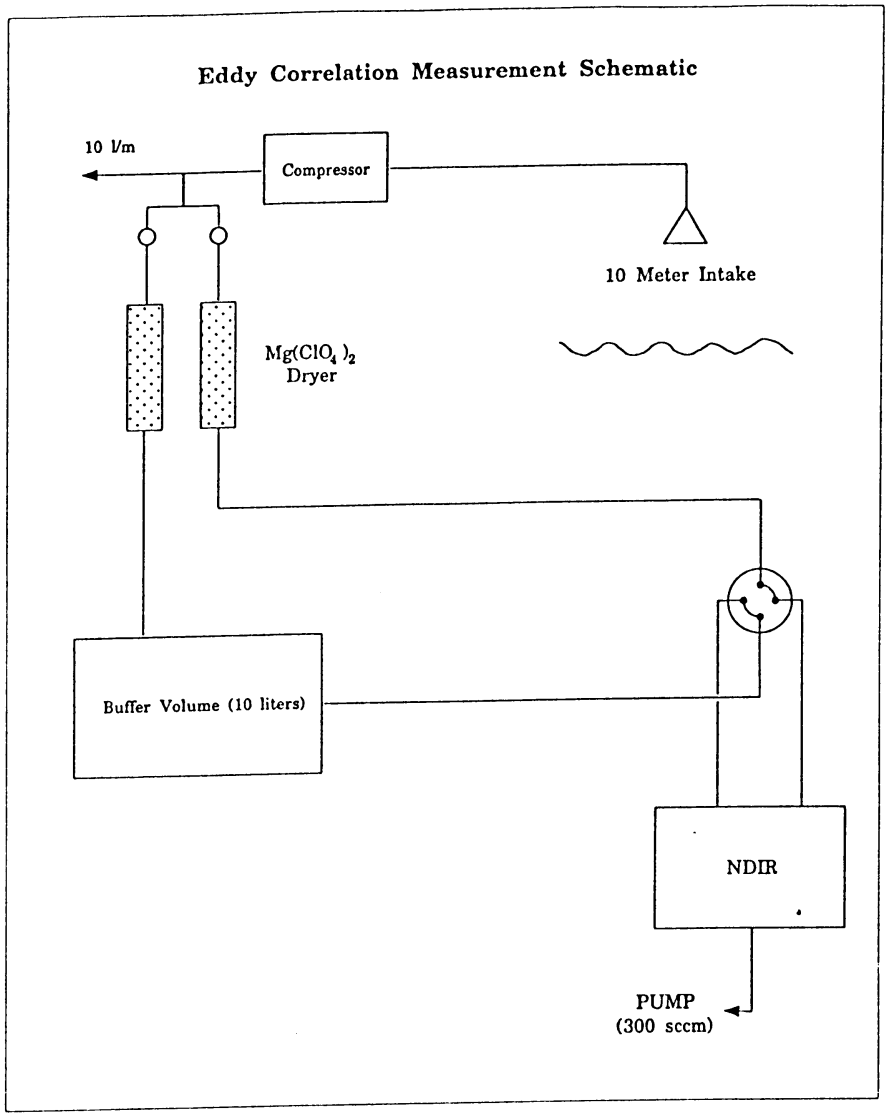

Figure 2

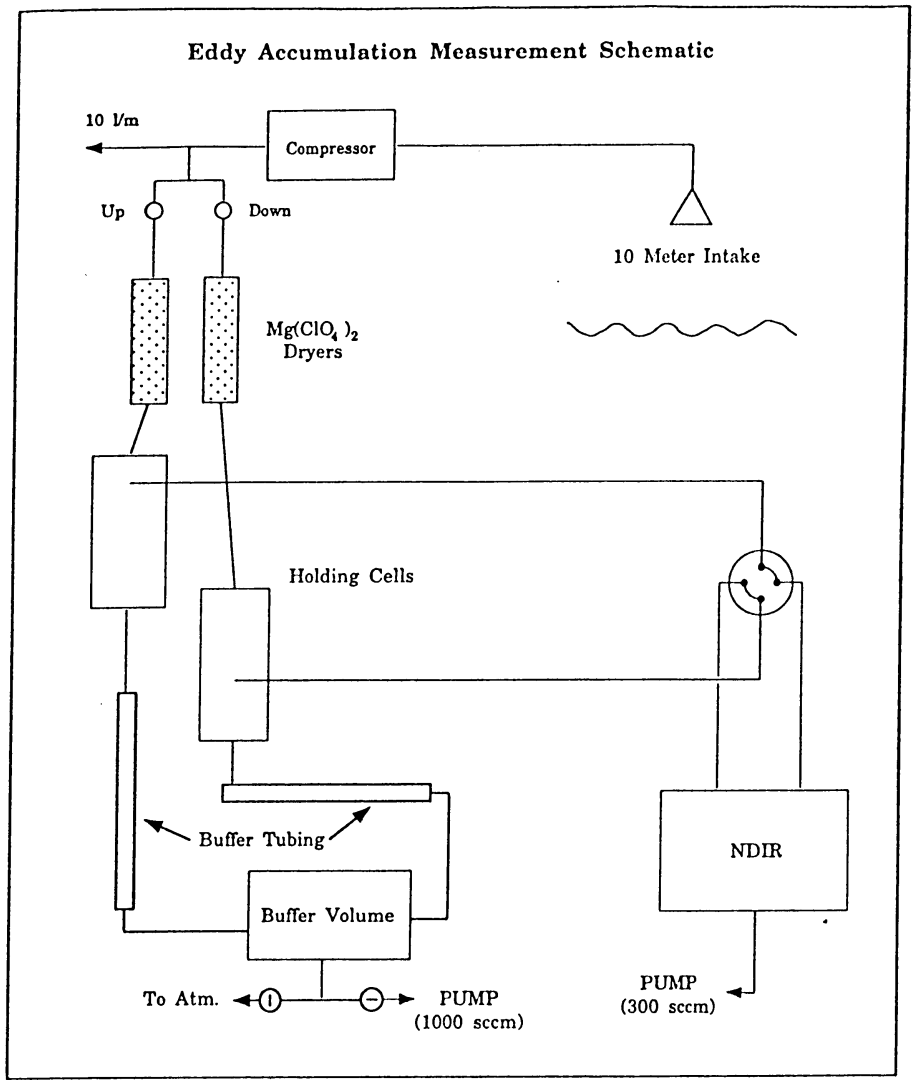

Figure 3

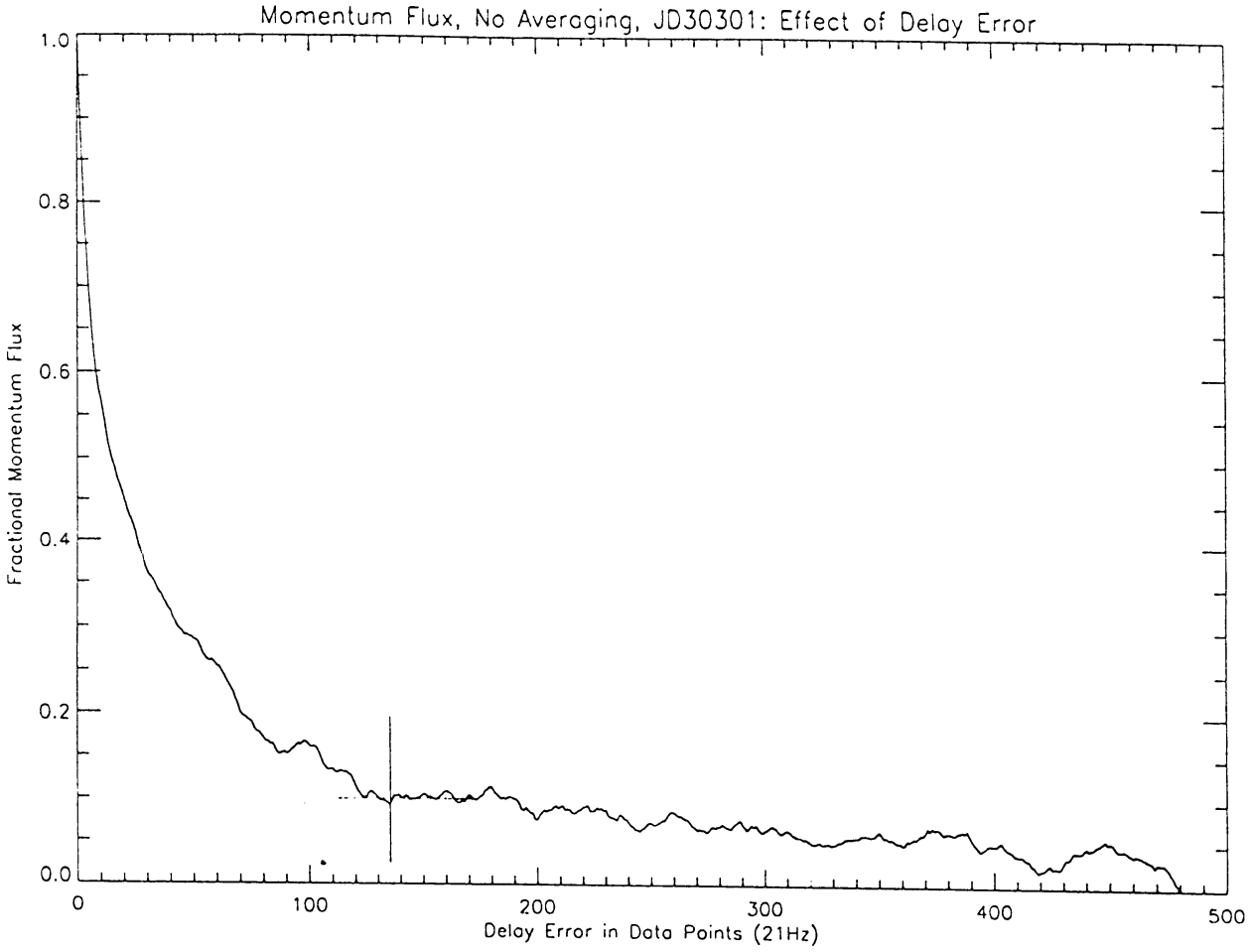
Momentum Flux, No Averaging, JD30301: Effect of Delay Error
Fractional Momentum Flux
1.0
0.8
0.6
0.4
0.2
0.0
0
100
200
300
400
500
Delay Error in Data Points (21Hz)

Figure 4

Possible Evidence of Greatly Enhanced CO2 Sea Exchange at High Wind Speeds from Vertical Gradient Measurements over the North Sea

Richard W. Dissly [1),2)], Jim Smith[3)], and Pieter P. Tans[2)].
[1)] CIRES, Campus Box 216, University of Colorado, Boulder, CO 80309
[2)] NOAA/CMDL,325 Broadway, Boulder, CO 80303
[3)] Atmospheric Observing Systems, 6372 Niwot Rd., Longmont, CO 80503

Abstract

In the fall of 1996, we participated in the second phase of the Air Sea Gas Exchange and Marine Aerosol Gas Exchange (ASGAMAGE) campaign, designed primarily as an international intercomparison of oceanic CO_2 flux measurement techniques. The campaign was based on the fixed platform Meetpost Noordwijk, located about 9 km off the Dutch coast in the North Sea. We made several measurements of the vertical CO_2 gradient in the surface layer of the planetary boundary layer (PBL), and have looked at how the gradient changes as a function of the wind speed at 10 m (U_{10}). Air samples were dried and thermally equilibrated prior to measurement, so that neither temperature or water vapor corrections were necessary. Our data indicate that CO_2 flux increases rapidly for wind speeds above 13 m s^{-1}, at a much higher rate than predicted by the parameterization of Wanninkhof [1992]. This trend suggests that there may be mechanisms at high wind speeds, such as bubble entrainment in breaking waves, that enhance gas transfer across the air-water interface.

Introduction

The ASGAMAGE experiment was primarily intended to better quantify the factors controlling air-sea exchange of CO_2, similar to the previous ASGASEX (Air-Sea GAS EXchange) experiment carried out in 1993 from the same platform [see Oost, 1995a, for details]. To assess the variability of flux over the short time scales during which environmental forcing factors, such as wind speed, air temperature, or tidal currents can change (less than 30 min), the focus of this campaign was on improving fast micrometeorological techniques, such as eddy correlation, eddy accumulation, and vertical profiling, to directly measure the CO_2 flux.

Previous attempts to measure air sea exchange using these techniques [e.g., Jones and Smith, 1977; Smith et al., 1991; Wesely et al., 1982; Crawford et al., 1993; Kunz et al., 1996] have been hampered by two problems. First, oceanic fluxes of CO_2 are typically very small, requiring high instrumental sensitivity and stability to make accurate measurements. If we approximate the flux as follows:

$$Flux \sim \sigma_w \Delta C$$

where σ_w represents the variability in the vertical wind speed and ΔC is the difference in CO_2 mixing ratio between up and down moving parcels of air, then the required instrumental resolution can predicted for a given flux. As discussed by Broecker et al. [1986], the globally averaged rate of bomb radiocarbon uptake limits the average net flux of CO_2 between the atmosphere and ocean over any large region to values less than 3 mol m^{-2} yr^{-1}. If σ_w is typically 0.2 m s^{-1}, then the CO_2 mixing ratio difference needs to be resolved to better than 1

part in $3x10^4$ of the atmospheric mixing ratio of CO_2 as a lower limit to the required measurement precision. A reasonable upper limit to this resolution can be determined by assuming a global net flux of 2×10^{15} g yr-1 of carbon into the oceans, a typical value inferred from ^{13}C isotopic constraints [Ciais et al., 1996], to be uniformly distributed globally. This leads to a net CO_2 exchange of 0.5 mol m^{-2} yr^{-1} and a resolution upper limit of nearly 1 part in $2x10^5$ of the atmospheric mixing ratio. This would require an instrumental precision of better than 2 nmol mol^{-1} which is very difficult to obtain. It should be pointed out, however, as stressed by Weseley [1986] and Smith and Jones [1986], that this net flux is a constraint only over long time periods and large spatial scales; there is no reason this has to be a fundamental limit for the small footprints and time scales typically covered in micrometeorological campaigns.

A second, more insidious, problem is that the fluxes of both heat and water vapor must be removed from any measurement to obtain the true flux of CO_2 [Smith et al., 1979; Webb et al., 1980]. A flux of water vapor is carried as a mixing ratio difference in H_2O between up and down moving air parcels. Accordingly, all other atmospheric species will be displaced differentially between up and down moving air, giving rise to an apparent flux. Similarly, a non-zero heat flux will require that upward parcels have a different temperature, and therefore a different density than downward moving parcels, which again gives rise to an apparent flux of any atmospheric species.

Fluxes of carbon dioxide measured with open-path sensors are determined by correcting the measured CO_2 values with direct measurements of both moisture and heat fluxes. However, these biasing fluxes are typically much larger than the CO_2 flux, giving rise to large errors in the corrected term. An alternative is to remove the competing fluxes by drying the air samples and bringing them to a uniform temperature prior to measurement. This neccessitates using a closed-path CO_2 sensor, which can severely degrade high-frequency sampling needed to observe the full range of turbulent frequencies that carry the flux [Leuning et al., 1996].

Our intent during ASGAMAGE was to address both problems outlined above from the outset. We designed a closed-path non-dispersive infrared (NDIR) CO_2 analyzer with both high sensitivity and stability, then dried and thermally equilibrated all air samples prior to measurement. Using this NDIR, we made measurements of the vertical gradient of CO_2 mixing ratio over a three-day period near the end of the campaign (Nov 4-6, 1996). We also attempted to make measurements using both eddy correlation and relaxed eddy accumulation, using the same NDIR with modifications to the inlet system. Neither of these latter techniques was successful; the instrumental frequency response limited our eddy correlation attempts, and poor specification of the delay time in our intake line (separate from the profile intakes) limited our ability to make flux measurements using relaxed eddy accumulation [see, e.g., Businger and Oncley, 1990, for details of this technique]. Consequently, only fluxes inferred from vertical gradient results are presented.

Measurement

A schematic of our measurement setup is shown in Figure 1. For sample acquisition, two intake lines were run to heights of approximately 4 m and 20 m above mean sea level. The end of each line was oriented down with a small funnel attached to the end to help avoid intaking rain or sea spray. Both intakes were located on the SWcorner of the platform, the direction of the prevailing winds during the course of this set of measurements. The respective

heights were chosen to avoid flow distortion from the platform as much as possible, being placed well above and below the bulk of the structure.

The intake lines were 5 mm ID polyethylene tubing, both about 30 m in length. Each line was split and run in parallel into a pair of four-port stream selection valves. The other two ports on each of these valves were connected to two calibration cylinders at 359.76 and 364.77 plus or minus 0.04 μmol mol^{-1} of CO_2, calibrated at CMDL prior to the campaign. During calibration, sample air from each of these cylinders was introduced into the measurement cells at ambient atmospheric pressure to avoid any systematic error due to a pressure differential between the measurement cells. The common outlet of each stream select was then run through separate magnesium perchlorate [$Mg(ClO_4)_2$] dryers, and finally to a two-position, four-port valve directly above the measurement cells of the NDIR. The entire system was pumped from downstream of these cells at a flow rate of 150 mL min^{-1} through each cell. The transit time of air samples through each intake line was therefore about 4 minutes.

During each gradient measurement, the two intakes were switched between the dryers using the stream selection valves a total of four times to detect any bias that may have been introduced by the drying material. Within each of these four positions, the two-position valve directly above the measurement cells was switched four times to monitor any bias due to differences in the measurement cells. Each full cycle lasted approximately 20 minutes. The estimated uncertainty within each 20 minute cycle was determined from the standard deviation of the sixteen measurements within each cycle. Any actual changes in the gradient during each 20 minute cycle are thus reflected in this uncertainty estimate. Bias due to differential uptake or release of CO_2 on the $Mg(ClO_4)_2$ was minimal when the chemical agent was fresh, however a rapid increase in this bias was clearly observed when the $Mg(ClO_4)_2$ neared saturation; data during these periods were rejected. The drying agent was changed approximately every six hours during our observations.

NDIR Analyzer.

At the heart of the analysis system was a closed-path non-dispersive infrared analyzer developed under contract with Atmospheric Observing Systems (Longmont, CO). The unit makes differential measurements of CO_2 mixing ratio between two measurement cells, each with a volume of 5 mL. The cells are designed to maximize flushing efficiency: at flow rates of less than 250 mL min^{-1}, the cells are totally flushed with less than 20 mL of gas. The cells act as a low-pass filter for fluctuations in mixing ratio, so increasing the useful frequency cutoff (defined as the frequency where the transmitted spectral power has attenuated by a factor of two) is important for measurements in the PBL where fluxes are carried by the full spectrum of turbulent frequencies. Measurements during this campaign were made with a flow rate of 150 mL min^{-1} through the cells; the half-power frequency was only ~0.1 Hz at this flow rate. This was a serious limitation for our eddy correlation measurements. Laboratory tests subsequent to the campaign show that the half-power frequency increases to 1 Hz for a flow rate of 1 L min^{-1}, so we remain optimistic that eddy-correlation measurements of CO_2 flux using this system will be viable in future campaigns.

The optical train incorporated a blackbody radiation source modulated at 1 kHz, a cooled PbSe detector, and silicon optical components to maximize the transmission of the 4.26 μm band used to make the differential CO_2 absorbance measurements. All components were mounted to a rigid breadboard, and placed inside of an insulated container to minimize drift due to thermal variations and fluctuations in CO_2 mixing ratio in the open paths between the cells and the source and detector. The container top was cooled with thermoelectrics as

both the blackbody source and the cooling system for the detector were significant sources of heat, but temperature was not actively controlled. The long thermal time constant of the analysis system made the bias drift between the measurement cells slow enough that it could be processed out of the data by the periodic switching of the two-position valve above the measurement cells. With this drift eliminated, it became possible to attenuate the random noise simply by increasing our integration times. In the lab, we routinely achieved instrumental precision from tank air of better than 5 nmol mol^{-1} in CO_2 mixing ratio for integration times of 20 min.

Results

To estimate surface fluxes from our gradient data, we assume neutrally stable conditions in the atmospheric surface layer. Wind speeds were moderate to high (U_{10} greater than 10 m s^{-1}) and the air-sea temperature difference was small (less than 2 °C) during our gradient measurements, so neutral conditions dominated.

For neutral conditions, the flux can be calculated with knowledge of the mixing ratio and wind speed at two heights [Lenshow, 1995]:

$$Flux = \frac{-k^2 (U_2 - U_1)(C_2 - C_1)}{[\ln(z_2 / z_1)]^2}$$

where k is the Von Karman constant (~ 0.4). The wind data were measured with a sonic anemometer at a single position above the ocean surface (4-6 m, depending on the tide), and corrected for platform flow distortion based on experience in previous campaigns at this location [Oost et al., 1994]. To determine the wind speed at the two measurement heights, we assume a logarithmic profile:

$$U(z) = \frac{u_*}{k} \ln[z / z_0]$$

where u_* is the friction velocity and z_o is the roughness length. A difference in windspeed between two heights is independent of z_o; for our measurement heights of 20 and 4 meters:

$$(U_{20} - U_4) \sim 4.0\ u_*$$

The drag coefficient is defined as:

$$C_D = [u_* / U_{10}]^2$$

An empirical relationship for C_D in terms of U_{10} has been determined at this location during a previous campaign [from HEXOS; see Smith et al., 1992]:

$$C_D = \frac{0.27 + 0.116 U_{10}}{1000}$$

We assume that this relationship is valid during our measurements, although the drag coefficient is certainly dependent on the wave field, and wind speeds during HEXOS were on average lower (5-12 m s^{-1}).

The calculated flux from ocean to atmosphere is shown in Figure 2 as a function of U_{10}. The specified wind speed is taken as an average over the hour immediately preceding the gradient measurement. Averaging over substantially longer or shorter time periods does not produce a single-valued function of flux in terms of U_{10}. Included is the flux predicted from the parameterization of Wanninkhof [1992], assuming an ocean temperature of 13°C and a salinity of 35‰, and using a ΔpCO_2 value of 110 µatm, typical for the few days immediately preceding the gradient measurements. The oceanic saturation state was measured up until one day prior to the gradient measurements shown here; it was stopped due to a pumping failure on the platform. As the wind direction and ocean current direction did not vary between the time of our measurements and the saturation state measurements, this value is probably representative for our measurement period. The ocean remained supersaturated with respect to the atmosphere by 70-120 µatm for the full campaign, with little or no stratification of dissolved CO_2 in the water column as seen during ASGASEX [Oost et al., 1995b]. Bakker et al. [1996] have suggested that such high carbon levels probably originate from the mineralization of accumulated organic matter in deeper waters, brought into the proximity of the platform by coastal upwelling.

There appears to be a clear functional dependence of flux on the wind speed. However, this trend is markedly different from that predicted by the parameterization of Wanninkhof. The deviation has two distinct features: calculated fluxes are substantially lower than that predicted by the parameterization for U_{10} less than 13 m s^{-1}, while the fluxes for U_{10} greater than 13 m s^{-1} are much higher, with an apparant trend that would suggest much higher fluxes at wind speeds greater than we experienced. The large fluxes calculated for U_{10} greater than 13 m s^{-1} are the result of large gradients measured in CO_2 mixing ratio, up to 638 nmol mol^{-1} over our fixed height difference.

Discussion

To date, attempts to parameterize the air-sea exchange of trace gases solely as a function of wind speed and saturation state have been inexact. The flux of a trace gas is usually defined as follows:

$$F = kS(\Delta p CO_2)$$

where k is a transfer velocity, S is the solubility, and ΔpCO_2 is the partial pressure difference of the gas between the air and water. Compiling estimates of the transfer velocity from various field and laboratory measurements shows a clearly increasing trend as a function of wind speed [Wanninkhof, 1992], but the scatter of data makes a unique relationship between the two difficult to quantify, and probably indicates that factors other than just the wind speed affect the transfer velocity. Given the lack of a unique functional dependence of transfer velocity on wind speed from previous studies, it is rather interesting that we should observe such a clear trend. Perhaps this is an indication that our measurements are representative of conditions over a large fetch, so that variability on small spatial and temporal scales is not seen.

The most striking feature of Figure 2 is the sharp deviation from standard parameterizations such as that by Wanninkhof. Are there reasonable physical explanations for our observed trend? The sharp transition in flux near U_{10} equal to 13 m s^{-1} is indicative of a change in the process mediating CO_2 exchange. Jähne et al. [1987] have shown that the onset of surface wave activity marks a transition in the diffusive scale length near the immediate surface. Increasing surface waves driven by wind brings turbulent diffusion closer to the surface on the water side, reducing the thickness of the boundary layer where molecular diffusion dominates, enhancing surface exchange with increasing wind speed. This transition corresponds with the onset of capillary wave activity which typically occurs at low wind speeds (U_{10} less than 5 m.s^{-1}). Surface roughness can be surpressed by the presence of surfactive organics [Goldman et al., 1988], which will shift this transition to higher wind speeds, but still far below our range of observed conditions.

A more probable enhancement of flux at moderate to high wind speeds is caused by the onset of wide spread wave breaking and associated bubble cloud formation. Bubble penetration will boost the transfer velocity of any trace gas, but the degree of enhancement is a complex function of both the volume flux of bubbles and the solubility of the gas. Bubbles will enhance the exchange of insoluble gases much more than soluble gases, such as CO_2, as shown in recent experiments [Wanninkhof et al., 1995, Asher et al., 1996]. Woolf [1993] ventures to give a reasonable estimation of the enhancement of CO_2 transfer velocity due to bubbles by relating the volume flux to fractional whitecap coverage, k_b=8.51(W/0.01) cm h^{-1}, where W is in turn a parameterized function of the wind speed. Using this functional dependence of Woolf with our highest observed wind speed of 15.5 m s^{-1} yields a bubble mediated transfer velocity of 37 cm h^{-1}. For an ocean temperature of 13 °C, a salinity of 35%, and a ΔpCO_2 of 110 µatm, this provides an enhanced flux of about 1.7 mmol m-^{2} h^{-1}, or a total flux of about 4.6 mmol m^{-2} h^{-1}. This is significantly less than our determined flux of 17 mmol m^{-2} h^{-1} based on the gradient measurements; this theoretical prediction is not adequate to explain our observations.

Casual inspection never revealed standing water in our intake lines, but we cannot rule out the possibility that our large measured gradients, and therefore large fluxes at high wind speeds, are an experimental artifact due to the presence of standing water from sea spray on the walls of the lower intake line. If sea water with a higher pCO_2 than the atmosphere enters the lower intake line and begins to equilibrate with the sample air stream, this will give anomalously high values measured at the lower intake height, yielding an artificially large gradient. Can we place some reasonable constaints on the importance of this process? Taking typical values from the campaign of $pCO_{2(Water)}$ = 470 µatm and $pCO_{2(air)}$ = 360 µatm, we can calculate the amount of excess CO_2 in the water coating the walls of the intake tubing that can come out of solution before equilibrium is reached. As most of the carbon involved in this process exists as bicarbonate (HCO_3^-) and carbonate (CO_3^{2-}) ions in solution, we must first calculate the total carbon content of the water for the given pCO2. At a water temperature of 13°C and a salinity of 35%, the solubility constant of CO_2 is about 0.04 mol $kg^{-1}atm^{-1}$ [Weiss, 1974], so the concentration of dissolved CO_2 is 1.88x10^{-5} mol kg^{-1} for a pCO_2 of 470 µatm. The total dissolved inorganic carbon (DIC) content can be approximated using the following relationship [eqn. 3-20 in Broecker and Peng, 1982]:

$$[CO_2] = \frac{1}{K'} \frac{(2[\Sigma CO_2] - [Alk])^2}{[Alk] - [\Sigma CO_2]}$$

where K' is the equilibrium constant for the following reaction,

$$H_2O + CO_2 + CO_3^{2-} = 2\,HCO_3^-$$

For our assumed salinity and water temperature, K' ~1565; thus, most of the carbon is in the bicarbonate form. If we assume an alkalinity of 2340×10^{-6} μeq kg^{-1}, close to the global average for surface waters [Takahashi, Broecker, and Bainbridge, 1981], the total DIC concentration in the water is 2200 μmol kg^{-1}. To bring this water into equilibrium with the air, $pCO_{2(Water)}$ must decrease by 110 μatm. The corresponding change in the total carbon content is buffered by the fact that the value of K' is so high. For a given change in ΔpCO_2, the corresponding change in the total DIC is smaller by roughly a factor of ten. This proportionality is known as the Revelle factor, defined as follows:

$$\Delta pCO_2 / pCO_2 = R(\Delta DIC) / (DIC)$$

If we assume R=10, then for our stated assumptions the change in the total carbon is ~50 μmol kg^{-1}, or 50 μmol L^{-1}; this is the concentration of carbon in seawater that is available to "contaminate" our airstream as CO_2. An atmospheric mixing ratio of 360 μmol mol^{-1} is equivalent to a CO_2 concentration of ~15 μmol L^{-1} in our airstream. To give the largest measured gradient of 638 nmol mol^{-1} in CO_2, the volume flow of water need only be 1 part in 2000 of the sample air flow (150 mL min^{-1}), or less than 5 mL h^{-1}, assuming full equilibration. This contamination rate is conceivable, especially in high seas, i.e., at high wind speeds. Although the mouth of the lower intake was a couple of meters above the normal swell, it is possible that rogue waves could have submerged the intake at the highest win speeds. We cannot discount this as a possible cause of our observed trend.

The low calculated fluxes at wind speeds less than 13 m s^{-1} relative to that predicted by the Wanninkhof parameterization are probably not the result of carbon depletion in the water column following episodes of high wind speed, i.e., high sea-to-air flux, although we cannot conclude this with certainty. We considered this possibility because the average wind speed decreased steadily over a 36 hour period in which most of the gradient measurements were made. Similarly, the observed gradient and calculated flux decreased steadily over the same time period. As ΔpCO_2 was not being measured simultaneously with this decreasing trend, we assume that the oceanic supersaturation of 110 μatm used to calculate the parameterized Wanninkhof flux in Figure 2 is valid for our measurement period. To investigate whether our highest calculated flux could lead to significant depletion of DIC during our measurement period, we can roughly predict the time it would take to bring the full water column into equilibrium with the atmosphere at this flux. The water depth at the platform location was 17m; the full column was well mixed for the campaign duration (particulary during episodes of high winds, as evidenced by sand being drawn into the equilibrators!). For a saturation excess of 110 μmol mol^{-1} relative to the atmosphere, the excess carbon concentration is roughly 50 μmol L^{-1}, as calculated above. Thus the carbon inventory that needs to be depleted for the full column is 0.85 mol m^{-2}. At our maximum calculated flux of 21 mmol m^{-2} h^{-1}, the time required for this column to equilibrate with the atmosphere would be 40 hours, neglecting the input of new carbon into the column. This is an extreme lower limit to the required equilibration time. Continual carbon input was likely, as the ocean remained superaturated for the full duration of the campaign. Perhaps the best evidence that sea-to-air flux did not appear to cause a loss of carbon is that oceanic pCO_2 was being measured during several protracted high-wind episodes prior to our gradient measurements; the partial pressure of CO_2 in solution did not change as a result of these episodes. The suppressed flux at

moderate wind speeds (U_{10} less than 13 m s^{-1}) is more likely the result of surfactants impeding the diffusion of CO_2 to the atmosphere when the surface is largely unbroken by whitecaps. The proximity of the platform to Rotterdam harbor and associated shipping lanes would make such surfactant coverage likely.

Conclusions

To our knowledge, these results represent the first vertical gradients of CO_2 measured in the surface layer over the ocean. Our measurements suggest that parameterizations of air-sea exchange may not be adequate at high wind speeds. However, it is possible that the direct equilibration of seawater supersaturated in CO_2 in the lower intake line can significantly affect the measurements. Still, the presence of wave breaking and associated exchange due to the deep penetration of bubble clouds into the water column should enhance the flux over that predicted by Wanninkhof [1992]. The magnitude of this enhancement at high wind speeds as predicted by theory is largely uncertain due to a lack of measurement under these conditions. If the trend presented here is correct, regions with high average wind speeds would need to be weighted more strongly in models of global carbon exchange than at present. Episodically high wind speeds, such as those in storms, would also play a more significant role in mitigating the exchange on a global scale. Obviously more direct measurements of flux are needed, particularly at high wind speeds, to verify this trend.

Acknowledgements

The authors would like to express our gratitude to Dr. Wiebe Oost and the staff of KNMI for the organization and technical assistance provided during ASGAMAGE, and for providing the corrected wind measurements. We would also like to thank Gerard Kunz from TNO for providing his ΔpCO_2 data, and both Søren Larsen and Finn Hansen from RISØ for allowing us to tap into their sonic anemometer data stream.

References

Asher, W.E., L.M. Karle, B.J. Higgins, P.J. Farley, E.C. Monahan, and I.S. Leifer, The influence of bubble plumes on air-seawater gas transfer velocities, J. Geophys.Res., 101, 12027-12041, 1996.

Bakker, D.C.E., H.J.W. de Baar, and H.P.J. de Wilde, Dissolved carbon dioxide in Dutch coastal waters, Marine Chemistry, 65, 247-263, 1996.

Broecker, W.S., J.R. Ledwell, T. Takahashi, R Weiss, L. Merlivat, L. Memery, T.-H. Peng, B. Jähne, and K.O Munnich, Isotopic versus micrometeorological ocean CO_2 fluxes: A serious conflict, J. Geophys. Res., 91, 10517-10527, 1986.

Broecker, W.S., and T.-H. Peng, Tracers in the Sea, Columbia University, Palisades, New York, 1982.

Businger, J.A., and S.P., Oncley, Flux measurement with conditional sampling, J.Atmos. Ocean Technol., 7, 349-352, 1990.

Ciais, P., P.P.Tans, J.W.C. White, M. Trolier, R.J. Francey, J.A. Berry, D.R. Randall, P.J. Sellers, J.G. Collatz, and D.S. Schimel, Partitioningof ocean and land uptake of CO_2 as inferred by ~13C measurements from the NOAA/CMDL global air sampling network, J. Geophys. Res., 100, 5051-5070, 1995.

Crawford, T.L., R.T. McMillen, T.P. Meyers, and B.B. Hicks, Spatial and temporal variability of heat, carbon dioxide, and momentum air-sea exchange in a coastal environment, J. Geophys. Res., 98, 12869-12880, 1993.

Goldman, Dennet, and Frew, Surfactant effects on air-sea gas exchange under turbulent conditions, Deep Sea Res., 35, 1953-1970, 1988.

Jähne, B., K.O. Münnich, R. Bosinger, A. Dutzi, W. Huber, and P. Libner, On the parameters influencing air-water gas exchange, J. Geophys. Res., 92, 1937-1949, 1987.

Jones, E.P., and S.D. Smith, A first measurement of sea-air CO_2 exchange by eddy correlation, J. Geophys. Res., 82, 5990-5992, 1977.

Kunz, G.J., G. de Leeuw, S.E. Larsen, and F. Aa. Hansen, Over-water eddy correlation measurements of fluxes of momentum, heat, water vapor, and CO_2, in Air-Water Gas Transfer, edited by B. Jähne and E.C. Monahan, pp. 685-702, AEON Verlag and Studio, Hanau, 1995.

Lenshow, D.H. Micrometeorological techniques for measuring biosphere-atmosphere trace gas exchange, in Biogenic Trace gases: Measuring Emissions from Soil and Water, edited by P.Matson and R. Harriss, pp. 126-163, Blackwell Science, Cambridge, MA, 1996.

Leuning, R., and M.J. Judd, The relative merits of open- and closed-path analyzers for measurement of eddy flw~es, Glob. Change Biol., 2, 241-253, 1996.

Oost, W.A., The ASGASEX '93 experiment,in Air-Water Gas Transfer, edited by B.Jähne and E.C. Monahan, pp. 811-816, AEON Verlag and Studio, Hanau, 1995a.

Oost et al., Flow distortion calculations and their application in HEXMAX, J. Atmos. Ocean Tech., 11, 366-386, 1994.

Oost, W.A., W. Kohsiek, G. de Leeuw, G.J. Kunz, S.D. Smith, B. Anderson, and O.Hertzman, On the discrepancies between CO_2 flux measurement methods, in Air-Water Gas Transfer, edited by B. Jähne and E.C. Monahan, pp. 723-733, AEON Verlag and Studio, Hanau, 1995b.

Smith, S.D., and E.P. Jones, Dry-air boundary conditions for correction of eddy flux measurements, Boundary Layer Meteorol., 17, 375-379, 1979.

Smith, S.D., and E.P. Jones, Isotopic and micrometeorological ocean CO_2 fluxes: Different time and space scales, J. Geophys. Res., 91, 10529-10532, 1986.

Smith, S.D., R.J. Anderson, W.A. Oost, C. Kraan, N. Maat, J. deCosmo, K.B. Katsaros, K.L. Davidson, K Bumke, L. Hasse, and H.M. Chadwick, Sea surface wind stress and drag coefficients: the HEXOS results, Bound.-Layer Meteor., 60, 109-142, 1992.

Smith, S.D., R.J. Anderson, E.P. Jones, R.L. Desjardins, R.M. Moore, O. Hertzman, and B.D. Johnson, A new measurement of CO_2 eddy flux in the nearshore atmospheric layer, J. Geophys. Res., 96, 8881-8887, 1991.

Takahashi, T., W.S. Broecker, and A.E. Bainbridge, The alkalinity and total carbon dioxide concentration in the world oceans, in Carbon Cycle Modeling, edited by Bert Bolin, pp. 271-286, Wiley, New York, 1981.

Wanninkhof, R., Relationship between wind speed and gas exchange over the ocean, J.Geophys. Res., 97, 7373-7382, 1992.

Wanninkhof, R., W. Asher, and E. Monahan, The influence of bubbles on air-water gas exchange: Results from gas transfer experiements during WABEX-93, in Air-Water Gas Transfer, edited by B. Jähne and E.C. Monahan, pp. 239-254, AEON Verlag and Studio, Hanau, 1995.

Webb, E.K., G.I. Pearman, and R. Leuning, Correction of flux measurements for density effects due to heat and water vapour transfer, Quaff. J. R. Met. Soc.,106, 85-100, 1980.

Weiss, R.F., Carbon dioxide in water and seawater: The solublity of a non-ideal gas, Marine Chem., 2, 203-215, 1974.

Wesely, M.L., D.R Cook, R.L. Hart, and R.M. Williams, Air-sea exchange of CO_2 and evidence for enhanced upward fluxes, J. Geophys. Res., 87, 8827-8832, 1982.
Wesely, M.L., Response to "Isotopic versus micrometeorologic ocean CO_2 fluxes: A serious conflict" by W. Broecker et al., J. Geophys. Res., 91, 10533-10535, 1986.
Woolf, D.K., Bubbles and the air-sea transfer velocity of gases, Atmos. Ocean, 31, 517-540, 1993.

Figure Captions

Figure 1. Gradient measurement schematic.

Figure 2. Measured CO_2 flux as a function of wind speed. The closed squares are fluxes inferred from the vertical gradient of CO_2 mixing ratio. The indicated errors for the gradient data are discussed in the text. The dashed curve represents the predicted flux from the parametrization of Wanninkhof (1992) assuming an ocean temperature of 13°C, salinity of 359‰, and a ΔpCO_2 of 110 μatm (ocean supersaturated with respect to air).

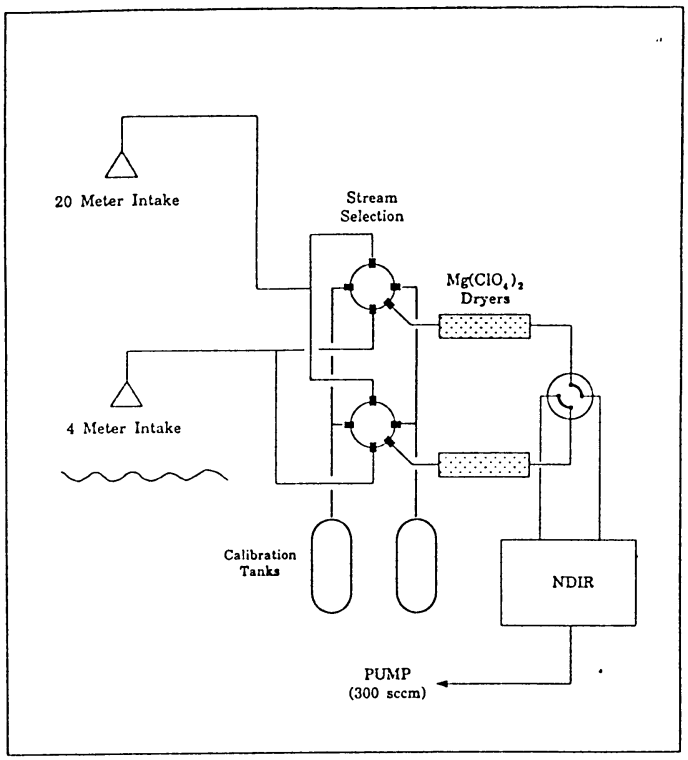

Figure 1

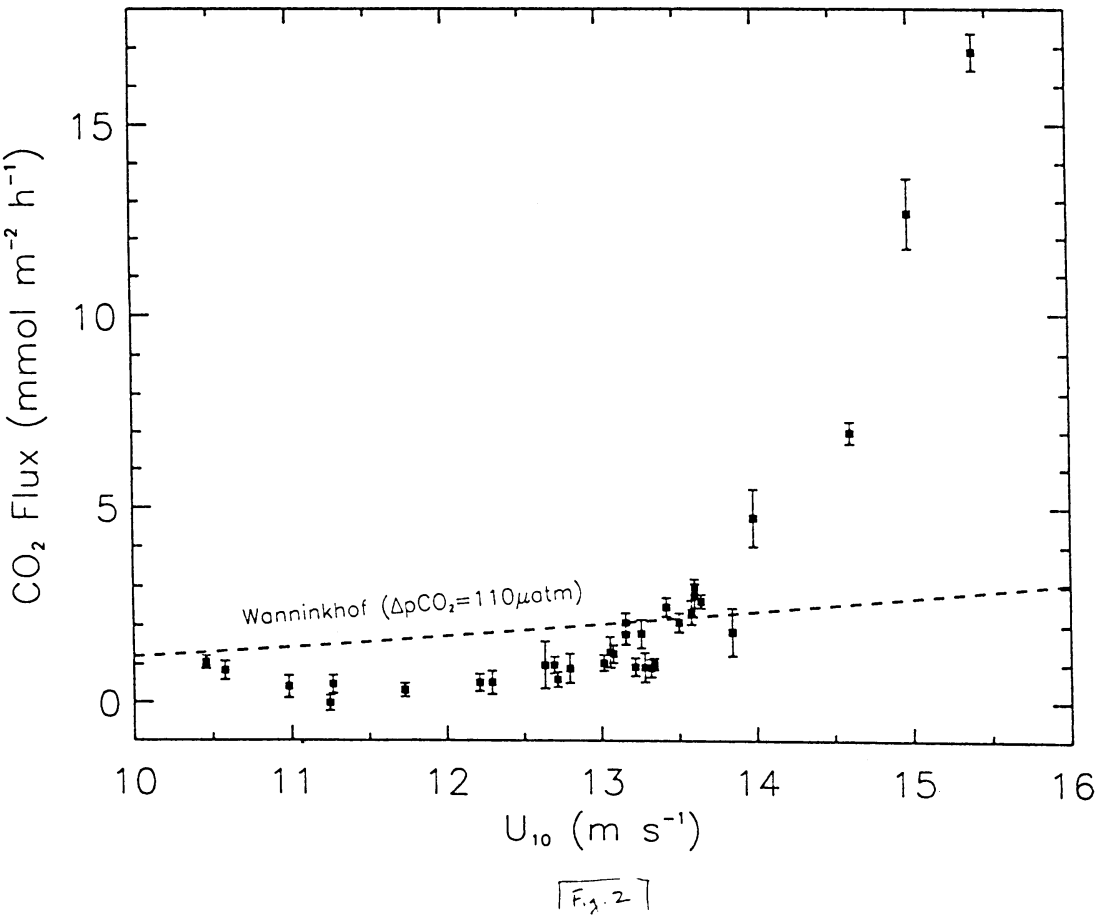

Fig. 2

MEASUREMENTS MADE DURING CHALLENGER 129: A CONTRIBUTION TO ASGAMAGE.

Phil Nightingale[1], Rob Upstill-Goddard[2], Gill Malin[3], David Ho[4], Peter Schlosser[4], Wendy Broadgate[3] and Tristan Sjöberg[1,3].
1) Plymouth Marine Laboratory, 2) University of Newcastle, 3) University of East Anglia, 4) Lamont Doherty Earth Observatory/Columbia University.

Measurements of transfer velocity using multiple tracers

The technique

Theoretically, it should be possible to be routinely measure gas transfer velocities at sea by deliberately and simultaneously releasing two tracers, one inert but volatile, the other inert but non-volatile. Concentration measurements for the volatile tracer would then be used to assess k_w, with corrections for dispersive dilution determined from measurement of the conservative tracer. However, at the time of the first dual tracer experiments to determine k_w in 1989 (Watson et al. 1991), an "acceptable" conservative tracer, i.e. one that was non-toxic, non-radioactive and detectable in trace quantities, had not been identified. Although conservative tracers such as rhodamine-B had been developed for tidal dispersion studies (e.g. Talbot and Talbot 1974), quoted limits of detection were impractical for our purposes (rhodamine-B is also designated a class 1 carcinogen).

An alternative "dual tracer technique" was therefore developed in which two volatile tracers with a large diffusivity contrast, in this case ^3He and SF_6, were released to seawater and their concentrations monitored with time as they escaped to the atmosphere at different rates. In this case it is the difference between the two transfer velocities (i.e. $k_{3He} - k_{SF6}$) that is actually determined from the equation shown below;

$$k_{3He} - k_{SF6} = [\ln (r_1/r_2) \times h] / t_2 - t_1$$

where r_i = $^3He/SF_6$ concentration at time t_i h = mean depth of the water column.

Clearly it is necessary to have a knowledge of how k_{SF6} and k_{3He} are related in order to obtain an estimate of k for either gas. Traditionally transfer velocities have been related to a power law dependence on the Schmidt number (Sc.) shown below;

$$k_{SF6}/k_{3He} = (Sc_{SF6} / Sc_{3He})^n$$

where Sc. = kinematic viscosity of seawater / molecular diffusivity of the gas
Modelling work (Ledwell, 1984), laboratory studies (Jahne et al., 1987) and lake experiments (Watson et al., 1991) all show that the value of n is expected to be -0.5 at wind speeds greater than 3.6 m s^{-1}. In calculating our results, we have assumed that this dependence is correct for wind speeds above 3.6 m s^{-1} and have corrected all values of k derived from the $^3He/SF_6$ tracer pair to Sc. 600. If bubbles/breaking waves are important in gas exchange at then our interpretation may be too simple, although the modelling work of Woolf (1995) has indicated that the Sc. dependency of He and SF_6 will remain close to -0.5 in the presence of bubbles.

Conservative Tracers

Ideally however, one of the tracers deployed should be non-volatile. Until now, a suitable marine tracer has not been identified. Microbial tracers have been used to investigate sewage dispersion in coastal waters (Pike et al. 1969) and to trace the movement of contaminating microbes in groundwater systems (Keswick et al. 1982). Bacterial spores were used in these studies as they persist in the water in their metabolically inactive state and have better

detection limits than commonly used chemical tracers. They are considered to be innocuous in use, incapable of growth in the environment and unlikely to interfere with the natural population. These characteristics suggested to us that bacterial spores could be an ideal conservative tracer for use in gas exchange studies in open seawater and we first used them in this context during Challenger Cruise 99A in 1993. Data obtained on that cruise facilitated the direct calculation of k_w for SF_6 and ^3He independently of each other and allowed us to determine the Schmidt number dependence of gas transfer, a significant advance on our previous capabilities. During the ASGAMAGE experiment our aim was to improve on our first results by using a higher initial spore concentration, minimising sample storage/handling and carrying out experiments to investigate whether spores are truly conservative with respect to light exposure and micro-zooplankton grazing.

Rhodamines WT and Sulpho-G are representative of a new generation of non-toxic tracer "dyes" which can be analysed at high dilution using improved techniques of analysis (Suijlen and Buyse 1994). Rhodamine WT is susceptible to mild photo-degradation and as such is not strictly conservative. However, by measuring its ratio to rhodamine sulpho-G which has a different photochemical loss rate, any non-conservatism can be corrected for. By deploying these compounds in conjunction with the other three tracers, we aimed to generate additional sets of estimates of k_w for SF_6 and ^3He. Thus, it would be possible for the first time to compare directly k_w determined with three different combinations of tracers.

Approach

Our preferred method of deployment is to dissolve the tracers in a known volume of water and then pump this water into the sea to create the tracer-enriched patch. Although this is time-consuming and the mass of tracer deployed is limited by the size of the tank, it avoids loss of gas to the atmosphere via direct bubbling of seawater and ensures that the ratio of the tracers is initially constant throughout the patch. The deployment was complicated by the use of the multiple tracers, as the rhodamines had to be prepared in a manner that was mutually exclusive for the preparation of the gaseous tracers.

Eight units of Biotrace ™, each containing $1 * 10^{14}$ spores of Bacillus globigii var. Niger (BG) per 2 litres of suspension, were added to one steel tank (~ 2500 dm^3). This was then filled with freshwater adjusted to a salinity of about 35 $^{o}/_{oo}$ by addition of sodium chloride. The tank was then sealed and saturated with SF_6 using the method described by Upstill-Goddard et al. (1991) over a period of about 24 hours. A known volume of ^3He was subsequently added to the headspace in the tank and this re-circulated through the water phase. Rhodamine WT (25 kg of 20% solution) was added to 50 kg of freshwater in a 1000 dm^3 steel tank, with continuous stirring via a submersible recirculation pump. 75 dm^3 of CH_3OH and 10 kg of rhodamine sulpho-G powder were then added and the tank filled to volume with ambient seawater and sealed. The release site was close to the Meetpost Noordwijk but specifically chosen to be away from any low saline water close to the coast. Unfortunately, this area of the North Sea is heavily used and allowance had to be made for possible movement of the patch either towards shipping lanes or the many gas production platforms in the vicinity.

Analytical

An automated on-line analytical system, capable of SF_6 analysis with a three minute repeat time, was used to obtain a near real-time representation of the patch while the ship was underway. The output from this system was interfaced to a GPS and the resultant information plotted for use as a first approximation to reduce the effects of the tidal oscillation. These continuously updated plots were used as a further aid in navigating the ship around the patch. Samples were collected for analysis from the centre of the patch. Concentrations of SF_6 and BG were determined on board the ship.

Samples were collected and stored for the later analysis of ^{3}He and rhodamines on return to land.

Preliminary Results

The use of the three non-volatile tracers appears to have been successful. Although there is evidence for BG contamination of the ship (or sampling bottles) that presumably occurred during the tracer release, this appears to have been limited to the first day of the experiment. After this time the ratio of BG to the rhodamines does not change significantly as would be expected if there was only a small loss of tracer from the water column. Indeed a line of least squares fit to the data suggests that the loss of rhodamine WT is about 5% in excellent agreement with the predicted photohemical loss rate of rhodamine WT.

The tracer data has been used to generate estimates of the transfer velocity from the following combinations of tracer pairs (He/SF_6, He/BG, He/Rhodamines, SF_6/BG and SF_6/rhodamines. The data are mutually supportive. The data are presently preliminary but lend support to the relationship of Liss and Merlivat.

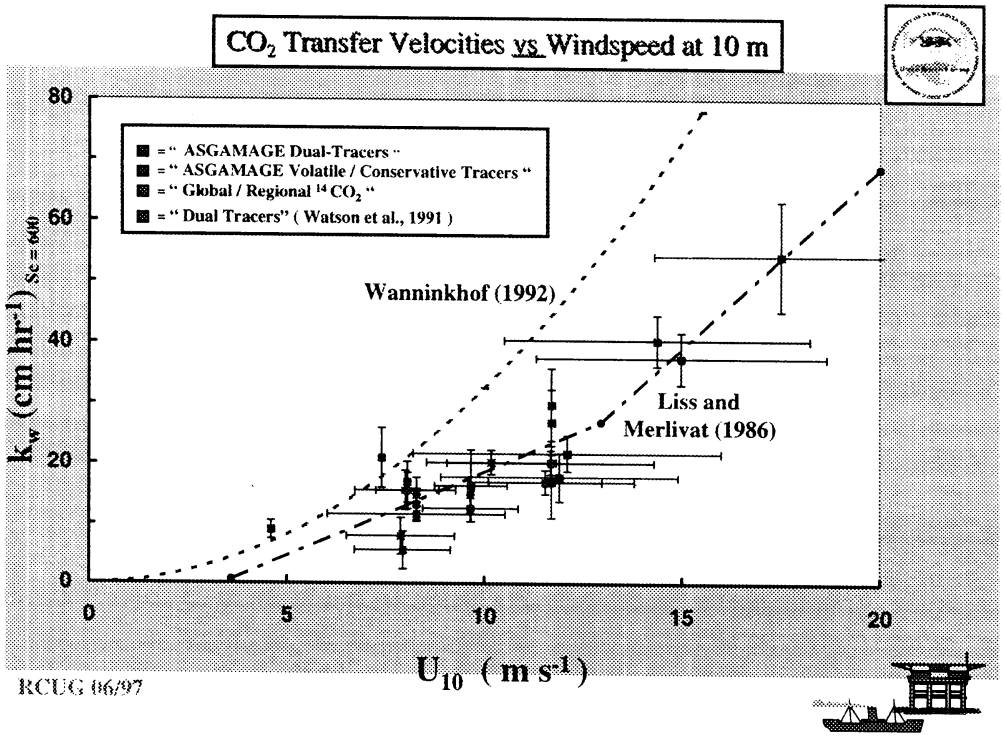

Future Work

It should be noted that the ship wind speeds were used to generate the above figure. It is likely that the platform derived winds to be used in the final data work up will be different as the ship was away from the patch for some period of time due to the very heavy weather that was encountered during the study. The SF_6 data is also awaiting a final calibration. The final data will also be used to investigate whether it is possible to reduce some of the scatter when k is plotted against wind only by including effects of bubbles, breaking waves and other parameters on gas exchange.

Other measurements made as part of ACSOE/ASGAMAGE

A whole host of other measurements were made during Challenger Cruise 129. These are summarised below and some brief results from studies on carbon monoxide and non-methane hydrocarbons presented later.

Underway (i.e. continuous) measurements

Water Based:	Depth, sea surface temp, salinity, optical attenuance, Total suspended matter, fluorescence, oxygen, ADCP
Meteorological:	Wind speed (cup anemometer), wind direction, air temperature (wet bulb plus dry bulb), barometric pressure, solar radiation, PAR, wind stress (Taylor and Yelland).

Underway (5 mins – 5 hrs)

Tracer:	SF_6
Chemical:	Dissolved oxygen, chlorophyll, non-methane hydrocarbons (NMHC) (air and water), carbon monoxide (CO), nutrients, suspended matter, methane (CH_4) (air and water).

Vertical Profiling

Physical:	Depth, salinity, temperature, transmission, PAR (upwelling and downwelling)
Tracers:	SF_6, ^3He, bacterial spores, rhodamines,
Chemical:	Fluorescence, oxygen, NMHC, CH_4, CO, nutrients,
Biological:	Chlorophyll, phytoplankton species,

A CD-ROM containing all of the above fully calibrated data should be available by May 98.

Non-Methane Hydrocarbons

Isoprene (2-methyl 1,3-butadiene) is reactive hydrocarbon with a lifetime of about 4 hours in the atmosphere where it affects the balance of oxidants, such as the hydroxyl radical and ozone. The major source of atmospheric isoprene is terrestrial plants. However, recent work has shown that isoprene is also input from surface seawater and that production is closely associated with biological activity (Broadgate *et al.*, 1997). During the ASGAMAGE experiment the concentration of isoprene in the surface water generally decreased as the wind speed increased. Variations within the patch are likely to be due to changes in the biology in the patch (linear regression of isoprene and chlorophyll, $r^2 = 0.45$) and salinity which indicates isoprene does not have a riverine source.

There is good agreement between the flux of isoprene to the atmosphere calculated by the Liss-Merlivat relationship and that calculated using the estimates from tracer technique. The exception is the period of very high winds towards the end of the experiment when the ship was sheltering off the coast of England.

The loss of isoprene to the atmosphere was calculated from the average flux over the period (using the wind speeds measured on the ship and the Liss-Merlivat relationship) and compared with the measured loss in the water column. An *in situ* net production rate of isoprene was calculated to be 1.7 pmol l^{-1} dy^{-1}. This is a very crude approximation but represents the first calculation of *in situ* production of isoprene in the ocean.

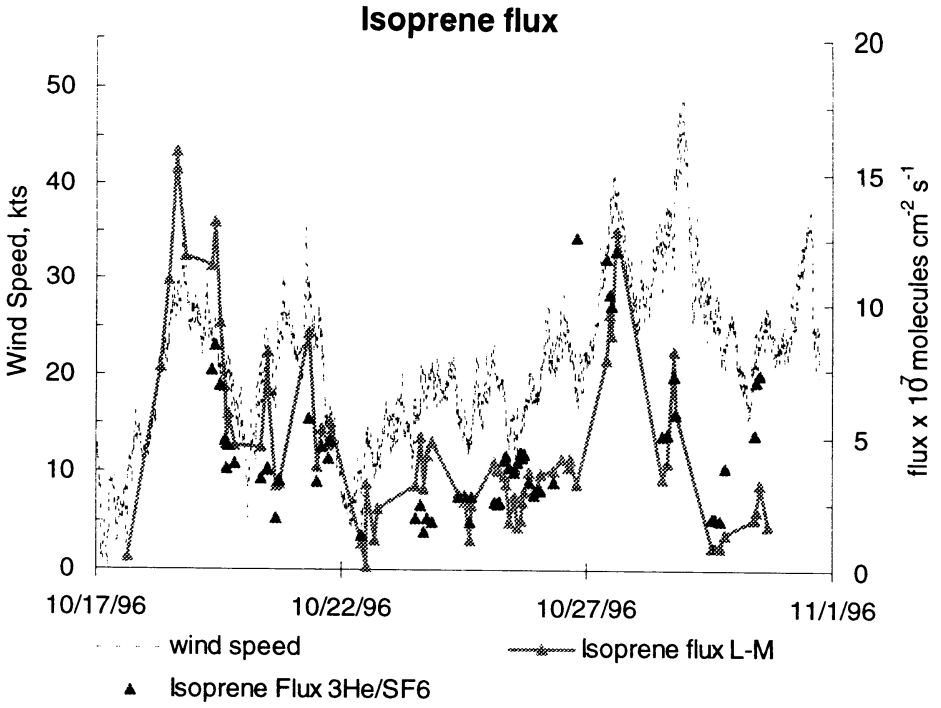

Carbon monoxide

CO was measured on a semi-continuous basis throughout the cruise while atmospheric levels were determined hourly. Advantage was made of the SF6 tracer patch to make a lagrangian study of surface water dissolved CO. Measurements were made over several 24 hr periods and seemed to follow a diurnal pattern, with the maximum concentrations between 2 - 4 hours after local noon followed by a gradual decline throughout the evening and night. Levels start to rise approximately 1 hour after sunrise. This trend was clearly evident on sunny days.

Atmospheric CO levels were more easily correlated to wind speed and direction rather than time of day. Easterly winds were associated with elevated levels, 400 - 600ppbv, whereas northerly winds were associated with lower concentrations, 30 - 80ppbv consistent with previous observations from the UK coast (Cardenas et al. 1997).

It is hypothesised that the dominant production mechanism for dissolved carbon monoxide is the photo-degradation of dissolved organic matter (DOC) by UV light. The main sink is loss to the atmosphere. The results from the ASCAMAGE cruise are in harmony with these theories.

Acknowledgements

This study was made possible by a large collaborative effort between staff from the Plymouth Marine Laboratory, the University of East Anglia, the University of Newcastle, Southampton Oceanography Centre, NIOZ, Lamont Doherty Earth Observatory, the British Oceanographic Database Centre and the UK Research Vessel Services. Aspects of this project received funding from the UK NERC Community Project, Atmospheric Chemistry in the Oceanic Environment (ACSOE).

References:

Broadgate, W. J., P.S. Liss and S.A. Penkett, "Seasonal emissions of isoprene and other reactive hydrocarbon gases from the ocean", *Geophys. Res. Letts.*, **24** (21), 2675 - 2678, 1997.

Cardenas L.M., J.F. Austin, R.A. Burgess, K.C. Clemintshaw, S. Dorling, S.A. Penkett and R.M. Harrison Correlations between CO, NOy, O3 and non methane hydrocarbons and their relationships with meteorology during winter 1993 on the North Norfolk coast, UK. Atmos. Environ. (in press).

Jahne B., K.O. Munnich, R. Bosinger, A. Dutzi, W. Huber and P. Libner (1987), On the parameters influencing air-water gas exchange, J. Geophys. Res. 92 1937-1949.

Keswick, B.H., Wang, D-S. & Gerba, C.P. (1982). The use of microorganisms as ground water tracers: a review. Groundwater 20, 142-149. (1982)

Ledwell J.J., (1984) The variation of the gas transfer velocity with molecular diffusivity, in; Gas transfer at water surfaces, eds. W. Brutsaert and G.H. Jirka, Riedel.

Pike, E.B., Bufton, A.W.J. and Gould, D.J. (1969). The use of Serratia indica and Bacillus subtilis var niger spores for tracing sewage dispersion in the sea. J. Appl. Bacteriol., 32, 206-216.

Talbot, J.W. and Talbot, G.A. (1974). Rapp. P.-V. Reun. Cons. Perm. Int. Explor. Mer 167, 93

Suijlen, J.M. and Buyse, J.J. (1994). Potentials of photolytic rhodamine WT as a large scale water tracer in a long-term experiment in the Loosdrecht lakes. Limnol. Oceanogr., 39, 1411-1423.

Upstill-Goddard, R. C., Watson, A. J., Wood, J. and Liddicoat, M. I. (1991). Sulphur hexafluoride and helium-3 as seawater tracers: deployment techniques and continuous underway analysis for sulphur hexafluoride. Anal. Chim. Acta, 249, 555-562.

Watson, A. J., Upstill-Goddard, R. C. and Liss, P. S. (1991). Air-sea exchange in rough and stormy seas measured by a dual tracer technique. Nature 349, 145-147.

Woolf D.K., (1997) Bubbles and their role in gas exchange, in The sea surface and global change, eds P.S. Liss and R.A. Duce Cambridge University Press.

Air-Sea Exchange Processes and their Remote Measurement by the Southampton University Department of Oceanography

Angus Graham and David Woolf
Southampton University Department of Oceanography, United Kingdom

1. Introduction

This report contains abstracts of two talks given as part of a meeting called in September 1997, to review progress of partners in ASGAMAGE, an international programme of experimental research into air-sea gas fluxes. Most of the experimental work took place in 1996 from a platform, Meetpost Noordwijk, 8 km off the Dutch coast, where the water is of mean depth 18 m. It was performed in two phases, May to June and October to November, and superseded a similar experiment, ASGASEX, conducted from the platform in September 1993. The objectives and methods employed by SUDO are fully described in the Report (February 1997), in which further details of the observed processes may also be found. The analysis is still under way, so results given here are necessarily preliminary.

A general discussion of pertinent near-surface processes is given by the second author in Section 2, an account of progress of the thermal imaging techniques then following. The acoustic work that has been conducted, in which surface waves and the bubbles generated as they break have been imaged, is described by the first author in Section 3.

2. Physical Processes of Air-Sea Exchange and Their Measurement

The study of air-sea gas transfer coefficients has been dominated by discussion of the relationship of transfer velocities with wind speed. Consideration of the processes by which air-sea gas exchange occur lead us to conclude that there is unlikely to be an absolutely systematic relationship between transfer velocity and wind speed, rather it is necessary to consider the strength of various processes in the prevailing environmental conditions.

The rate-limiting process in the air-sea exchange of poorly soluble gases is the efficiency of transfer of dissolved gases across the marine microlayer. This transfer may occur either by a combination of molecular and turbulent transport directly across the microlayer, or indirectly through the entrainment of air bubbles into the sea and the subsequent transfer of gases across the surface of the bubbles (Figure 2.1). The rate of direct transfer depends on the intensity of small and large eddies and their interaction with the sea surface. The rate of bubble-mediated transfer depends on the rate of generation of bubbles and their advection and dispersion. Considering the generation of turbulence and bubbles by the wind (Figure 2.2), we find a complicated relationship. The transfer of momentum to the sea by the wind depends significantly on factors such as atmospheric stability. More importantly, most of the momentum is initially transferred to the wave field, not current and shear. This is highly significant as the eventual transfer from the waves to the surface layer is greatly separated in space and time from the initial transfer from the wind. Furthermore, the specific results of momentum transfer to the surface layer (e.g., small eddies, large eddies and bubbles) might depend significantly on the stage of development of the wave field. As a result there are strong theoretical grounds for suspecting a dislocation between instantaneous wind and instantaneous gas transfer coefficients. The degree to which this contributes to scatter in transfer velocity - wind speed relationships is presently unknown but demands attention.

The thickness of the marine microlayer is only ~ 1mm, therefore there are few techniques for engaging this layer. We are developing the use of thermal imagery to study the influence of eddies and breaking waves on the sea surface. We report the analysis of a few hours of data from late on 3rd of June, from a longwave (8-12 micrometre) scanning thermal imager looking at 030°, when the wind was 6-8m/s from the Southwest (unfortunately wind and waves will have been distorted by the platform). The current was carrying water towards the imager at up to 0.5m/s.

A raw image is shown in Figure 2.3. This features an exceptionally large breaking wave (for the conditions) entering from the lower left. The crest appears exceptionally hot; this is largely a consequence of high emissivity; the water in the wake of the breaking wave is generally warmer than usual implying some surface disruption.

The raw images cover ~10x10m of sea surface but are geometrically distorted. Also the thermal noise of each pixel (=80mK) obscures all but the strongest features. We have processed the images as follows. The image is warped (with the greatest possible preservation of individual pixels) to a 128x128 pixel, 6.4m x 6.4m subsample at the centre of the original image. The images are detrended and then optimally (Weiner) filtered to remove high wavenumber noise while retaining low wave number information. The results imply the influence of large (1 metre scale) eddies on surface renewal, with streaks of warm and cold water aligned preferentially in approximately the wind direction. Calculation of the standard deviation of temperature in the Weiner filtered images is plotted against time in Figure 2.4. Dramatic increases and then falls in Weiner standard deviation are observed on time scales of 10 minutes. The standard deviation within the detrended images is plotted against the standard deviation of the Weiner filtered images in Figure 2.5 (diamonds); there appears to be a remarkably clear relationship with an extrapolated Ay-intercept@ almost exactly equal to the manufacturer*s stated noise level (80mK). In Figure 2.5, we have also plotted the predicted total standard deviation if this consisted solely of thermal noise and the Weiner standard deviation (squares), or thermal noise and twice the Weiner standard deviation (triangles). It is clear that there is in fact a considerable high frequency signal, which apparently is closely related in magnitude to the low frequency signal. Statistics of a series of 26 consecutive images (separated by 10 seconds each) at ~2200, around one of the peaks in standard deviation, are plotted in Figure 2.6. The earlier members of the series are characterised by a strong positive skewness, possibly associated with outbursts of warmer water from the bulk. As the standard deviation declines, the skewness drops to negative values (and later returns to near zero).

Thermal imagery is capable of detecting the influence of breaking waves and large eddies on the sea surface, and provides evidence of their importance to surface renewal and gas exchange. There appears to be a strong link between large eddies and smaller eddies.

3. Observing and Parameterising the Marine Bubble Layer

3.1 Introduction

Sonar observations of the sea surface made from the platform and the analysis techniques that have correspondingly been developed are here summarily described. The main purpose was to study the near-surface bubble layer, resulting from wind waves as they break, and responsible for most of the backscatter. Following breaking, large bubbles rapidly fragment, lose gas to

solution or return to the surface, but a near-surface cloud of microbubbles remains distinct within the layer for several minutes.

Bubbles figure prominently in air-sea exchanges. Much of the work done in breaking is against their buoyancy. They offer an extra, subsurface, interface for the exchange of heat and gas (the transfer rate of the latter greater at their hydrostatically-enhanced pressure). They also disrupt the microlayer when they surface, oscillate and burst. They ferry particulates scavenged in their passage through the water to the surface, and generate an aerosol in bursting. They are also important as tracers. They move in the orbits associated with surface and internal waves, and are drawn into zones of surface convergence and separation delineating fronts and Langmuir circulation, the downwelling helping sustain them by opposing their buoyancy.

3.2 Methodology

Pulsed upward-looking high-frequency sonars were used. Three were side-scans, narrow in the horizontal and broad in the vertical, inclined upward at about 20E, and with a range of 100 m or more. One of these was a 500 kHz sector-scanner, swept in the azimuth and deployed at a mean depth of 14 m from the south-west platform corner. The other two were a fixed perpendicular pair, frequencies 90 and 250 kHz, placed on the seabed 150 m north-west of the platform. Three narrow-beam near-vertical sonars, frequencies 86, 250 and 500 kHz, were also deployed 50 m from this, all profiling the same patch.

3.3 Observations

The sector-scanner's operation is sketched in Fig. 3.1. The side-scans all essentially reveal the depth-averaged backscatter along a narrow surface sector, bubble backscatter dominant over that directly from the surface at oblique incidence. Dispersion of the pulse by the bubbles is negligible, and clouds at far range are unshadowed by those nearer. As the distribution of clouds is systematically invariant over the beam, the effect of attenuation may be removed by dividing the signal at each range by the azimuthal mean, in the case of the sector-scanner, or by the temporal mean otherwise. Objective measurements may thus be made from the records without calibrating the signal.

Side-scan records, shown in Figs. 3.1-3.3, show wavefronts associated with the dominant surface waves, and continuous curvilinear features resulting from filamentary bubble bands aligned close to the wind, lying in the zones of surface convergence of Langmuir circulation. Waves are most clear in the sector-scanner sonographs, producing curved features as the phase and scan speeds are comparable. All the dominant wave characteristics, the phase velocity, wavelength and slope, may be measured from such images (wave height following from the surface as imaged along the shortest, vertical, path). The phase of the wavefronts is also under scrutiny, as is whether some of the short-wave features reflect the motion of bubbles generated when the wave spills as a long wave overtakes it (the motion thus that of particles). Bubble bands are, in contrast, best imaged by the fixed beams. Expiration of the band features reflects the dissolution, dispersal or return to the surface of the bubbles, or the passage of the band out of the span or breadth of the beam.

3.4 Parameterisation

Sonographs from the narrow-beam sonars, such as that of Fig. 3.4a, show clouds in detail as they pass through the beam or as waves break in it. The image extends to the first subsurface bin, the surface identified from each pulse by the steep signal gradient, and the vertical wave-motion thus removed prior to the temporal averaging (dispersion of sound by bubbles is not sufficient to produce an apparent displacement of the surface).

Key statistics of the bubble layer may be derived from these records. Its structure may be parameterised without calibrating the signal. Shapes are extracted, as shown in Fig. 3.4b, from points where the signal exceeds the medial value at each depth. Statistics then computed, as shown in Fig. 3.5, include the frequency and duration of shapes in the beam, measures of breaking frequency and decay of clouds in the limit of zero current, and the excursion of shapes about their surface positions, from which their tilt may be derived. Fig. 3.5a suggests that wholly subsurface clouds last less long in the beam.

The signal is calibrated by calculating the scattering cross-section pertaining volumetrically, M_v (acoustic wavelengths are much smaller than cloud scales). Losses due to bubble scattering and absorption are allowed for, but coherent scattering effects, dominant for air volume - void - fractions of order 10^{-5} or more, are ignored. To invert M_v, if known accurately, and obtain bubble densities, the size density must be partially prescribed, as no more than three frequencies were simultaneously active. A model form is, therefore, adopted (see Fig. 3.6a). The two most important variables, the peak radius and total number density, then remain to be determined.

An r.m.s. model error may be calculated for the period yielding Fig. 3.4, as there are more frequencies than unknowns: it is 50%. On average, the total bubble area is 0.17% of the sea surface, and the bubbles displace the surface upward by 43 nm. Other statistics are shown in Fig. 3.6. The ambient size spectrum falls less sharply than the instantaneous form prescribed, the result of the variability in the instantaneous peak. A decline in the mean bubble number density and void fraction is evident in the top two metres (this about four times the significant wave height).

Figure Captions

Figure 2.1 A schematic of direct and bubble-mediated transfer.

Figure 2.2 A schematic of the connections between wind and gas transfer.

Figure 2.3 A thermal image featuring a large breaking wave.

Figure 2.4 Time series of the standard deviation of temperature within a processed (detrended and Weiner filtered) image.

Figure 2.5 A plot of the standard deviation in detrended images against the standard deviation in detrended and Wiener filtered images. See text for details.

Figure 2.6 Plots of the statistics of 26 consecutive images. See text for details.

Figure 3.1 The sector-scanning sonar deployed, a) sonograph, commencing at 13:42:20 UTC on October 31st 1996, b) features identified, c) schematic of the sweep. The

sonograph shows the scattering over compass angle and slant range, the latter calculated from return time via the standard sound-speed polynomial. No correction for attenuation has been applied. The image is accrued over 89 s. The pulse repetition rate is 12 Hz. The broad radial bands of absent backscatter result from obstruction of sound by the platform legs and mounting pole.

The (10 m) wind is 13 m s^{-1} from 205°. The current is 7 cm s^{-1} heading to 225°, as measured by a current meter mounted at a mean depth of 10 m on the south-west platform leg. The significant wave height is 2.4 m (wave-period data from a wave rider deployed off the platform are not yet available).

Figure 3.2 Sonographs from the sector-scanner sweeping westward over a 20 s interval, commencing at a) 23:40:56 on October 29th, b) 18:02:58 on November 1st, c) 16:38:20 on November 3rd. The pulse repetition rate is 6 Hz for (a), specifications otherwise as for Fig. 3.1.

During (a), the (10 m) wind is 12 m s^{-1} from 304°. The (10 m) current is 31 cm s^{-1} heading to 224°. Significant wave height is 3.8 m. During (b), the (10 m) wind is 9 m s^{-1} from 245°. The (10 m) current is 54 cm s^{-1} heading to 39°. Significant wave height is 1.6 m. During (c), the (10 m) wind is 12 m s^{-1} from 228°. The (10 m) current is 4 cm s^{-1} heading to 7°. Significant wave height is 2.4 m.

Figure 3.3 Sonograph from a fixed 90 kHz side-scan, commencing at 22:12 on September 24th 1993 (obtained in ASGASEX). The range is that along the surface, the origin 15 m from the point above the sonar to exclude the zone in which specular reflection dominates over bubble backscatter. Surface range is calculated from slant range by taking the bubbles to lie wholly at the surface. Averages of eight pulses, the pulse repetition rate 4 Hz, have been used. Given the mean current vector, measured at the south-west platform leg, it follows that the features developing from A and B are of at least 50 m length. Shown below are the directions relative to the beam of the wind and current, and the gradient of a feature induced by a bubble band aligned with the wind and advected passively by the current (line length has no significance).

The (10 m) wind is 10.3 ± 0.6 m s^{-1} from $67 \pm 3°$ right of the beam (beam pointing to 280°). The (5 m) current is 38 ± 5 cm s^{-1} heading $133 \pm 5°$ right of the beam. The dominant wave period is 5.0 s, the significant height 1.6 m.

Figure 3.4 Sonograph from the 250 kHz narrow-beam sonar, commencing at 07:41 on October 18th 1996, a) unprocessed signal level, proportional to the r.m.s. backscatter pressure, b) reduction according to signal strength, commencing 20 mins into (a). The pulse repetition rate is 4 Hz, and averages of eight are calculated every 25 cm in depth. Shapes extracted in (b) are of scale five or more bins in both depth and time. Those of lighter shade lie entirely subsurface. The dark lines in the remainder delineate the excursions identified.

The (10 m) wind speed is 7.3 ± 0.1 m s^{-1}.The (10 m) current is 34 ± 3 cm s^{-1}, the wind heading $26 \pm 4°$ to its left. The dominant wave period is 3.1 s (computed from the record prior to surface detection and averaging), the significant height 0.6 m.

Figure 3.5 Statistics, in profile, of the shapes identified in Fig. 3.4b: mean shape a) duration, b) frequency, c) excursion. Crosses denote values for the full ensemble of shapes, asterisks those for subsurface shapes. Excursions are positive when shapes recede from the sonar.

Figure 3.6 Statistics of the period of Fig. 3.4, a) bubble size density at depth 0.6 m, and profiled moments of b) size density, c) total number density, d) void fraction. The histogram is cut off at a radius, a, of 120 μm. The dashed line shows the prescribed instantaneous size density, here assigned the same peak radius, a_p, and scaled and nondimensionalised by a factor $7.6H10^{-2}a_p$. This density falls off ultimately as a^{-5}, with a cubic dependence on smaller bubbles, the simplest smooth unimodal density that is both flat in the limit of very small or large bubbles and consistent with a finite (subunity) void fraction. Crosses denote means, asterisks the coefficient of variation, the former nondimensionalised in (b) and (c) by the mean at 0.4 m depth, 38 μm in the case of (b) and 87 dm^{-3} in the case of (c).

Schematic of Bubble Evolution

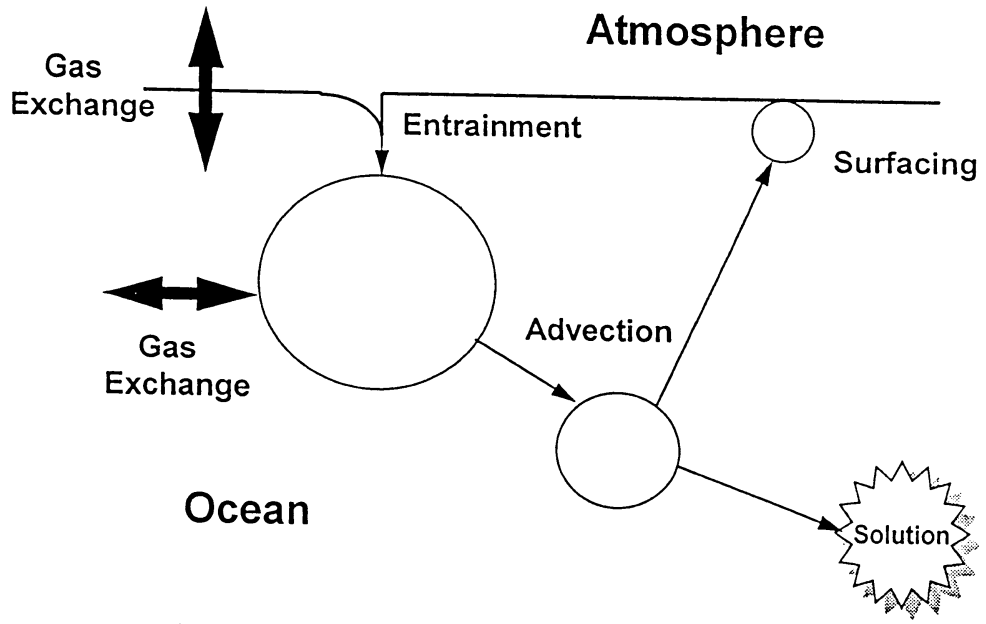

Fig 2.1

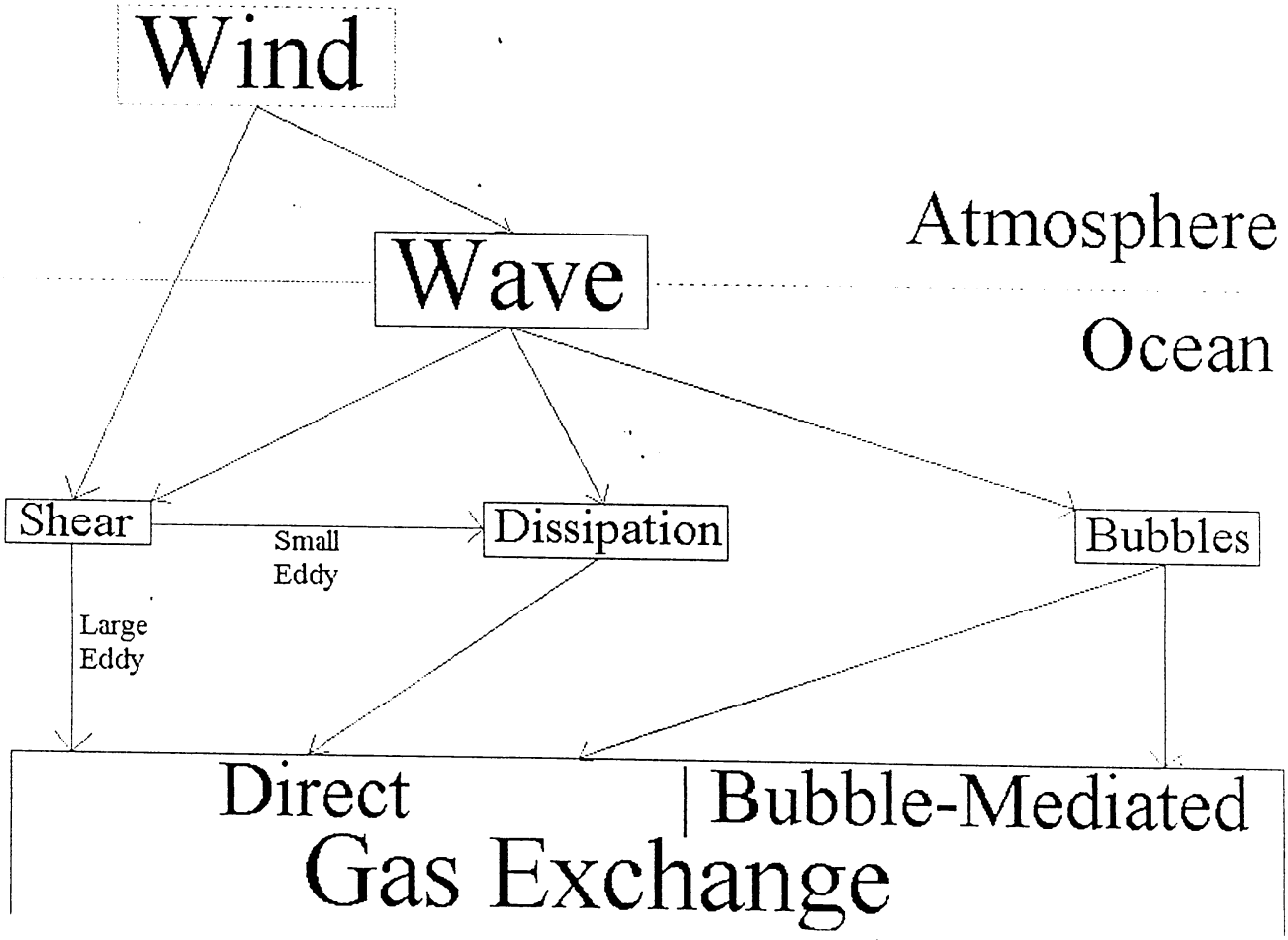

Fig 2.2

Breaking Wave

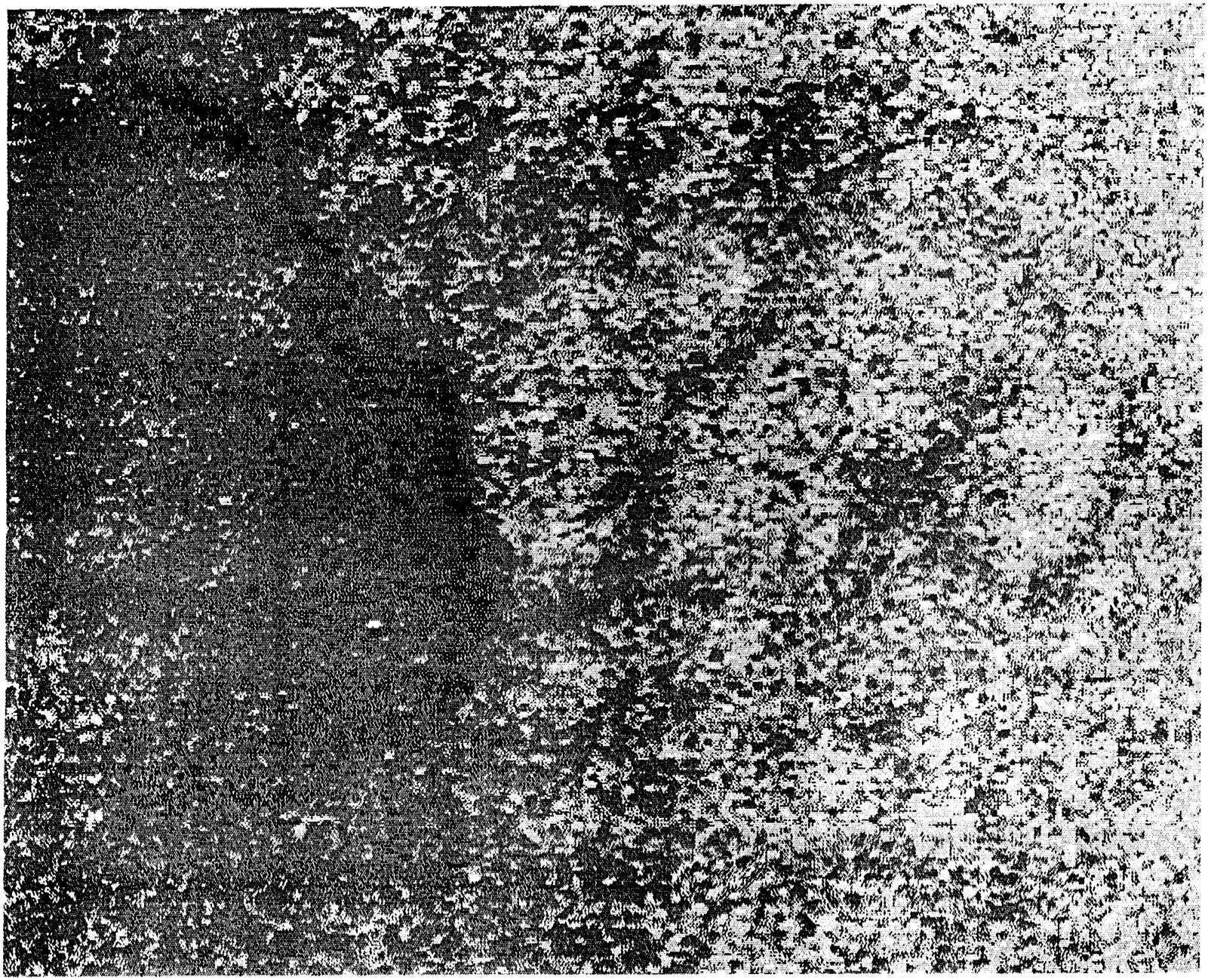

Fig 2.3

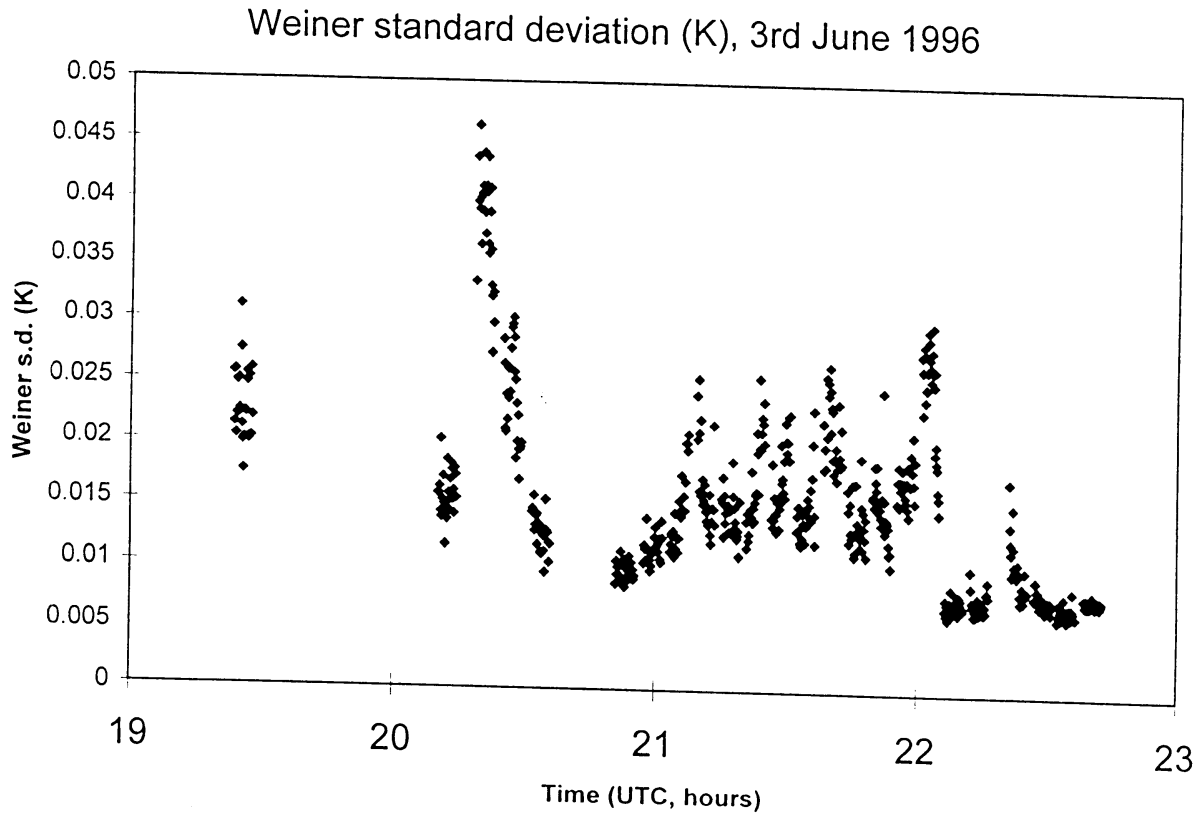
Weiner standard deviation (K), 3rd June 1996
Weiner s.d. (K)
0.05
0.045
0.04
0.035
0.03
0.025
0.02
0.015
0.01
0.005
0
19
20
21
22
23
Time (UTC, hours)

Fig 2.4

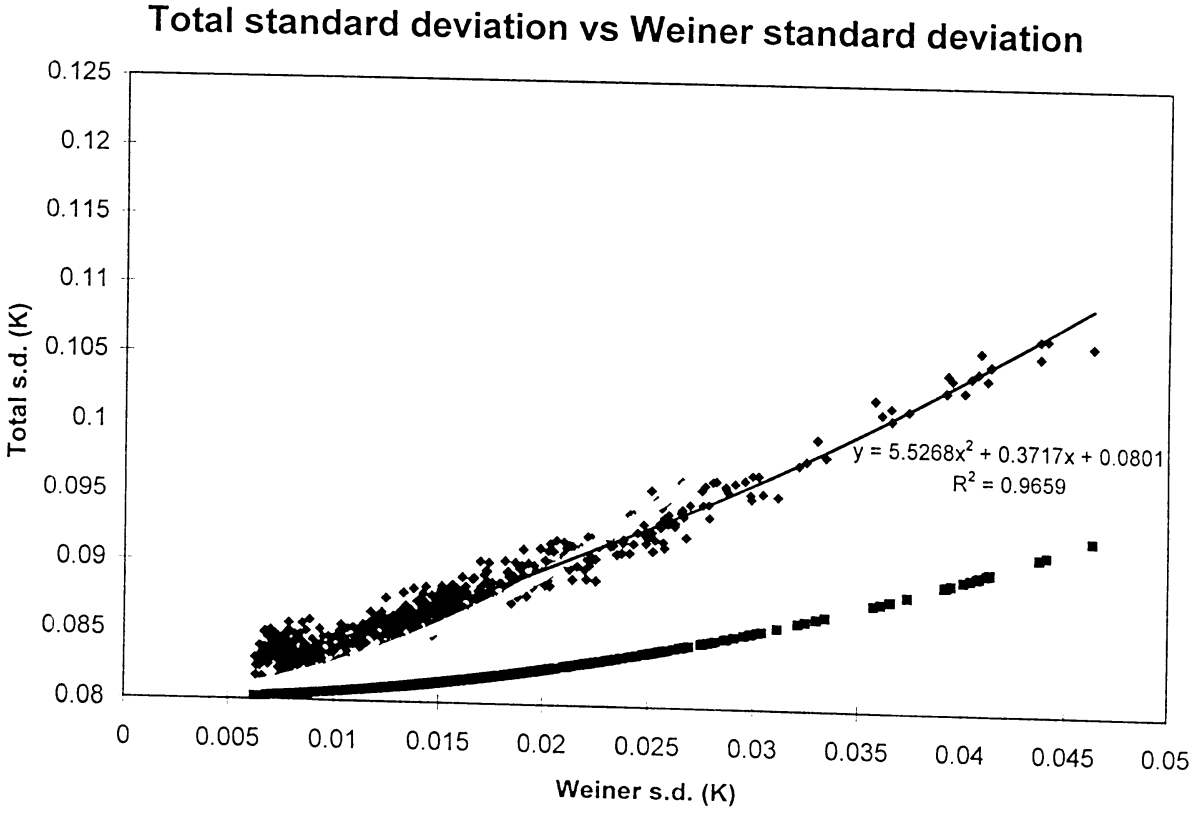
Total standard deviation vs Weiner standard deviation
Total s.d. (K)
0.125
0.12
0.115
0.11
0.105
0.1
0.095
0.09
0.085
0.08
y = 5.5268x² + 0.3717x + 0.0801
R² = 0.9659
0
0.005
0.01
0.015
0.02
0.025
0.03
0.035
0.04
0.045
0.05
Weiner s.d. (K)

Fig 2.5

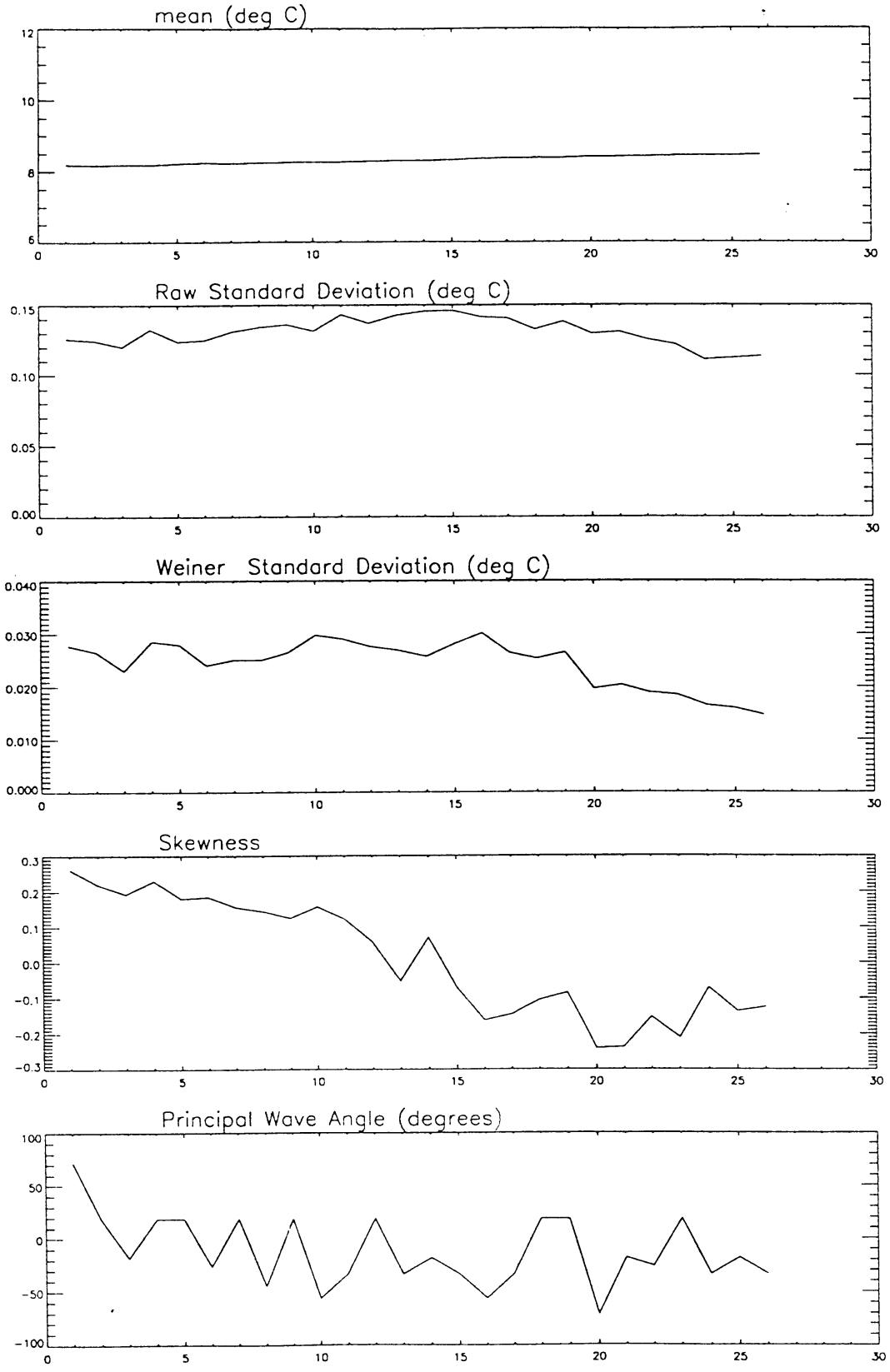
mean (deg C)
12
10
8
6
0
5
10
15
20
25
30
Raw Standard Deviation (deg C)
0.15
0.10
0.05
0.00
Weiner Standard Deviation (deg C)
0.040
0.030
0.020
0.010
0.000
Skewness
0.3
0.2
0.1
0.0
-0.1
-0.2
-0.3
Principal Wave Angle (degrees)
100
50
0
-50
-100

Fig 2-6

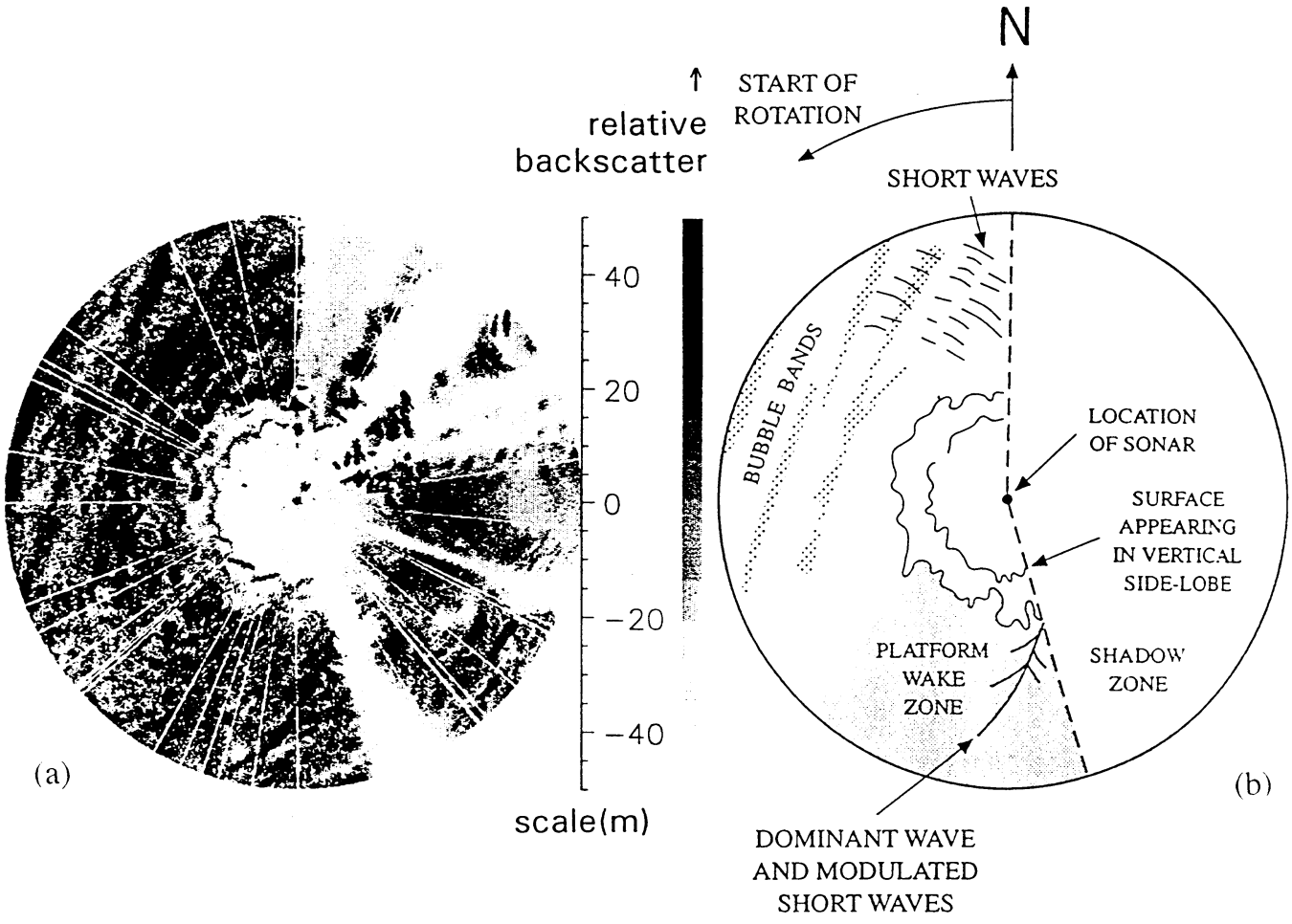
relative backscatter
40
20
0
−20
−40
scale(m)
(a)
N
START OF ROTATION
SHORT WAVES
BUBBLE BANDS
LOCATION OF SONAR
SURFACE APPEARING IN VERTICAL SIDE-LOBE
PLATFORM WAKE ZONE
SHADOW ZONE
(b)
DOMINANT WAVE AND MODULATED SHORT WAVES

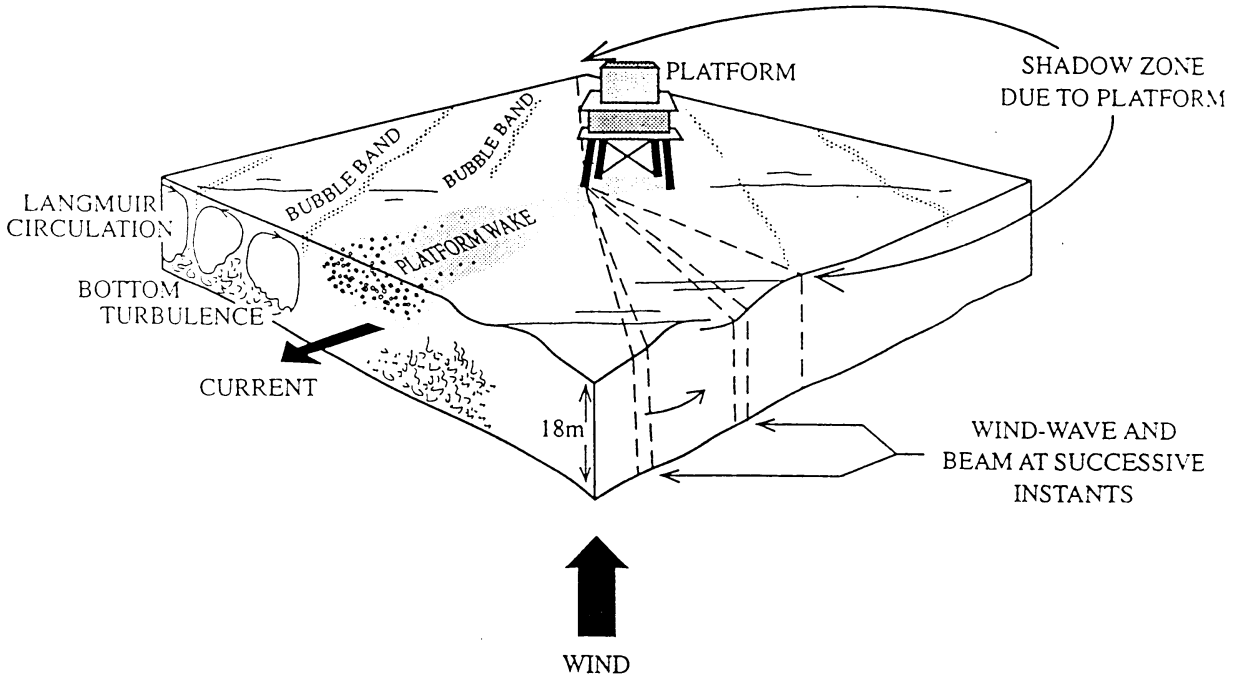
PLATFORM
SHADOW ZONE DUE TO PLATFORM
BUBBLE BAND
BUBBLE BAND
LANGMUIR CIRCULATION
PLATFORM WAKE
BOTTOM TURBULENCE
CURRENT
18m
WIND-WAVE AND BEAM AT SUCCESSIVE INSTANTS
WIND

(c)

Fig 3.1

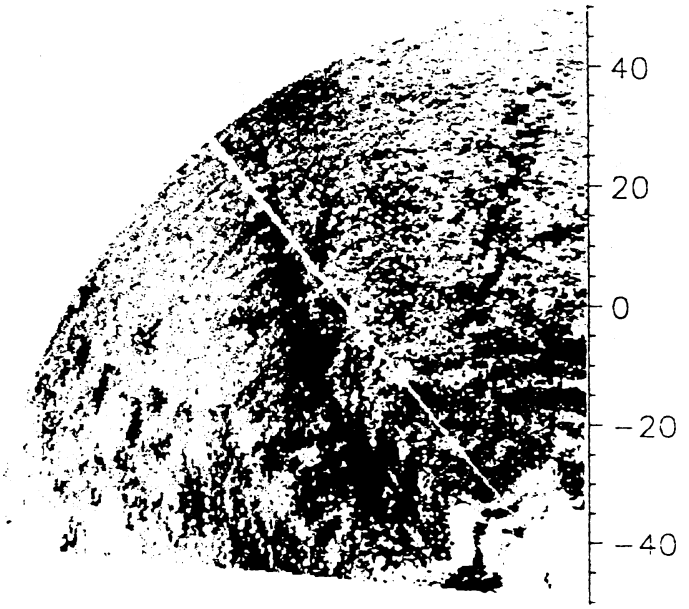

(a)

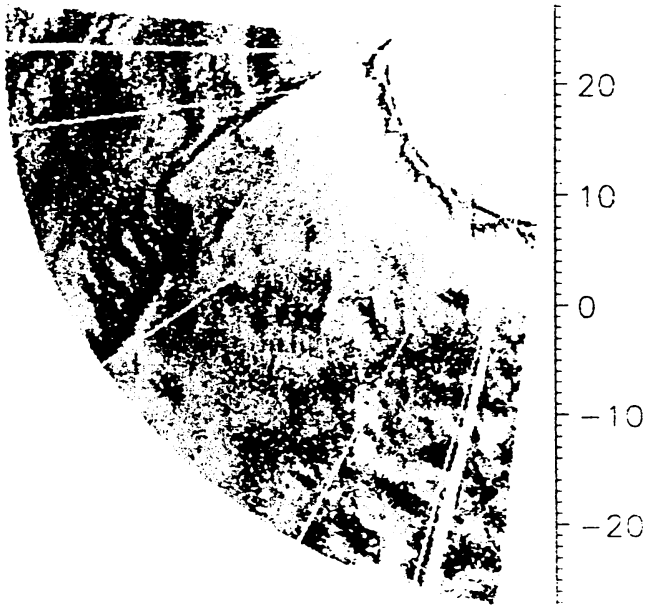

(b)

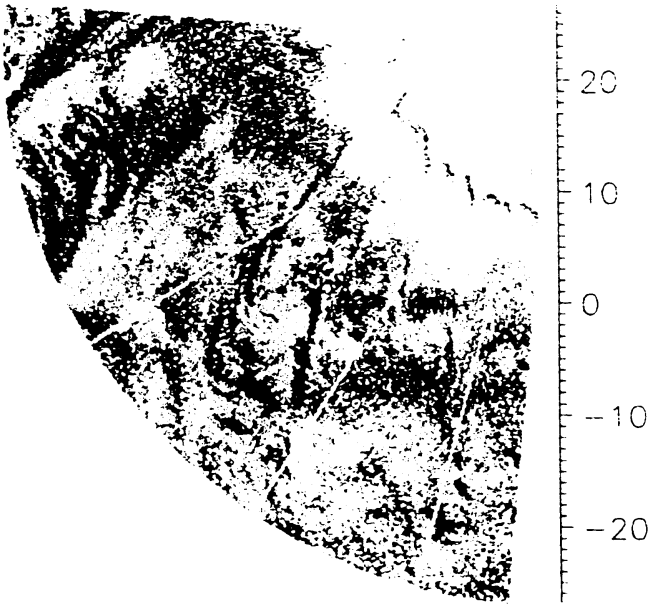

(c)

Fig 3.2

distance(m)
0
20
40
60
80
100
120
140
time(mins)
0
5
10
15
20
25
30
A
B
wind
current

Fig 3.3

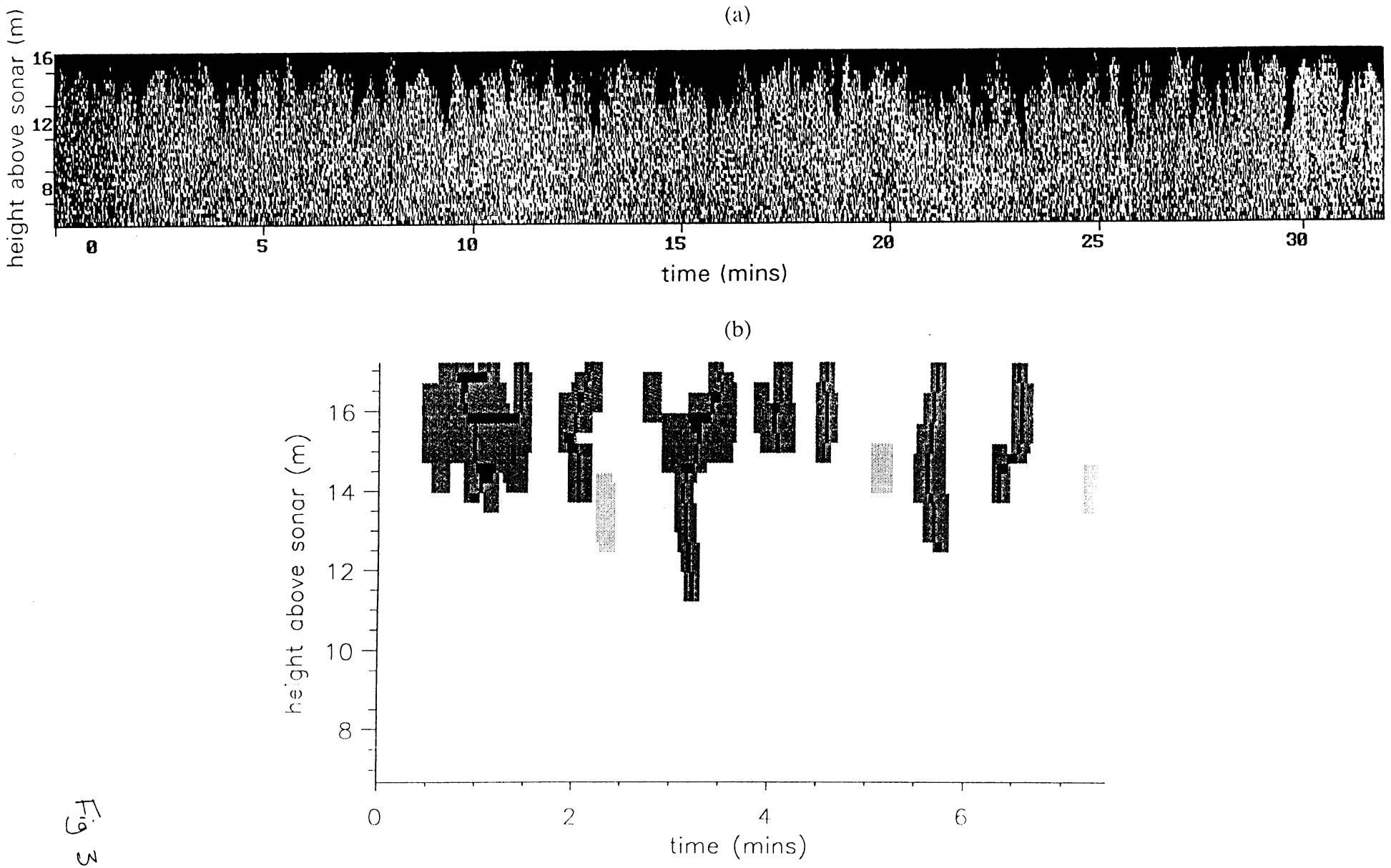
(a)
height above sonar (m)
16
12
8
0
5
10
15
20
25
30
time (mins)
(b)
height above sonar (m)
16
14
12
10
8
0
2
4
6
time (mins)

Fig 3.4

(a)

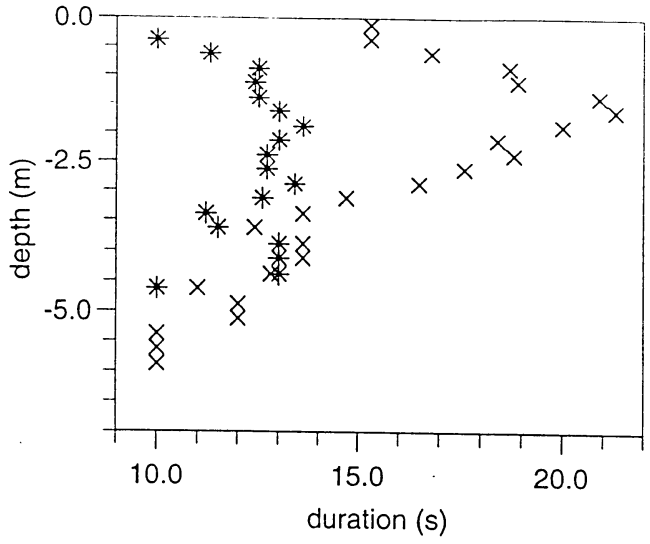
0.0
-2.5
-5.0
depth (m)
10.0
15.0
20.0
duration (s)

(b)

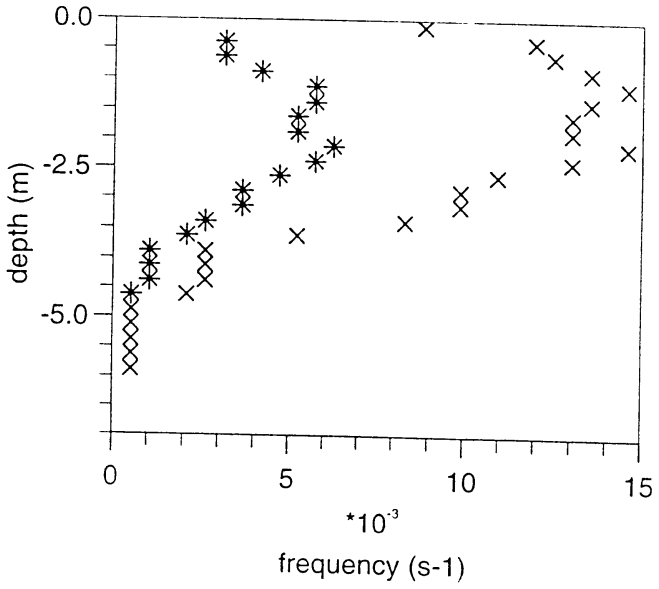
0.0
-2.5
-5.0
depth (m)
0
5
10
15
*10-3
frequency (s-1)

(c)

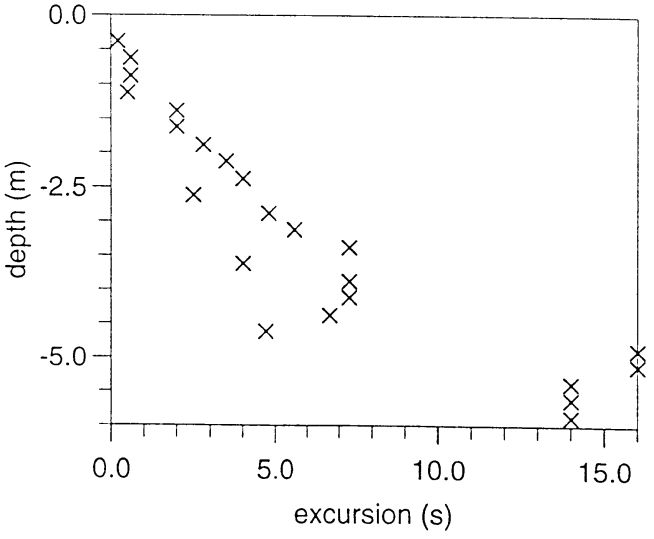
0.0
-2.5
-5.0
depth (m)
0.0
5.0
10.0
15.0
excursion (s)

Fg 3.5

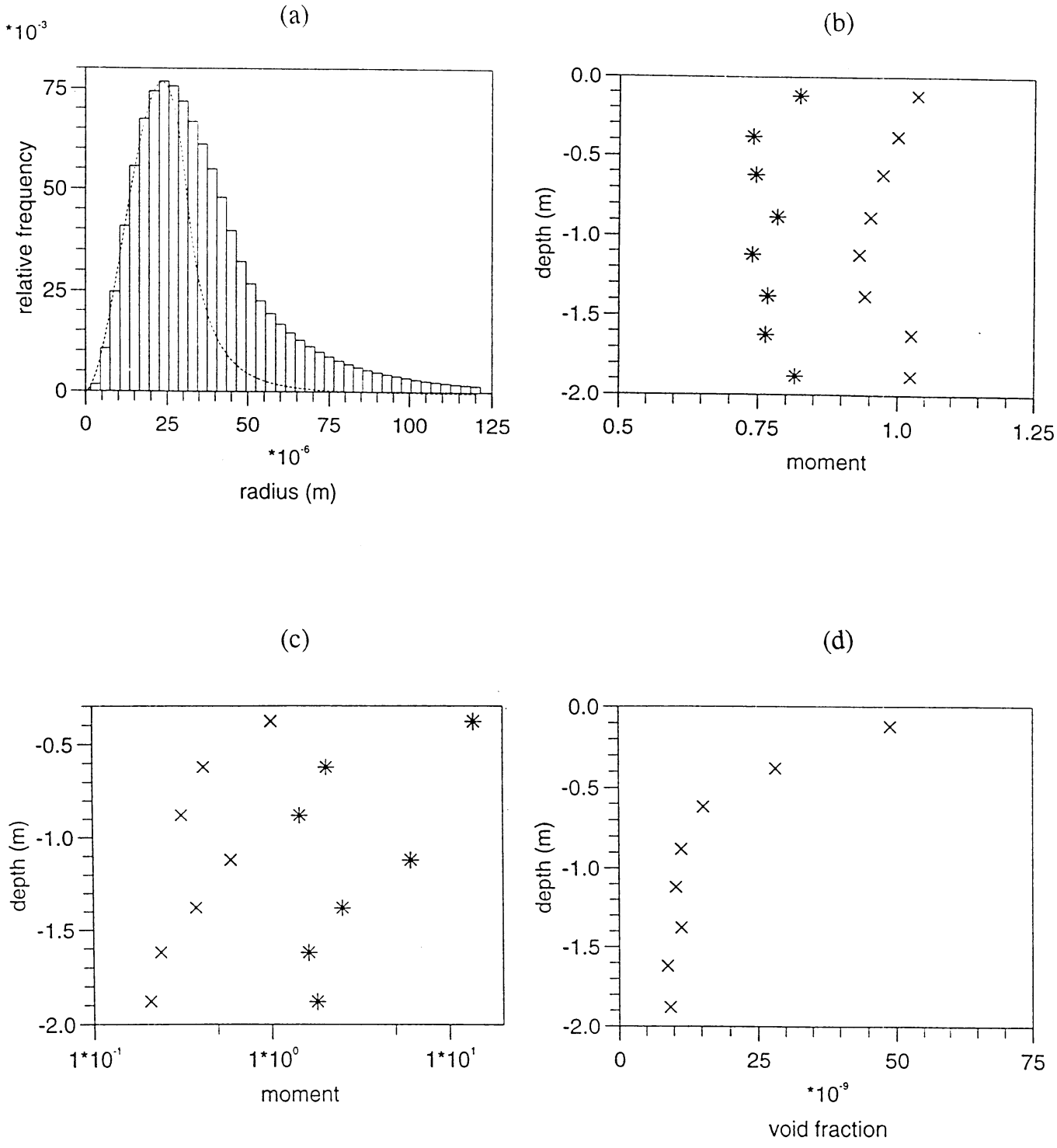
(a)
*10-3
relative frequency
75
50
25
0
0
25
50
75
100
125
*10-6
radius (m)
(b)
depth (m)
0.0
-0.5
-1.0
-1.5
-2.0
0.5
0.75
1.0
1.25
moment
(c)
depth (m)
-0.5
-1.0
-1.5
-2.0
1*10-1
1*10^0
1*10^1
moment
(d)
depth (m)
0.0
-0.5
-1.0
-1.5
-2.0
0
25
50
75
*10-9
void fraction

Fig 3.6

CO_2 Gas Concentrations, Gradients and Air-Sea Exchange during ASGAMAGE (TNO-FEL results)

Gerard J. Kunz[1)], Gerrit de Leeuw[1)], Søren E. Larsen[2)], Finn Aa. Hansen[2)] and Søren W. Lund[2)]

[1)] TNO Physics and Electronics Laboratory, P.O. Box 96 864, 2509 JG The Hague, The Netherlands

[2)] RISØ National Laboratory, Department of Meteorology and Wind Energy, DK-4000 Roskilde, Denmark

ABSTRACT

The ASGAMAGE experiments were co-ordinated by the Royal Netherlands Meteorological Institute (KNMI) from the Meetpost Noordwijk (MPN), a research platform in the North Sea 9 km off the Dutch coast. TNO-FEL and RISØ measured among others, the atmospheric concentration of CO_2 at four different levels (between 2 and 30 m above the mean sea level) and the CO_2 concentration (fugacity) in the sea using an equilibrator system. The key instrument, a LI-COR 6262 differential, non-dispersive, infrared gas analyser, was calibrated using four standard gases (accuracy 0.1 ppm). The performance of the instrument was verified every 2 hours using three reference gases. Air-sea fluxes of CO_2 were calculated using the gas transfer rate and the solubility proposed by Wanninkhof, 1992. In addition, fluxes of CO_2 were estimated from atmospheric gradients, the wind speed and the bulk transfer coefficient for carbon dioxide, C_c which was assumed similar to C_q the bulk transfer coefficient for water vapour. The dry air atmospheric mole fraction of CO_2 during on shore wind (maritime) conditions in October/November 1996 was 359±2.5 ppm. Air from rural and industrial areas could clearly be distinguished from maritime air during periods of off shore winds. In those periods, the CO_2 mole fraction increased by about 25 ppm and 80 ppm respectively. Values of p_{CO2} in the water varied slowly from about 41.0 Pa to about 48.5 Pa with tidal variations of about 1.5 Pa (but generally not in phase with the tide). CO_2 fluxes (upward) calculated from the air-sea concentration difference, ranged from about 0.00 mg/(m^2.s) to about 0.06 mg/(m^2.s) ± 10 %. As a result of the strong wind speed dependence of the transfer velocity k, the fluxes are strongly correlated with the wind speed. The CO_2 fluxes calculated from the gas concentration gradients in the atmosphere varied in the range from 0.00 mg/(m^2.s) to 0.02 mg/(m^2.s) ± 50 %. The fluxes obtained with the two methods do not correlate. This may be explained from the time required to equilibrate the partial-pressure difference between the sea and the overlaying air or from the low SNR in the data from the air-gradient method.

1. INTRODUCTION

Based on a LI-COR 6262 differential, non-dispersive, infrared (NDIR) H_2O/CO_2 gas analyser, TNO-FEL constructed a programmable and automatic sensor package to measure the CO_2 gas concentrations in the air and in the water. Air from levels of about 2, 6, 12 and 30 m above the mean sea level was continuously aspirated in and transported towards the laboratory at a rate of several litres per minute using polythene impermeable tubing (Stuifmeel, PE 100 8x6 Series 1500) and membrane pumps (Cole-Parmer, Air Cadet 07530-50/65). Fractions of these air flows were sampled at a rate of about 150 ml/min for some minutes. The remaining part of the flow and the analysed air samples were vented in the laboratory at atmospheric pressure. The partial-pressure of CO_2 in the water (fugacity) was measured using an equilibrator system constructed at TNO-FEL in combination with the gas sensor. The

equilibrator is based on the principles of Dr. Watson. A shower head in the head-space sprayed sea water at a rate of about 2 litres per minute in the head-space. The air in the equilibrator was continuously circulated in the closed equilibration volume at a rate of about 4 litres per minute. The equilibrator was kept at sea-water temperature by flushing the jacked around the system with sea water at a rate of about 10 l/min. Air samples taken from the equilibrator system were returned in the closed circuit after analysis. The reaction time of the equilibrator system (*1/e* folding time) was about 1.2 minutes. Water from 2, 3.5, 5, 7, 11 and 15 m depth could be sampled using submersible water pumps. Air and water measurements were carried out in a cycle of about 20 minutes. Prior to measurement the appropriate valves were set and the system was flushed during several minutes for stabilisation. The performance of the system was verified every 2 hours by analysing three reference gases (N_2, nominal about 248 ppm CO_2 and nominal about 440 ppm CO_2). The influence of water vapour on the measured CO_2 concentration was suppressed by operating the LI-COR in the default water vapour pressure broadening and dilution correcting mode (FCT 76-2; BndBrd, Dil→Ref:). Afterwards the CO_2 data can be corrected using air temperature and the relative humidity. Automatic atmospheric pressure correction was carried out by routing the output of the optional internal barometer (Terminal 15) through the pressure channel (FCT 43).

The conditions during the experiment were mainly slightly unstable with air-to-sea temperature differences (ASTD) down to about -6 °C (except during days 307 to 309 when the ASTD was about +1.5 °C) with wind speeds U_{10} from about 4 m/s to about 23 m/s. The water temperature decreased slowly from about 15.5 °C to about 13.5 °C whereas the CO_2 partial-pressure in the water, pCO_{2w} varied from about 41.0 Pa to about 48.5 Pa. This large increase is about a factor of 2 larger than can expected on the basis of the increase in the solubility due to the temperature decrease of the water. Dry air, atmospheric mole fractions of CO_2 of about 360 ppm were measured during maritime wind conditions whereas values up to 405 ppm were measured during periods of off-shore winds. As a result, an upwards directed CO_2 flux is expected (out of the water) during the experiment.

2. CALIBRATION

The LI-COR 6262 gas sensor was absolutely calibrated using four highly accurate (0.1 ppm) gas mixtures in the range from 246 ppm to 361 ppm CO_2, made available by NIOZ (Netherlands Institute for Sea Research) during the experiment. Three calibration runs were carried out. A second order polynomial was fit through the data points which left a least squares systematic uncertainty of 0.43 ppm (over the range of the test gases). Using this transfer function the actual values of our reference gases appeared to be respectively 247.88±0.43 ppm and 454.15±0.43 ppm. It is be noted that the calibration uncertainty of 0.43 ppm is much larger than the uncertainty obtained from the automatic reference measurements carried out every 2 hours. These gave least squares variations of about 0.06 ppm (24 samples of 5 seconds each) for all three reference gases.

During continuous operation over two periods of twelve days, the drift of the gas sensor was about 1.2 ppm. The stability of the sensor is visualised in a pair of scatter plots Figure 1a+b showing the relationships between the responses of the reference gases.

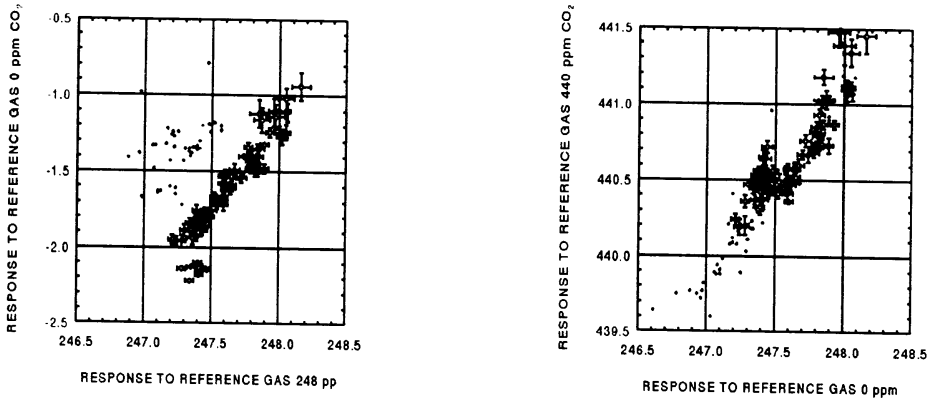

Figure 1: (a) Relationship between the response of the LI-COR 6262 to the reference gases N_2 and 248 ppm CO_2 (top figure) and (b) between the reference gases 248 ppm and 440 ppm CO_2 (bottom figure). One standard deviation error bars indicate the variability of the reference measurements. During the first few days the calibration procedure was not fully optimised and the data (dots) are not representative for this analysis.

The results of the reference measurements are an indication for the reliability of the performance of the instruments during the experiment. The uncertainty (spread of the data points) is in the range between about 0.1 ppm and 0.2 ppm. Note that this deviation is also better than the uncertainty in the calibration of 0.43 ppm CO_2. We therefore estimate that after the offset and gain correction (parameters obtained every 2 hours) the accuracy of our data is about 0.5 ppm.

3. RESULTS

The dry air atmospheric CO_2 concentrations are indications for the actual background values. A time series and a polar diagram of these data are shown in Figures 2a+b.

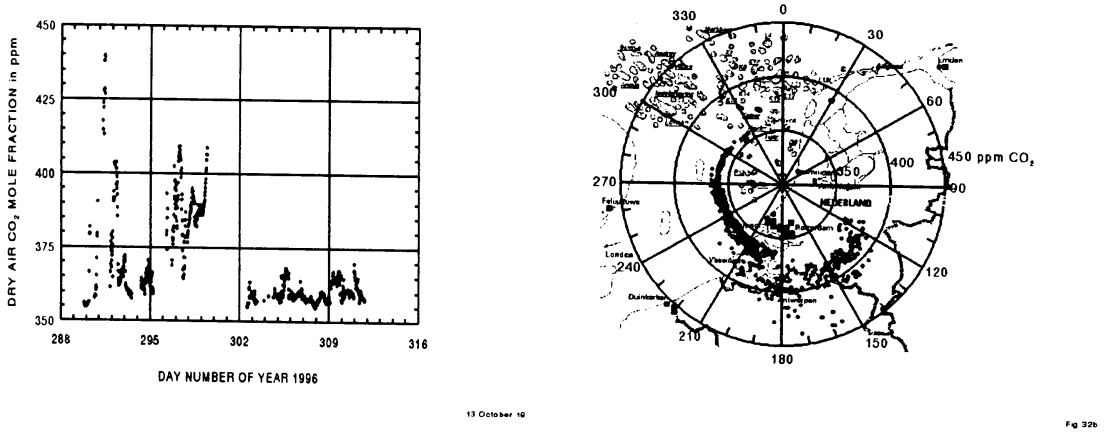

Figure 2a: Time series of the measured atmospheric dry air CO_2 mole fraction. The variability -one standard deviation- in the data is about 0.5 ppm (error bars not shown).

Figure 2b: Polar diagram of the dry-air CO_2 mole fraction. MPN is in the center of the figure.

The polar diagram of the dry air CO_2 mole fraction clearly indicates the direction of the Europort industrial regions with refineries (Rotterdam/Pernis) at about 40 km from MPN, urban areas and areas with intensive flower and vegetable growing (greenhouses). Other chemical plants from Flushing (The Netherlands) and Antwerp (Belgium) are at about 100 km. The large variability in the data is probably caused by the difference in production rate and dispersion during the experiment. The somewhat lower values around 135 degrees are from the rural central part of The Netherlands. These values are similar to the values measured in Cabauw in 1993 (Kunz and De Leeuw, 1994) in a similar period of the year. The relatively stable values in the dry air CO_2 mole fractions between about 230 and 340 degrees are measured during conditions of maritime air. From these values, it is estimated that at this location and in this period of 1996, the background mole fraction is 359±2.5 ppm. The influence of other (production) platforms in the North Sea, e.g., P12 and Rijn at about 40 km, direction about 270 degrees) is not clearly visible in these data.

The partial-pressure of CO_2 in the sea water (fugacity), pCO_{2w}, around MPN during the experiment is presented in Figure 3. The tide is also indicated in this figure.

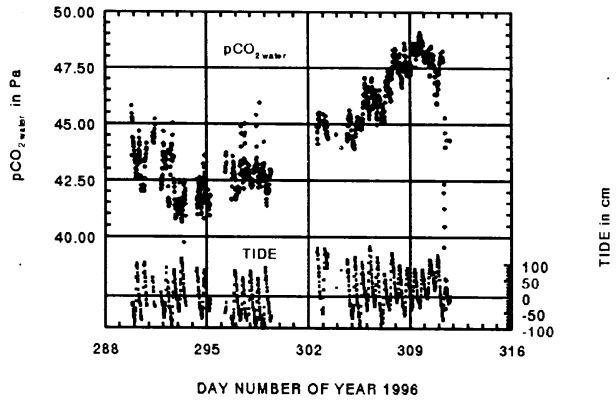

Figure 3: Partial-pressure of CO_2 gas in sea water near MPN during October/ November 1996. The tide is plotted in the bottom of the figure. The variability in the data -one standard deviation- is about 0.1 Pa (error bars not shown).

The results in Figure 3 show considerable variations of pCO_{2w}: the short term variations of about 1.2 Pa and a long term variations of about 7.5 Pa which are both much larger than the 0.05 Pa uncertainty in the measured data. (The steep decrease in the data at the end of the experiment is caused by a defect in the water supply system.) A closer look at these data indicates that the short term effects have a reasonable relationship with the tide which brings fresh water from the river Rhine and may be also from the river Scheldt resulting in a variability of the salinity and the gas contents. However, there is no clear correlation between the phases of the tide and of the variations of pCO_{2w}. A similar but much stronger effect was also noticed during the ASGASEX experiment carried out at the same location in September 1993 (Oost *et al.* 1995a,b, Smith and Anderson, 1995 and Wilde and Duyzer 1995). The slow term variation of pCO_{2w} is much larger and appears to be strongly correlated with the water temperature as shown in Figure 4.

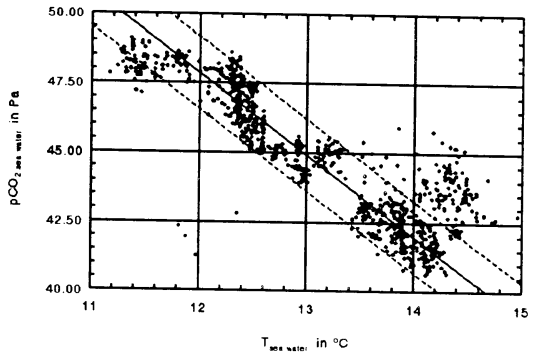

Figure 4: Scatter diagram of pCO_{2w} in the sea-water and the (equilibrator) sea-water temperature. The variability in the data -one standard deviation- is about 0.1 Pa (error bars not shown)..

The width of the spread in the data (about ±1.2 Pa) is caused by tidal effects and the large effect seems to be highly correlated with the water temperature. We have checked the effect of temperature and salinity on the solubility of CO_2 gas in sea water (see, e.g., Wanninkhof, 1992). This analysis shows that for a fixed value of the salinity of 35 per mille, the solubility varies by about 3 % per degree Celsius and that at 10 °C, the solubility varies by about 2 % per 5 per mille salinity. An other cause of the temperature effect might be the redistribution of the carbon system (CO_2 gas, bicarbonate and carbonate) in the water. It is known that the dissociation constants are a function of temperature. Correlation with wind speed is only marginal

Mass fluxes of CO_2 gas, F_m were derived from the air-sea partial pressure differences (ΔpCO_2) using Wanninkhof's wind speed and temperature dependent gas transfer velocity (k), and the temperature dependent solubility (K_0) of carbon dioxide gas in sea-water assuming a salinity (S) of 35 per mille. The slight correction for the carbon dioxide fugacity is not carried out. The time series of ΔpCO_2 and of the 10 m wind speed (U_{10}) are presented in Figure 5a. The fluxes, calculated using $F_m = k\, K_0\, m_{CO2}\, \rho\, \Delta pCO_2$, with m_{CO2} the molecular mass of CO_2 and ρ the density of sea water, are presented in Figure 5b.

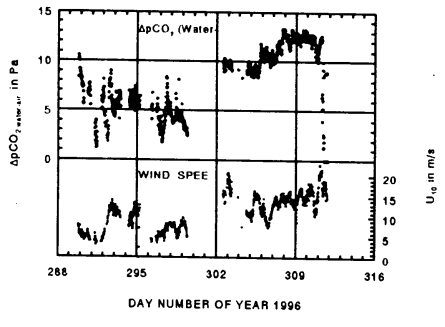

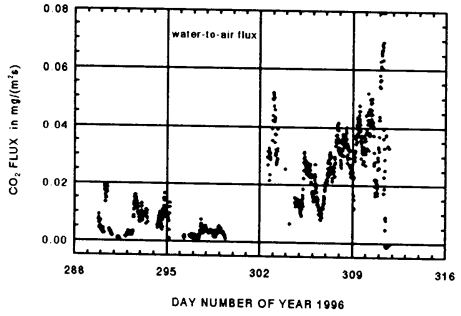

Figure 5a: Time series of ΔpCO_2. The variability in the data -one standard deviation- is about 0.15 Pa (error bars not shown). The line in the bottom shows the MPN values of U_{10}.

Figure 5b: Time series of the mass fluxes of CO_2 calculated from the air-water partial-pressure difference ΔpCO_2. The variability in the data -one standard deviation- is about 0.005 mg/(m^{2}s) (error bars not shown).

The measured values are comparable with those during ASGAMAGE in 1993 (Kunz *et al.*, 1995a,b and Oost *et al.*, 1995a,b).

Although the wind speed data in Figure 5a indicate a positive correlation with the pCO_{2w} (thus also with ΔpCO_2), this correlation is too weak (variations of about ±2.5 Pa) to explain the observed extra decrease of pCO_{2w} with temperature as shown in Figure 4. The calculated mean CO_2 flux increases slowly during the experiment to about 0.05 mg/(m^2 s) with some peaks to higher values. Of course, the CO_2 flux increases with wind speed because both the gas transfer rate and the concentration difference increases with wind speed. Largest values occur at the lowest temperatures. This is shown in Figure 6.

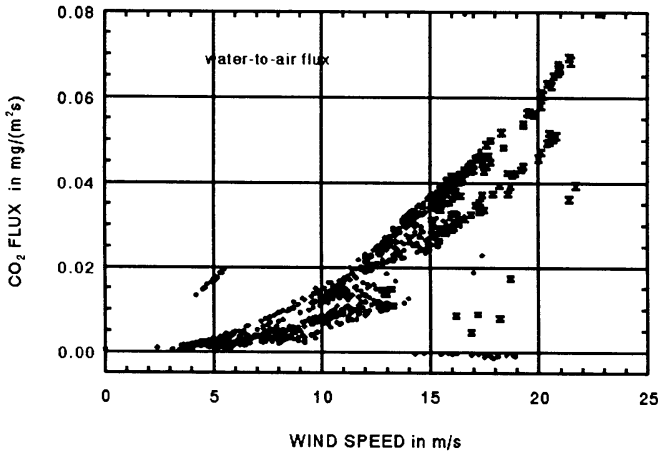

Figure 6: CO_2 mass flux F_m versus wind speed. F_m calculated from the air-sea partial-pressure difference. The variability in the data -one standard deviation- is about 0.005 mg/(m^2 s) (error bars not shown).

During ASGAMAGE, the atmospheric mole fraction of CO_2 was measured at several heights (about 2, 6, 12 and 30 m above the mean sea-level). To minimise undesired effects of water vapour the LI-COR was operated in the water vapour correcting mode. During data processing the results can be corrected for this effect using relative humidity and air temperature. (The profiles of temperature and relative humidity can be calculated from the MPN meteo data using a surface layer bulk model, e.g., from Smith, 1988 or Kunz, 1996, to calculate the actual micro-meteorological conditions and to estimate the atmospheric the stability.) Differences in the mole fraction between 2 m and 30 m were in the range from about -1 ppm up to about 2 ppm with intermediate values at the levels in between. The differences between 30 m and 6 m level are presented in Figure 7a. (The values between 30 m and 2 m are up to a factor of two larger but could not always be measured because the air inlet was sometimes overwashed by waves during periods of strong winds.) The air-sea temperature difference, which may serve as an indication for the atmospheric stability, is also shown in this figure. The CO_2 fluxes are calculated from the differences in the mole fraction, the wind speed differences and the bulk transfer coefficient C_c for carbon dioxide gas (see e.g. Kunz *et al.*, 1995b). Similarity theory suggests that C_c will be similar to the bulk transfer coefficients for water vapour and/or for heat which are both about 10^{-3}.

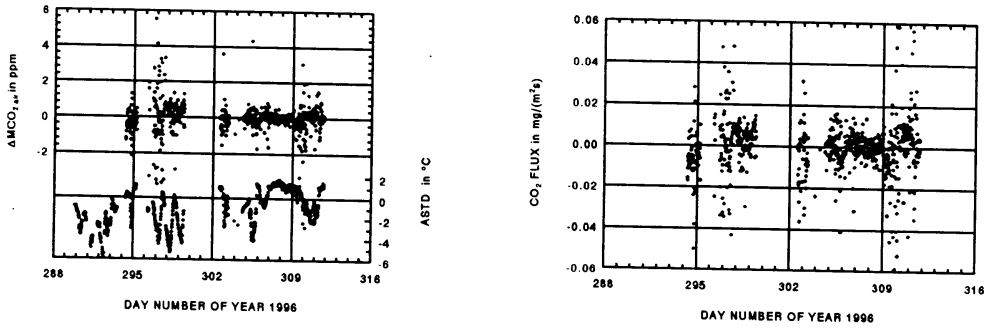

Figure 7a: Differences in mole fractions of atmospheric of CO_2 between 6 m and 30 m above the mean sea level. The variability in the data -one standard deviation- is about 1 ppm (error bars not shown).

Figure 7b: Fluxes of CO_2 calculated from the mole fraction differences, the wind speed and the gas. The variability in the data -one standard deviation- is about 0.025 mg/(m^2s) (error bars not shown).

The relatively large excursions of the mole fraction differences in the first two weeks are caused by the relatively high concentrations of antropogenic CO2 in the atmosphere during off shore winds. Under these conditions, the fetch over the water towards MPN is too short to obtain an equilibrium condition of the gases in the water and in the atmosphere. The time constant to obtain equilibrium is estimated as follows:

The mass of CO_2, M_{CO2} required to increase the partial pressure in volume V with ΔpCO_2^i is given by:

$$(1) \qquad M_{CO2} = \Delta pCO_2^i \frac{m_{CO2} V}{RT},$$

where m_{CO2} is the molecular weight of CO_2, R the gas constant and T is the temperature of volume V.

The CO_2 mass evasion (or invasion) between the air-water interface is a function of the mass flux (F_m,) the area considered (A) and the duration (t). Thus:

$$(2) \qquad M_{CO2} = F_m A t.$$

The mass flux is, in turn, a function of the gas transfer velocity (k), the solubility (K_0,) the density of sea water (ρ) and the air-sea CO_2 partial-pressure difference (ΔpCO_2^d). If the slight correction for fugaciy is skipped, the mass flux is expressed as:

$$(3) \qquad F_m = m_{CO2} k \rho K_0 \Delta pCO_2^d.$$

Considering that CO_2 is heavily buffered in sea-water (it is assumed in this case that the sea acts as a constant source or sink), an estimation of the time required to change the CO_2 partial pressure in volume V by ΔpCO_2^i is:

(4) $$t = \frac{\Delta pCO_2^i}{\Delta pCO_2^d} \frac{V}{A} \frac{1}{k \rho K_0 RT}.$$

This equation is further simplified by assuming that the increase in the CO_2 partial pressure in the volume is equal to the air-sea partial pressure difference and that the ratio *V/A* is equal to the height (*H*) of the volume considered. These assumptions lead to an estimate for the equilibration time (*t*) given by:

(5) $$t = \frac{H}{k \rho K_0 RT}.$$

Substitution of the following quantities:

R = 8.3145 J/(mol.K);
T = 288 K;
H = 1 m;
k = $5.6 \cdot 10^{-5}$ m/s (at U_{10} =8 m/s);
ρ = 10^3 kg/m^3;
K_0 = $0.04 \cdot 10^{-5}$ mol/(kg.Pa).

results in a time constant of about $2 \cdot 10^4$ seconds (or about 5.5 hours) for each meter thickness of the layer considered. In practice this time will be larger because the partial pressure difference decreases with time.

Because of the relatively long equilibration time across the air-water interface, only the data from the two-week period at the end of ASGAMAGE-B is useful for comparison of the air-gradient method and the air-sea differential method. In that period the wind was mainly from westerly directions. Figure 7a shows that a slightly negative CO_2 gradient in the atmosphere was present during days 307 to 309 which seems to be correlated with the positive ASTD, displayed in the bottom of that figure.

Comparison of the fluxes calculated from the air-sea concentration differences (Figure 5b) and from the gradients of the gas in the air (Figure 7b) shows that in the first period the fluxes are comparable and that in the period of maritime conditions the fluxes differ by about a factor 2. A detailed analysis does not show a correlation between these fluxes. The reason for this might be twofold. First, the accuracy of the air-gradient fluxes is lower due to the small CO_2 gradients in the atmosphere and second, from the point of view of the equilibration time, it is not expected that the gas concentrations in the atmosphere follow instantaneously the air-sea gas concentration difference near MPN. Nevertheless, we are convinced about the quality and the uniqueness of these data. To the best of our knowledge, this is the first time that CO_2 concentrations have been measured at several heights above the sea surface over such a long period. The similarity between the values of the fluxes calculated from the gradients and the partial pressure differences is encouraging.

4. CONCLUSION

Concentrations of CO_2 in sea water, and in the air at several heights above the water were measured from a platform in the North Sea, about 9 km off the Dutch coast in October/November 1996. The measurements were carried out during the ASGAMAGE experiments co-ordinated by the KNMI (Royal Netherlands Meteorological Institute). Using accurate calibration gases in combination with a (slight) offset and gain correction derived from reference measurements, we estimate that the absolute accuracy of the measurements is

about 0.5 ppm (on 300 to 400 ppm). Major part of this accuracy is caused by uncertainties in the absolute calibration measurements. If it is necessary to increase this accuracy, it is recommended to also perform these calibration measurements automatically and more often. The (dry air) atmospheric background mole fraction of CO_2 during periods of on shore wind was 359±2.5 ppm. In periods of off shore wind, a discrimination could be made between Rotterdam industrial areas (at about 40 km) and rural areas (about 10 km). The partial gas pressure of CO_2 in the sea water was measured using a closed circuit equilibrator system at atmospheric pressure (basis Dr. Watson) in combination with the gas sensor. Although the equilibrator operated satisfactorily during the whole experiment it required continuous attention either to prevent drowning of the head-space due to foam formation or to prevent clogging of the shower head in periods of high sediment concentration, e.g., during periods of strong wind. It is recommended to further optimise the equilibrator on these points. The partial-pressure of CO_2 in the water varied from about 41.0 Pa to about 48.5 Pa. Short term variations of about 1.5 Pa are related to the tide but with random phase whereas the long term variation can partly be explained from the decreasing water temperature. The correlation with wind speed was very low. Air-sea fluxes of CO_2, calculated from the air-sea CO_2 partial-pressure differences, the wind speed dependent transfer rate (k) and the temperature and salinity dependent solubility (K_0,) ranged from about 0.00 mg/(m^{2}s) to about 0.06 mg/(m^{2}s) ± 10 %. These values are comparable with the results obtained during ASGASEX in 1993. Air samples simultaneously taken from four levels between about 2 m and 30 m above the mean sea level, revealed the possible existence of a CO_2 gradient in the atmosphere. These values varied from about -0.05 ppm/m (during stable conditions) to about 0.1 ppm/m. Assuming similarity between the bulk transfer coefficient for water vapour and carbon dioxide, fluxes of CO_2 were also calculated from this gradient. Although the results obtained in this way and the results from the air-sea partial-pressure difference are of the same order of magnitude (but with different uncertainties) no correlation was found between these two data sets. This might be caused by the very long time required to equilibrate the gas concentrations between the air and the sea.

ACKNOWLEDGEMENT

We are grateful to Wiebe Oost from KNMI for the excellent organisation of the ASGAMAGE experiments and to Cor Jacobs from the Royal Netherlands Meteorological Institute (KNMI) for the stimulating discussions on fluxes derived from the air-gradient data. The technical assistance during the experiment from Ed Worrel (KNMI), and the ongoing discussions with Wim Kohsiek and Hendrik Wallbrink (KNMI) to continuously improve the quality of the measurements were very valuable to us. We also like to acknowledge Dr. Spyridon Rapsomanikis from the Max-Planck-Institut für Chemie (MPIC, Mainz, Ge) for his advises on the use of the LI-COR 6262 in the very beginning of the ASGAMAGE experiment in May 1996. Furthermore we are indebted to the Netherlands Institute for Sea Research (NIOZ) for their willingness to provide us with their calibration gases. We also like to thank Guus Goossens and Jaap van der Horn with their crew for their hospitality and pleasant atmosphere at MPN. And last but not least, we gratefully acknowledge Leo Cohen and Marcel Moerman (TNO-FEL) for their excellent and invaluable co-operation during the developing phase of the CO_2 sensor package, the installation of the equipment at MPN and their motivating assistance throughout the whole experiment. Without these people we would not be able to continuously run the sensor package during four periods of two weeks and to attain the high quality of the obtained data.

The work described in this paper was carried out under EC contract DG XII, MAS3-CT95-0044 and supported by the Dutch Ministry of Defence, grant A95KM785.

REFERENCES

Kunz, G.J. and G. de Leeuw, 'TNO-FEL contributions to a pilot experiment for CO_2 flux measurement comparisons', TNO-FEL report FEL-94-A163, 28 pp., TNO Physics and Electronics Laboratory, The Hague, The Netherlands, 1994.

Kunz, G.J., 'A bulk model to predict optical turbulence in the marine surface layer', TNO-FEL report FEL-96-A053, 54 pp., TNO Physics and Electronics Laboratory, The Hague, The Netherlands, 1996.

Kunz, G.J., G. de Leeuw, S.E. Larsen and F.Aa. Hansen, 'Eddy correlation fluxes of momentum, heat, water vapor and CO_2 during ASGASEX', in Report of the ASGASEX '94 workshop, ed. by W.A. Oost, KNMI, De Bilt, October 3-5, 1994, pp. 12-16, 1995a.

Kunz, G.J., G. de Leeuw, S.E. Larsen and F.Aa. Hansen, 'Over-water eddy correlation measurements of fluxes of momentum, heat, water vapor and CO_2', in Selected Papers from the Third International Symposium on Air-Water Gas Transfer, eds. B. Jähne and E.C. Monahan, Heidelberg, July 24-27, pp. 685-701, 1995b.

Oost, W.A., 'Trying to make is make sense', in Report of the ASGASEX '94 workshop, ed. by W.A. Oost, KNMI, De Bilt, October 3-5, 1994, pp. 42-47, 1995a.

Oost, W.A., W. Kohsiek, G. de Leeuw, G.J. Kunz, S.D. Smith, R. Anderson and O. Hertzman, 'On the discrepancies between CO_2 flux measurements methods', in Selected Papers from the Third International Symposium on Air-Water Gas Transfer, eds. B. Jähne and E.C. Monahan, Heidelberg, July 24-27, pp. 723-733, 1995b.

Smith, S.D., 'Coefficients for sea surface wind stress, heat flux, and wind profiles as a function of wind speed and temperature', J. Geophys. Res. 93, 15, pp. 15,467-15,472, 1988.

Smith, S.D. and R.J. Anderson, 'BIO analysis of CO2 and H2O flux in ASGASEX '93', in Report of the ASGASEX '94 workshop, ed. by W.A. Oost, KNMI, De Bilt, October 3-5, 1994, pp. 17-21, 1995.

Wanninkhof, R., 'Relationship between wind speed and gas exchange over the ocean', J. of Geophys. Res., 97, C5, pp. 7373-7382, 1992.

Wilde de, H.P.J. and J. Duyzer, 'Methane emissions off the Dutch coast: air-sea concentration differences versus atmospheric gradients', in Selected Papers from the Third International Symposium on Air-Water Gas Transfer, eds. B. Jähne and E.C. Monahan, Heidelberg, July 24-27, pp. 763-773, 1995.

Measurements of total gas saturation, bubble population and acoustic scattering during ASGAMAGE by University College Galway

Peter Bowyer
Department of Oceanography, University College Galway, Galway, Ireland

1. Total gas measurements

Measurements were made during Asgamage A and B from two UCG total gas meters (1).Results are shown in figs 1 and 2:

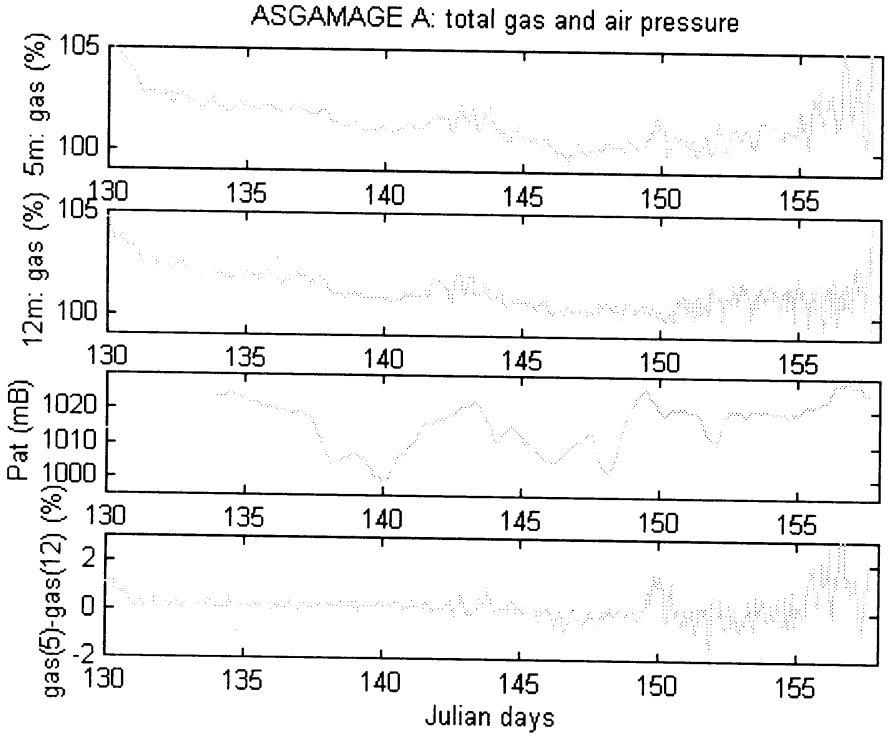

Figure 1

Figure 1 shows a steadily decreasing saturation, possibly biological in origin. The gas also follows the changes in atmopspheric pressure. The difference in gas tension between 5 and 12m is small apatrt from day 144 and 149-158. The latter periods are probably stratified (with the interface between 5 and 12 m: the other periods may also be sttratified with the interface outside these limits).

Figure 2 shows the B results. The top panel is the difference between the atmospheric pressure and the total gas tension, positive if the gas is being pushed into the water. Note the low aitr pressure on day 303 and 308-313. The second panel id the rate of change in gas concentration in the wayter: only a small negative signal is seen on day 303 and some outflow

on 309 and 311. Thois probably reflects the gas

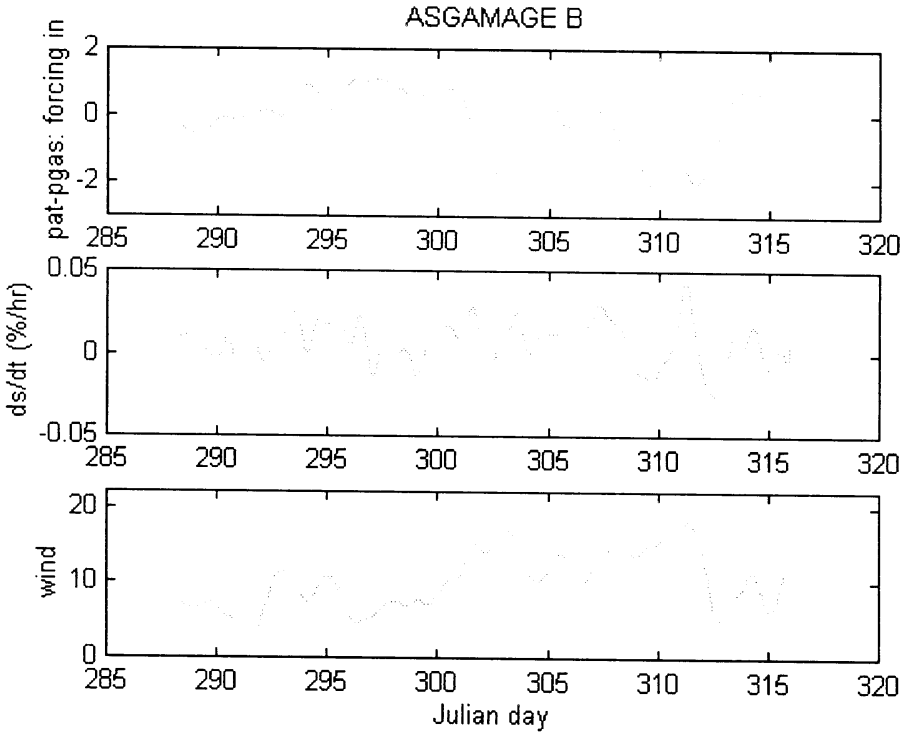

induced supersaturation of the water column.Attempts are under way to model this dataset, although the large advective changes intemperature are causing some problems.

Acoustic measurements

Analysis of the data from the upwardly pointing narrow beam sonar deployed in asgamage a in in progress. example shown is from the A period, with the sonar at about 4m depth. The strong red line is the surface and the increased scattering from the breaking waves shows clearly beneath the surface. Associated with the breaking event is a thickening of the surface. In addition the return signal, apparent above the surface shows the subsurface structure of the bubble clouds. These images will be analysed for
depth of cloud penetration and frequeny of breaking.

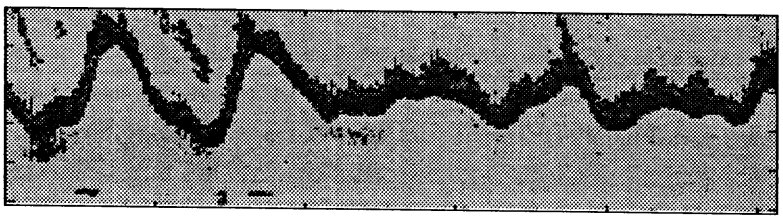

Hydrographic measurements

The progressive vector plot from the MPN RCM is shown in fig.4. This shows much more recterlinear currents than does the ADCP (deployed by SOC) for the same period. However, the currents show a pronounced onshore tendencyat day 303 and offshore at day 311, corresponding to a positive surge and negative surge, tespectively. These events, driven by the high winds, are also correlated with high rates of change in the water temperature, indicating a strong advective influence at these times.

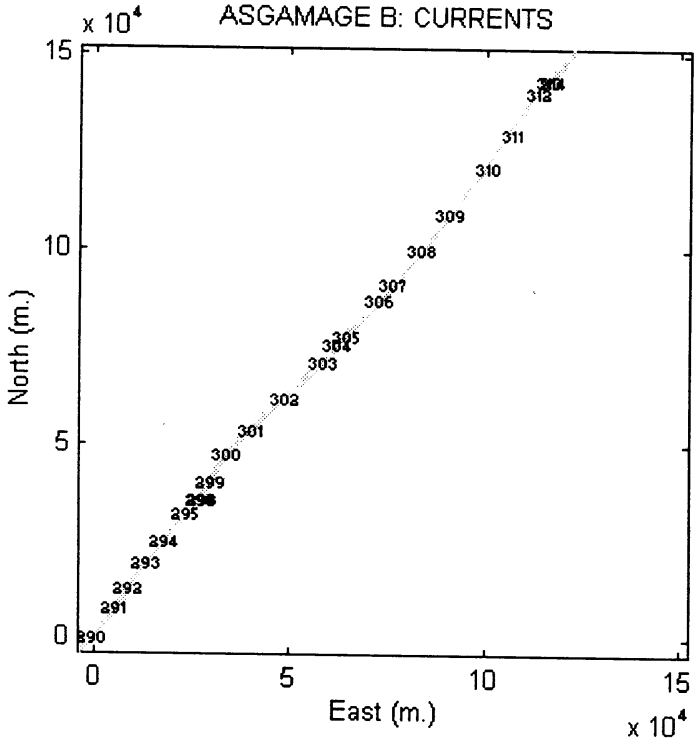

Measurements of bubble spectra

A video system was deployed during the B phase of the experiment. Unfortunately it failed after 3 hours, but some data was obtained of the near surface and 40 cm depth bubble spectra. The optics were maladjusted, so the numbers can be treated as accurate to +/-50%.

The same system has been deployed off a pier in Lough Corrib, Co Galway, also in a force 6, but with a fetch of only one mile. In this case the optics were better adjusted.

Figure 5 shows the data. The similarity in the spectra is striking, and probbably fortuitous, although at these large sizes, fresh and salt water may produce similar populations of bubbles.

The rapid fall off in concentration with depth is apparent, and supports descriptions of bubble distribution in models of bubble enhanced CO2 flux.

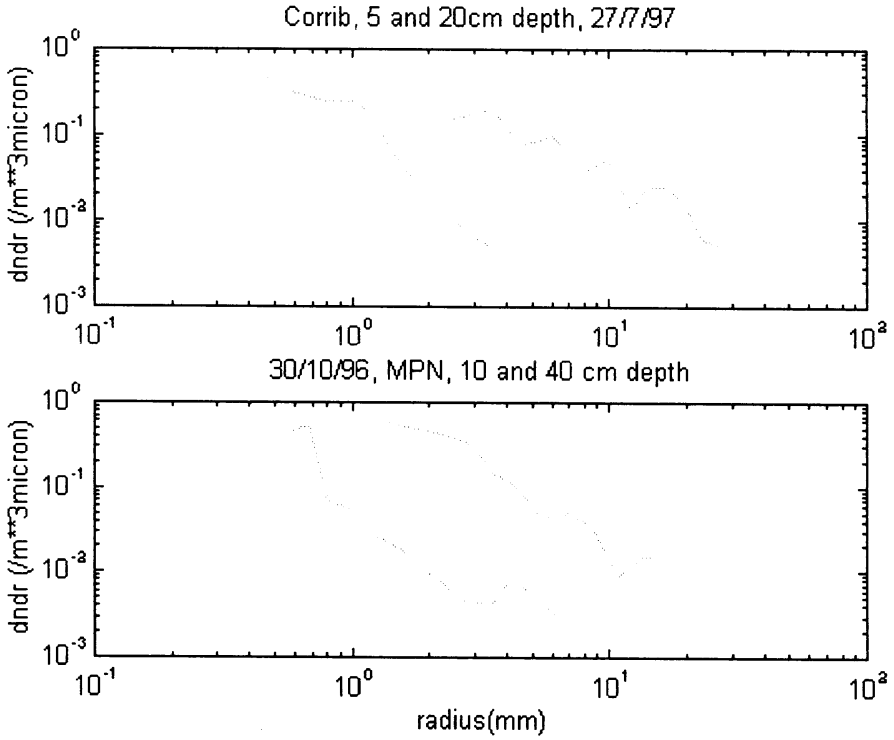
Corrib, 5 and 20cm depth, 27/7/97
dndr (/m**3micron)
10^{0}
10^{-1}
10^{-2}
10^{-3}
10^{-1}
10^{0}
10^{1}
10^{2}
30/10/96, MPN, 10 and 40 cm depth
dndr (/m**3micron)
10^{0}
10^{-1}
10^{-2}
10^{-3}
10^{-1}
10^{0}
10^{1}
10^{2}
radius(mm)

DATA WORKSHOP REPORT FROM BIO - ASGAMAGE-B

Robert J. Anderson and Stuart D. Smith
Bedford Institute of Oceanography (BIO), PO Box 1006, Dartmouth, N.S., Canada B2Y 4A2

Eddy fluxes of momentum, heat, water vapour and CO2 have been calculated from time series data logged with the BIO system, using the BIO Kaijo Denki DAT-300 sonic anemometer-thermometer, microbead thermistor probes and an ERC Lyman-alpha (ultraviolet absorption) H_2O sensor. Data from the aspirated KNMI IFM (henceforth IFM) IR (infrared absorption) H_2O and CO_2 and KNMI Lyman-alpha (ultraviolet) H_2O sensors, KNMI sea surface temperature and wave wire, NOM Oak Ridge IR (henceforth OAKR) CO_2 and H_2O sensor were also logged on the BIO system. TNO Advanet CO_2 and H_2O data were logged as well but are not used in this report. The aspirated KNMI sensors worked most of the time, while the OAKR sensor and BIO Lyman-alpha data were useful only in the absence of rain. The OAKR sensor claims a resolution of 20 $\mu g/m^2s$ for a 1 hour average CO_2 flux. All IR CO_2 sensors at times gave some indications of contamination by accumulation of sea salt or moisture, and on windy days we expect the best
results to come from periods just after the sensors were cleaned.

The BIO data system, which logs and gives preliminary results on-line (Fairall et al., 1997), worked well during the entire experiment. A total of 323 data runs were logged and processed in wind speeds of 3-16 m/s, directions from 171-331 degrees and with fairly constant upward $\Delta\rho CO2$ or $\Delta pCO2$. Rain or drizzle occurred during many runs. Inertial dissipation estimates of wind stress were also computed on-line.

During the first two weeks NOAA-ETL logged data from the TNO-RISO Solent sonic anemometer, the OAKR CO_2 and H_2O sensor, the KNMI wave wire and an Ophir IR H_2O sensor for intercalibration of mean and fluctuating humidity. The NOAA data system failed mid-way through the experiment and data from this system are not presented in this report.

A preliminary evaluation of CO_2 flux

The BIO analysis results use the BIO sonic vertical wind, and the Webb et al. (1980) corrections to CO_2 fluxes are based on data from the BIO temperature and their respective H_2O signals. Since the experiment we have re-analysed much of the data set. Adjustments have been made for tidal and other variations in sensor height, phase shifts due to positions of sensors relative to the wind direction, phase shifts due to response time of aspirated and other sensors, intercalibration and re-calibration of the sensors, and adjustment of wind speed for currents and flow distortion. The results to follow are from the re-analysed data.

Oak Ridge CO_2 Sensor Calibration

This sensor was calibrated in the field on two occasions using reference gases with 249, 358.5 and 443 ppm CO_2. In both cases the calibration results were nearly identical to those of the manufacturer. The mean sensor rms. level was 0.382 ($\pm$ 0.029) mg/m^3 CO_2 and mean humidity was 0.5$\pm$0.005 g/m^3 for the three calibration gases. This would suggest that the instrument noise level for CO_2 is approximately 0.4 mg/m^3 and that the humidity of the calibration gases was very low.

Offshore wind cases

CO_2 data in periods of offshore winds have high CO_2 variability that is probably generated from sources on the land and is unrelated to ocean boundary layer processes. These data provide an opportunity to compare sensor calibration and response time without the complication of allowing for H_2O-CO_2 crosstalk and sensor and system noise. Figure 1 compares CO_2 spectra from the OAKR and IFM CO_2 signals for BIO run 118. The spectra show agreement up to a frequency of 1 Hz, above which the OAKR spectrum appears to be noisy. We do not know if this noise is inherent in the sensor, or arises from the interface to the BIO data system. Also shown in Figure 1 is a noise level spectrum of the hooded OAKR sensor during calibration with a reference gas. The spectral shape is close to an $f^{-5/3}$ power law as indicated by the straight dashed line.

Onshore winds

CO_2 data in periods of onshore winds have much less variability and are often not very coherent between the two sensors. Much of the CO_2 signal may be noise or drift. For BIO run 175 (Figure 2) the OAKR CO_2 spectrum is higher than the KNMI spectrum, and this suggests that it may be contaminated by noise, drift or "crosstalk" sensitivity to other variables such as humidity or temperature. Again we are not sure if this problem is inherent in the OAKR sensor, or arises from the interface to the BIO data system.

Humidity spectra and influence of aspirators

The IR and UV water vapour sensors show excellent agreement (Figure 3). The KNMI sensors were in aspirators which allowed them to operate in rain and spray when the optics of open-path sensors would become contaminated. A Comparison of humidity spectra for BIO run 099 shows rolloff of the KNMI IFM and Lyman Alpha humidity signals relative to the OAKR humidity beginning at a frequency of about 0.1 Hz. At 3 Hz the IFM humidity spectrum rolls off by a decade, indicating attenuation by a factor of $1o^{1/2}$ in the IFM aspirator at this frequency. Rolloff of the IFM CO_2 signal would be similar.

CO_2 fluxes

CO_2 fluxes from the IFM and OAKR humidity signals and the BIO sonic anemometer are shown in Figure 4. The humidity crosstalk correction factor has been set to values believed to be appropriate to several modes of operation of the IFM CO_2 sensor. In nearly every case the CO_2 flux from the OAKR is higher than that from the IFM. It remains to be seen if this difference can be explained by influence of humidity or thermal crosstalk. In spite of this systematic difference there is an encouraging correlation in the hour-to-hour variations of CO_2 fluxes derived from the two sensors.

Wind stress, evaporation and heat flux Coefficients

Wind stress coefficients from the BIO sonic anemometer (Figure 5), corrected for distortion of mean wind speed by the MPN structure and adjusted to neutral stratification as in the HEXMAX data analysis (Smith et al., 1992), increase with wind speed with a trend that is between the HEXMAX line from Smith et al. (1992) and the lower line characteristic of open-ocean studies (Anderson, 1993; Smith, 1988). There is no significant difference between drag

coefficients derived from eddy flux (solid squares) and inertial-dissipation analyses, as implemented in the BIO AIRSEA data system.

Evaporation coefficients for each run have been averaged over eddy flux analyses of all humidity sensors logged by the BIO system, and adjusted to neutral stability (Figure 6). They replicate the HEXMAX results (DeCosmo et al., 1996), as do heat flux coefficients derived from eddy fluxes with the BIO microbead thermistor and sonic anemometer (Figure 7).

REFERENCES:

Anderson, R.J.: 1993, A Study of Wind Stress and Heat Flux over the Open Ocean by the Inertial Dissipation Method, J . Phys. Oceanogr., 23, 2153-2161.

DeCosmo, J., K.B. Katsaros, S.D. Smith, R.J. Anderson, W.A. Oost, K. Bumke, and H. Chadwick.,1996; Air-sea exchange of water vapour and sensible heat: The Humidity Exchange Over the Sea (HEXOS) results, J.Geophys. Res., V101,C5, 12001 -12016.

Fairall, C.W., J.E. Hare, S.D. Smith, R.J. Anderson, W. Kohsiek, R. Dissly, J. Smith and F. Hansen, 1997: Preliminary results on CO2 flux measurements during ASGAMAGE-B. Proc. IAMAS/IAPSO, Melbourne, Australia.

Smith, S.D., 1988; Coefficients for sea surface wind stress, heat flux and wind profiles as a function of wind speed and temperature. J.Geophys.Res.,V93,15467-15472.

Smith, S.D., R.J. Anderson, W.A. Oost, C. Kraan, N. Maat, J. DeCosmo, K.B. Katsaros, K.L. Davidson, K.Bumke, L. Hasse and H.M. Chadwick,1992: Sea Surface Wind Stress and Drag Coefficients: the HEXOS Results, Boundary-Layer Meteorol. 60, 109-142.

Webb, E.K., G.l. Pearman and R. Leuning,1980: Correction of Flux Measurements Due to Heat and Water Vapor Transfer. Quart. J. Roy. Meteorol. Soc., 106, 85-100.

FIGURE CAPTIONS

1. Comparison of spectra from KNMI-IFM and NOM-OAKR CO_2 sensors for offshore wind conditions.

2. Comparison of spectra from KNMI-IFM and NOAA-OAKR CO_2 sensors for marine wind conditions.

3. Humidity spectra from KNMI Lyman-alpha, IFM and OAKR sensors.

4. BIO analysis of CO_2 fluxes.

5. C_{10N} vs U_{10N} from BIO sonic anemometer for eddy flux and inertial-dissipation methods.

6. Neutral humidity flux coefficient C_{EN} as a function of U_{10N}. Fluxes have been averaged for sensors used during each data run.

7. Neutral heat flux Coefficient C_{TN} as a function of U_{10N}, eddy flux analysis of BIO microbead thermistor and sonic anemometer.

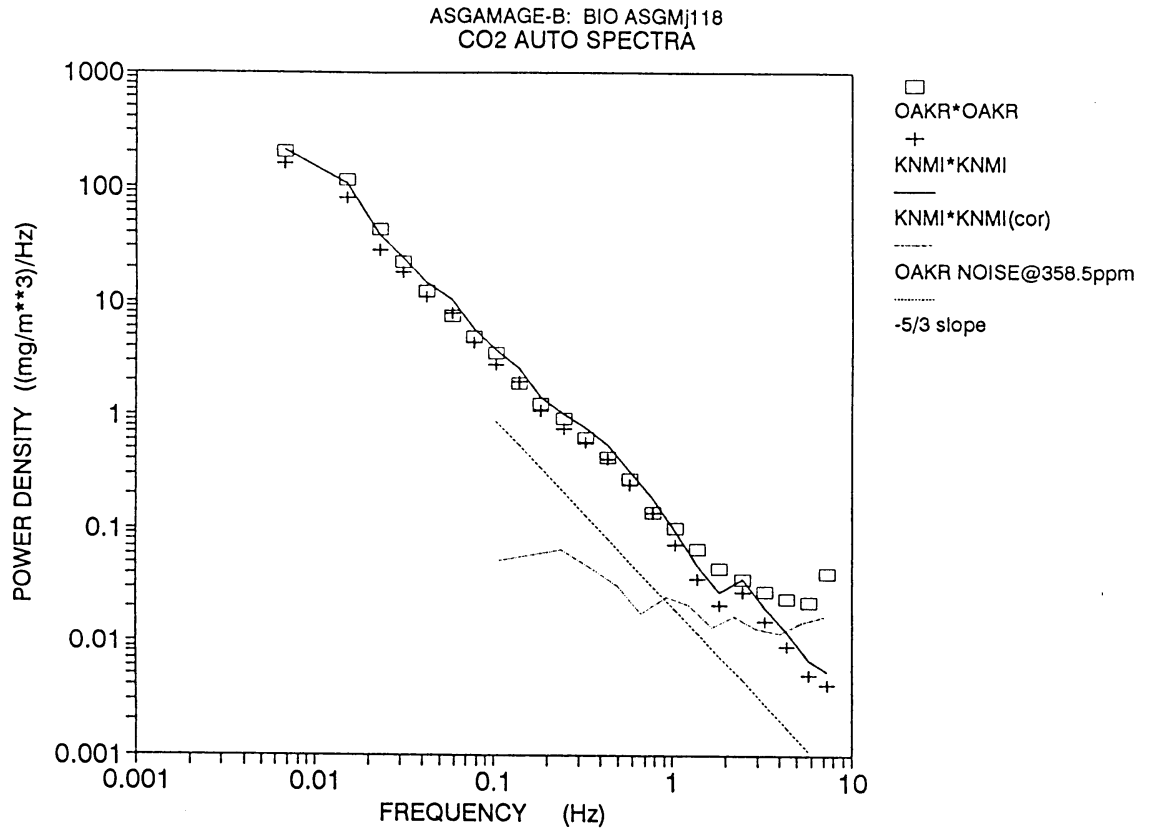

Figure 1

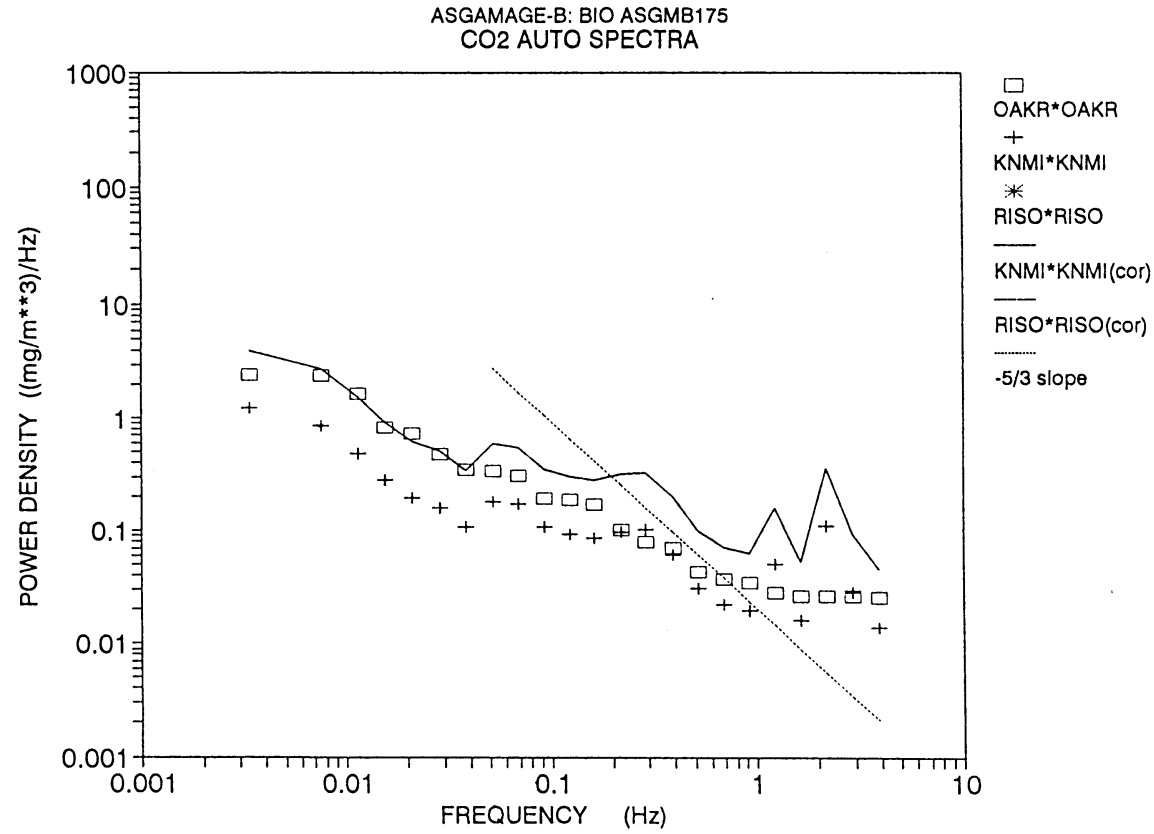

Figure 2

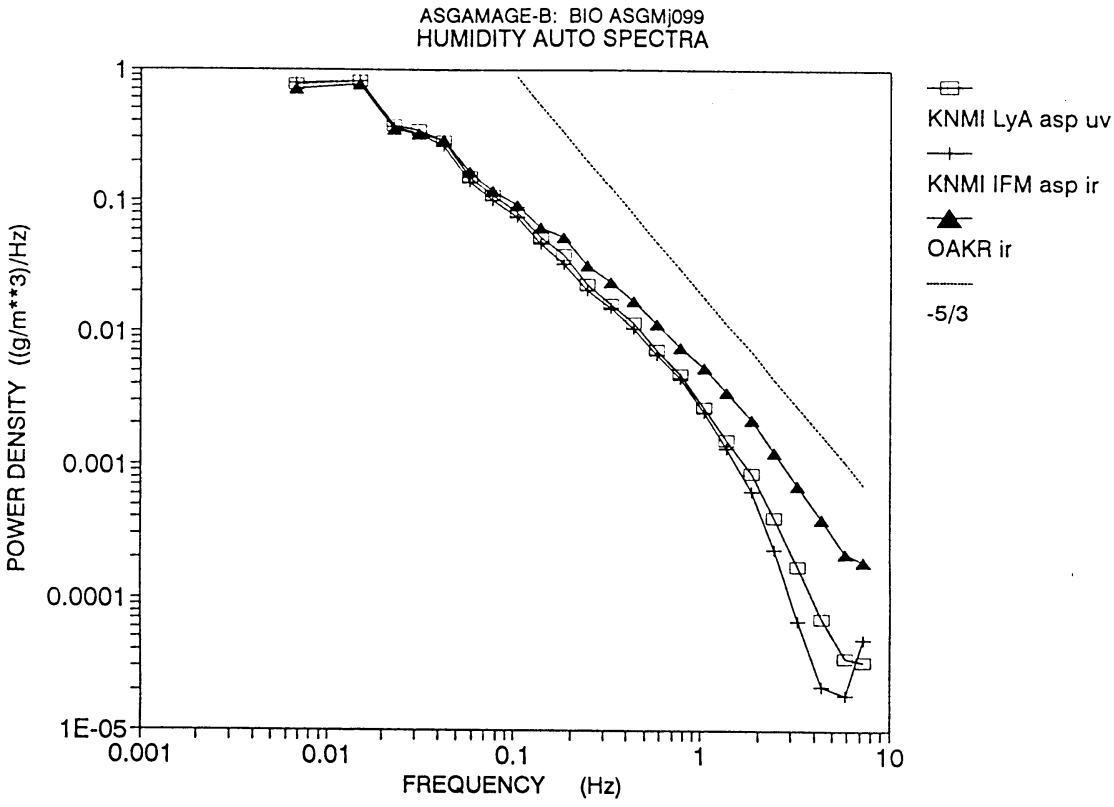

Figure 3

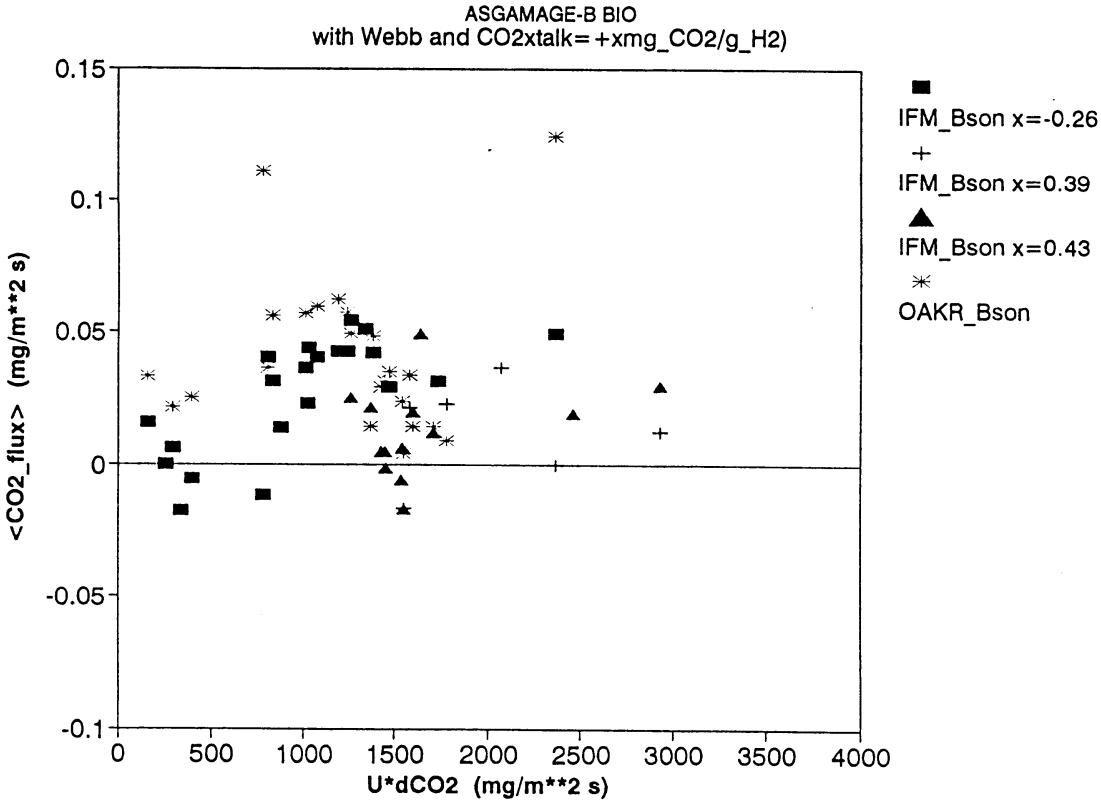

Figure 4

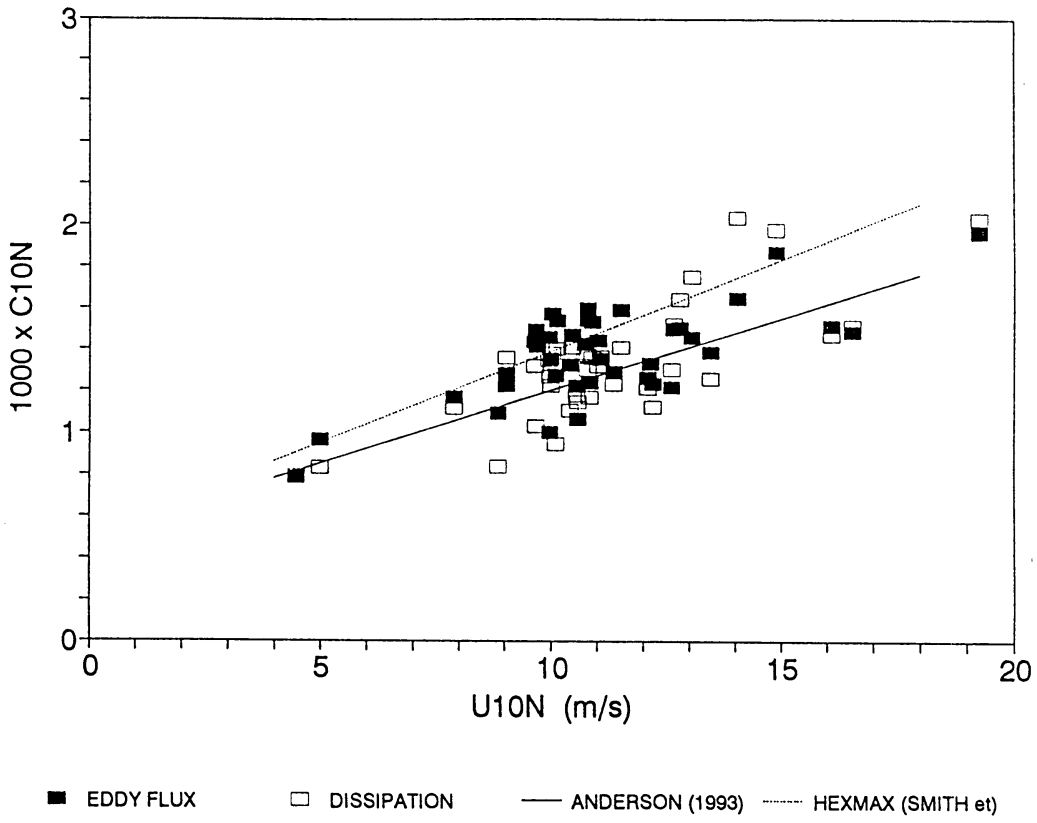

Figure 5

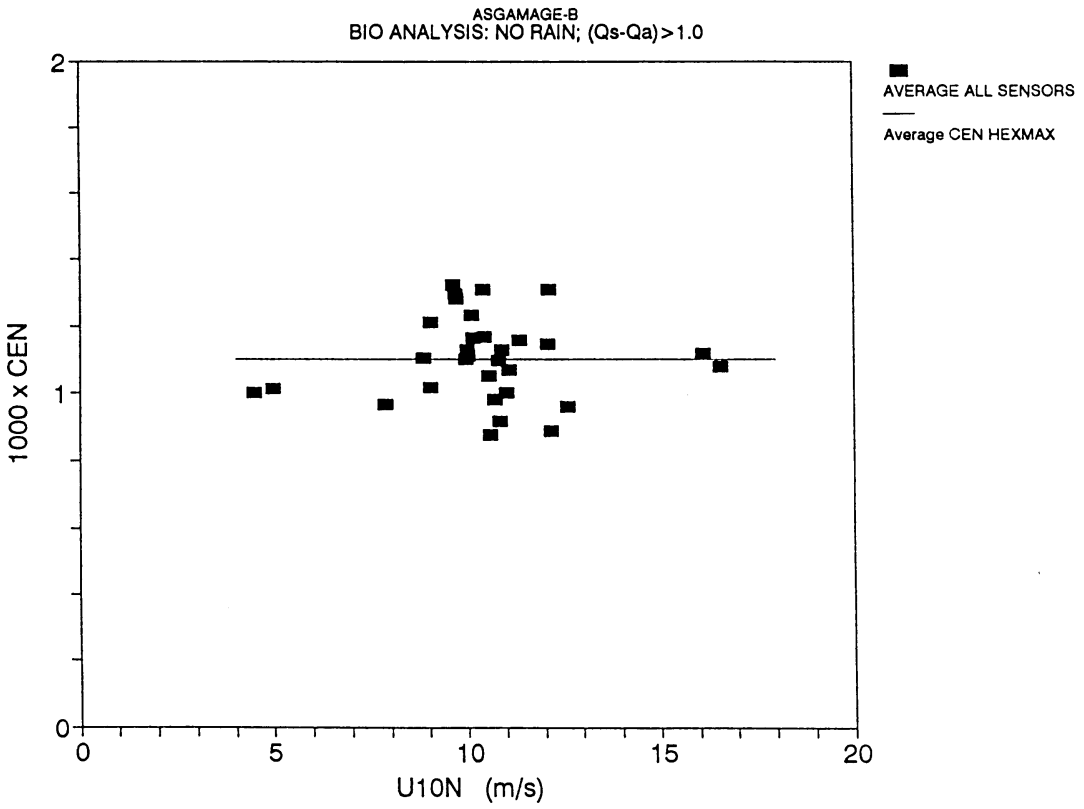

Figure 6

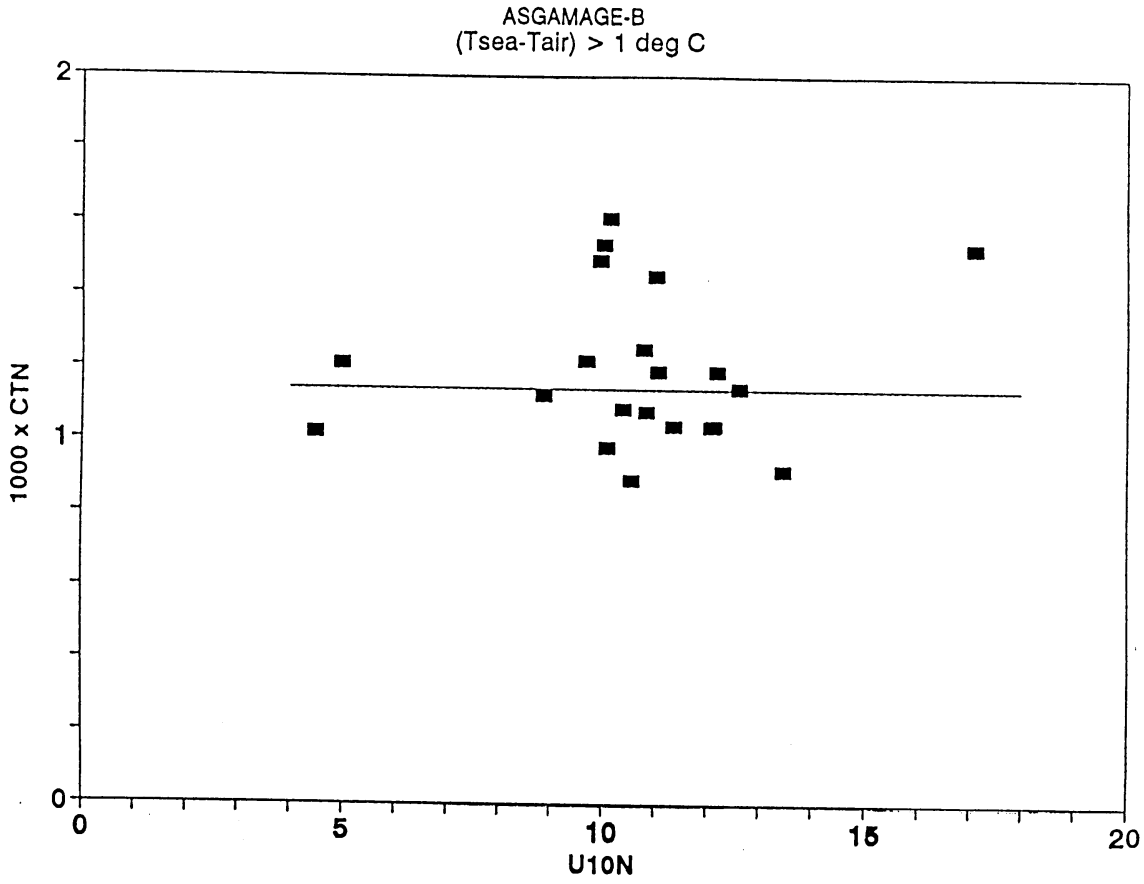

Figure 7

Experimental and Modeling study of Air-Sea Exchange of Carbon Dioxide.

S. E. Larsen[1)], F. Aa. Hansen[1)], J. F. Kjeld[1)], S. W. Lund[1)], G . J. Kunz[2)] and G. de Leeuw[2)]
[1)]Wind Energy and Atmospheric Physics, Risø, Roskilde, Denmark
[2)]TNO-FEL,The Hague, The Netherlands

Introduction

Air-sea exchange of slowly dissolving gases is still associated with some uncertainties. The transfer-velocity relations based on the Liss and Merlivat, and the Wanninkhof studies offer integration of many data sets, although with substantial scatter. However the small transfer rates implied by these relations indicate that in the natural environment fluxes and concentrations will often not be in the equilibrium, implicitly assumed when employing the transfer velocity relations. It is therefore important to compare simultaneous flux estimates by different estimation methods.

Experimental Studies.

Within ASGAMAGE we measured the air-sea fluxes employing micrometeorological method of flux determination for the fluxes of momentum, heat, water vapor and CO_2. Until recently large differences have existed between CO_2-fluxes estimated by micrometeorological methods and the transfer-velocity methods.

In total we obtained 1354 30 minutes run during ASGAMAGE-A,B. The micrometeorological data from these runs have now been collected into a common data base together with the partial pressure measurements of TNO, and continuing data selection and analysis is presently being conducted.

Figure 1 shows the three key instruments used for the micrometeorological flux estimation, a Gill sonic anemometer/thermometer and two Advanet CO_2/water vapor IR sensors. Two CO_2 sensors were used to improve the marginal Signal/Noise with cross-correlation between the two sensors. The basic micrometeorological method for flux estimation is the eddy correlation between the vertical velocity and the concentration fluctuations. Here we have further employed the eddy-co-spectral method and the inertial dissipation method, both being less sensitive to flow distortion induced by the platform and its motion. The instrumentation used with background and theory is described most comprehensively in (Larsen et al 96,97). Results have further been reported in Kunz et al(95a,b).

The co-spectral methods employs the low frequency part of the co-spectra, Co(f) to derive fluxes:

$$\langle w'\gamma' \rangle \approx 5f\, Co_{w\gamma}(f) \text{ for } 0.01\,Hz < f < 0.1\,Hz,$$

where γ stands for any of the scalars, T, q or q_{CO2}.
The inertial dissipation method employs the laws for high-frequency small scale turbulence to derive the fluxes from estimates of the dissipation, derived from the high frequency inertial range of the power-spectra, S(f) .

$$u_* = \left[\frac{f\,S_u(f)}{\alpha}\right]^{1/2}\left[\frac{2\pi}{U}\frac{\kappa z}{\phi_\varepsilon} f\right]^{1/3},$$

$$|\langle w'\gamma'\rangle| = \left[\frac{\alpha}{\beta}\frac{\phi_\varepsilon}{\phi_{N\gamma}}\frac{f\,S_\gamma(f)}{f\,S_u(f)}\right]^{1/2} u_*^2,$$

Here usual micometeorological notation is used (Larsen et al., 1996), and it is understood that the spectral values have to be taken within the inertial subrange.
The importance of the Webb correction for the micrometeorological flux estimates is by now well established. For species with very small fluxes it account for that even extremely small average vertical velocities may contribute significant to the total flux. For q_{CO2} the total flux becomes:

$$F_{qCO2} = \langle w'q_{CO2}'\rangle + 1.61\langle q_{CO2}\rangle\langle w'q'\rangle + (1+1.61\langle q\rangle)\langle q_{CO2}\rangle\frac{\langle w'T'\rangle}{\langle T\rangle},$$

In Figure 2, we show co-spectra between the vertical velocity and the CO_2 fluctuations and the power-spectra of the two individual CO_2 sensors as well as their co-spectrum, showing the signal/noise improvement by use of two sensors. Figures 3 shows examples of raw CO_2 fluxes obtained from ASGAMAGE data . Figure 4 showns the same data plotted against one of the flux estimates for easier comparison.

Modelling

To study the behavior of the air-sea flux for inhomogeneous and non-stationary conditions, we have developed a diffusion model considering the vertical diffusion in the water and in the air, and the chemical buffer in the water as well the Webb corrections in the air.
Basically, the model looks as follows:

$$\frac{\partial C}{\partial t} + \frac{\partial UC}{\partial x} + \frac{\partial WC}{\partial z} = -\frac{\partial\, Flux}{\partial z} - \alpha(C - C_0),$$

$$Flux = WC + \langle w'c'\rangle - D\frac{\partial C}{\partial z}$$

Here $\alpha(C - C_0)$, with C_0 being the concentration of CO being in local equilibrium with the Dissolved Inorganic Carbon and α describing the reaction times of the chemical system, accounts for the buffer effect in the water. Average values are indicated by capital letters, while lower case letters are used to describe the turbulent part of the variables. In the air the mean vertical velocity, W, is derived from the formulation for the Webb correction shown above. The turbulent part of the flux is determined through a K-diffusivity closure. The exchange across the interfacial layer is described by the exchange coefficient expression. This concept is based on that the transfer coefficient method models situations where all the air-water concentration difference is found at the air-water interface, a situation that is most closely approximated for stationary and horizontally homogenous situations. The model solves for the flux-concentrations between an upper an a lower boundary, corresponding to typically to the levels for the water and the air inlets for the concentration measurements in an experimental situation. Model estimates of the flux response to concentration changes are illustrated for a Gaussian change in the water concentration at the lower boundary for CO_2 in Figures 5.

Conclusions.

The micrometeorological methods have been found to deliver results that in average are close to the transfer-velocity during the ASGAMAGE campaigns. Hence the road seems now open for more detailed comparisons between the two methods allowing for experimental studies of transient situations for the air-sea exchange of CO_2.

Such situations have simultaneously being studied by means of simple diffusion models combined with the description of the carbonate buffer system. Although simplistic, this modelling concept allow for both exploratory and production analysis of the air-ocean exchange of CO_2 for transient conditions.

Although the micrometeorological method has been found work well, and new methods developed and tested during ASGAMAGE were found to work, much sensor and system improvement still needs to be done before the measuring systems used can be considered mature. Both the sonic and the CO_2 systems used were found to perform less well than expected and desired.

References.

Kunz, G.J., G.deLeeuw, S.E.Larsen, F.Aa.Hansen, 1995a. Over-water eddy correlation measurements of fluxes of momentum, heat, water vapour and CO_2. In: Air-water Gas Transfer (Eds. B.Jähne and E.C.Monahan) AEON Verlag Studio, Hanau (GE), 685-701.

Kunz, G.J., G.deLeeuw, S.E.Larsen, F.Aa.Hansen, 1995b. Eddy correlation measurements of fluxes of momentum, heat, water vapour and CO_2 during ASGASEX. In: Report of the ASGASEX'94 workshop, KNMI, De Bilt, The Netherlands (Ed. W.A.Oost), Technical report TR-174, 12-16.

Larsen, S. E., F.Aa. Hansen, G.De Leeuw and G.J.Kunz, 1996 Micrometeorological estimation of fluxes of CO_2, heat, humidity and momentum in the marine atmospheric surface layer during OMEX. In: OMEX Final Report, SubProject F (ULB, Brussels, Belgium), F,1-F,37.

Larsen, S.E., F.Aa.Hansen, J.F.Kjeld, G.deLeeuw, and G.J.Kunz, 1997. Experimental and modelling work on CO_2 exchange. Proceeding of the NILU/MAST Workshop on Air-Sea Exchange, Oslo, Norway, 11-13 June, 1997.

Figure Captions

Figure 1. Sensor packet used for micrometeorological estimation of the CO_2 flux, showing sonic anemometer and two Advanet CO_2/Water vapor sensors.

Figure 2. Example on Co-spectra and power spectra involving CO_2 flux estimation by the co-spectral and the dissipation method from one of the MAST-ASGAMAGE campaigns. Note the improved Signal/Noise by cross correlation.

Figure 3. Raw CO_2 fluxes estimated by the co-variance method, by the two CO_2 sensors (Risr and TNO), the co-spectral method, G, and by the inertial dissipation method (disp.), during the ASGAMAGE Experiment at Meetpoost Nordweijk.

Figure 4. The raw CO_2 fluxes of Fig.3 plotted versus the covariance estimate by the TNO-CO_2 sensor, illustrating similarities and differences between the different estimates.

Figure 5. The air and water concentration over a negative Gaussian concentration perturbation with a horizontal scale of 2 km at 6 meters depth, with limitted penetration to the surface. Also shown is the associated flux distribution in the air.

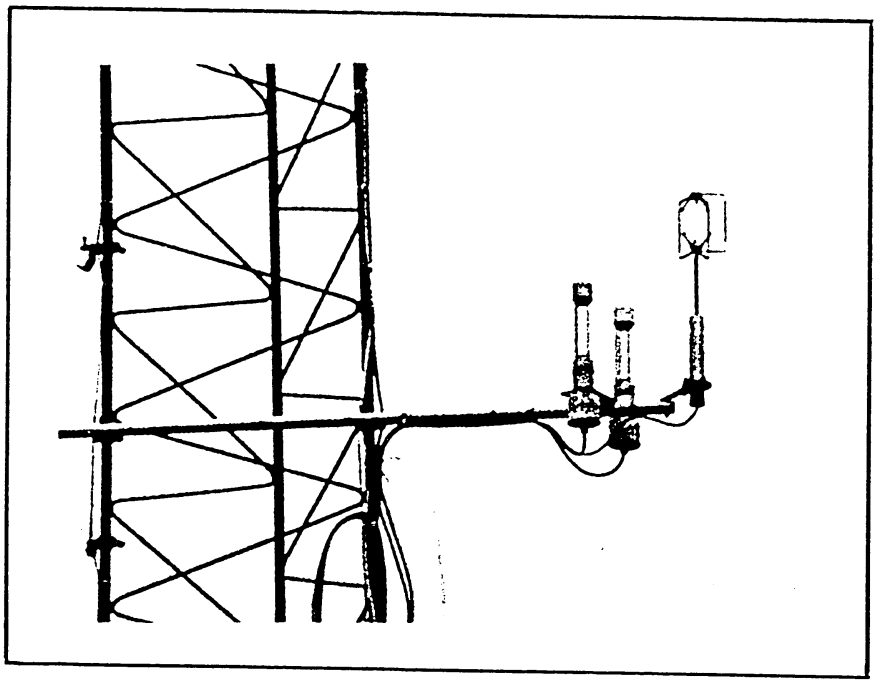

Figure 1

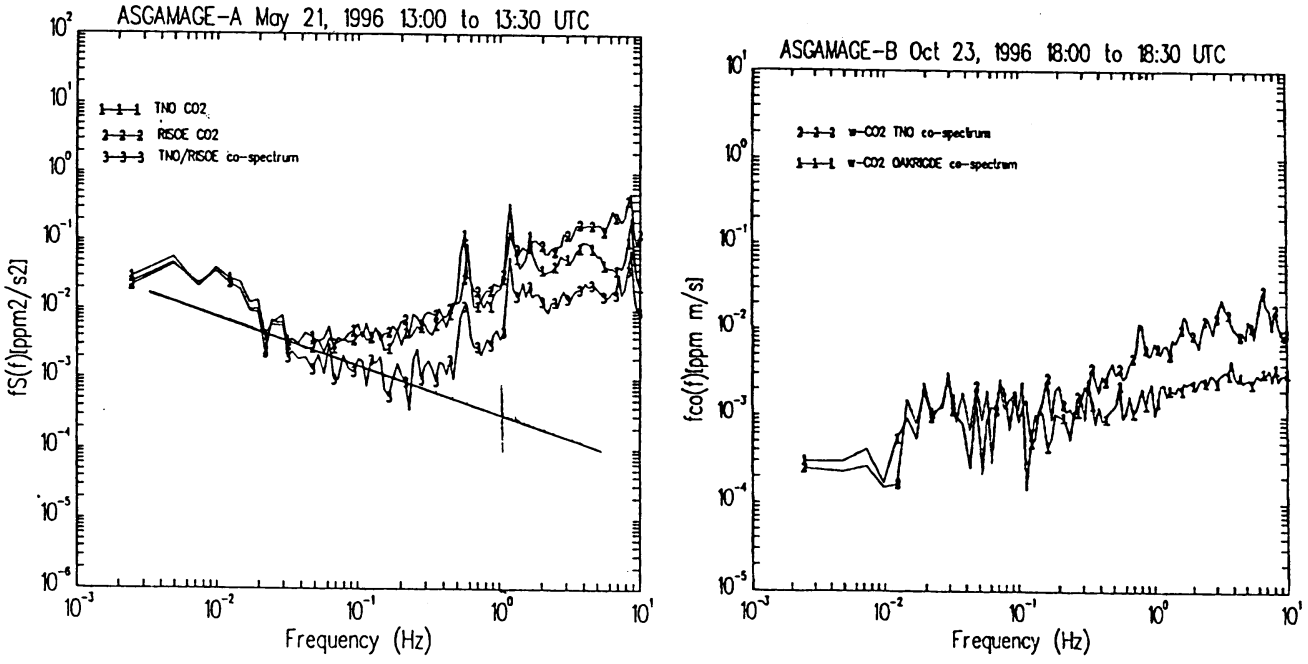

Figure 2

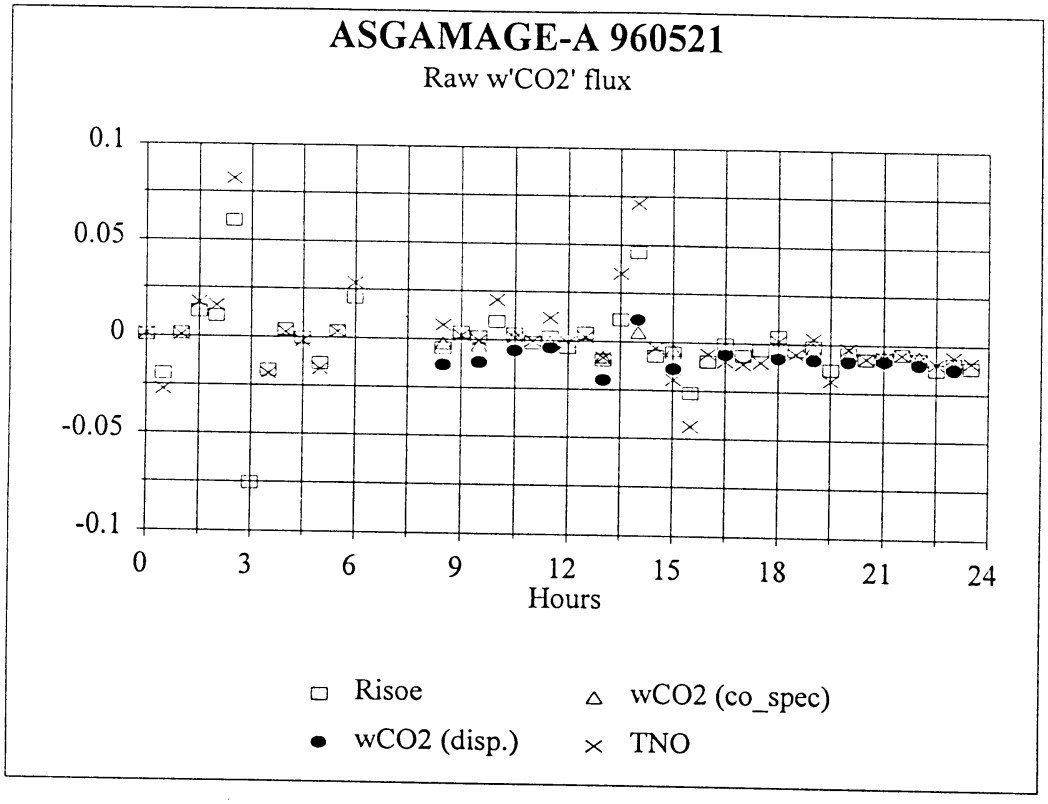

Figure 3

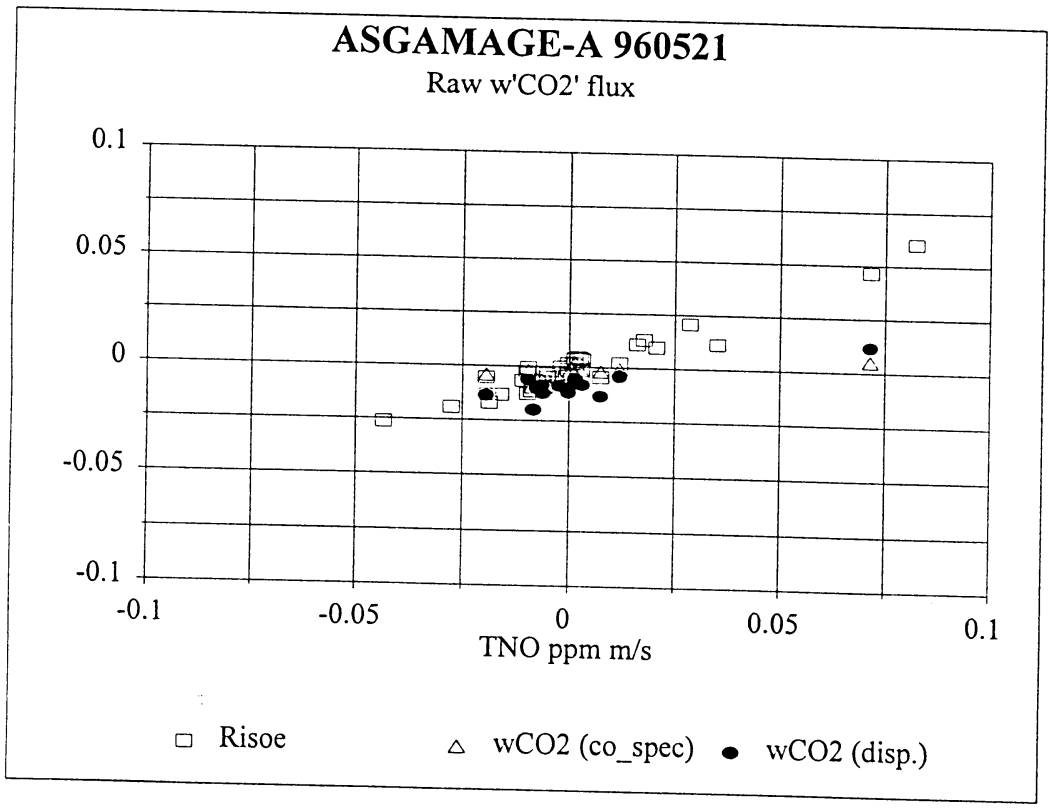

Figure 4

Concentration and flux distributions for a stationary situation
No vertical advection velocity in the air
Buffer mechanism included
u_{*a}= 0.4 m/s

Sc = 864 (CO_2, T = 18 °C, Seawater)

Concentration distributions in air and water (measured in mg/l)

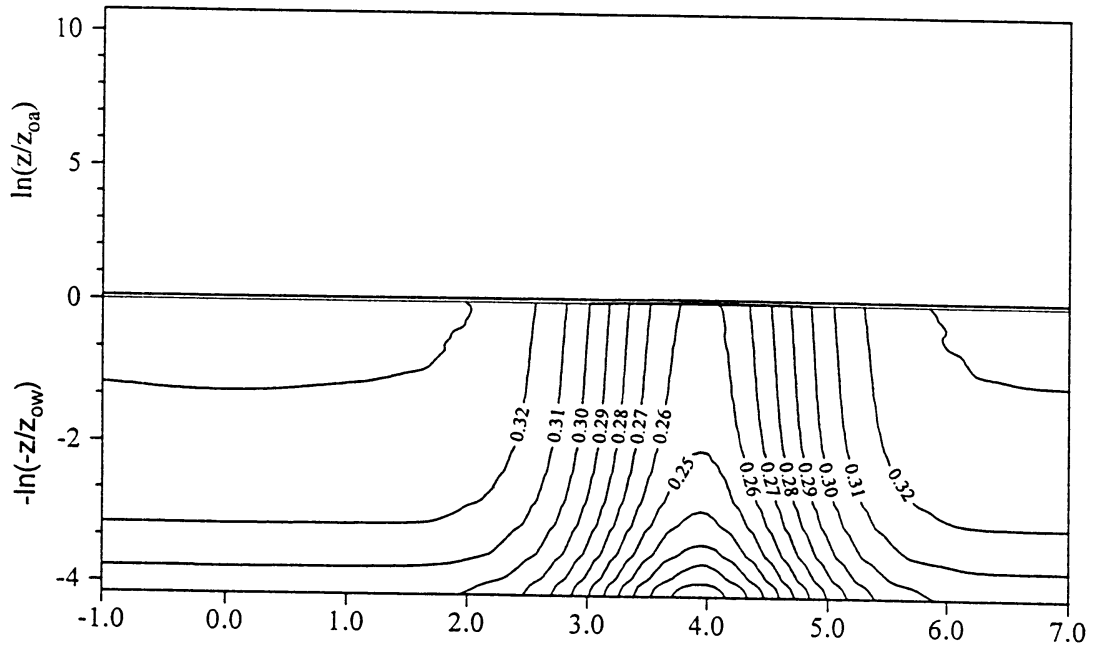

Flux distribution in the air (measured in mg/m²s)

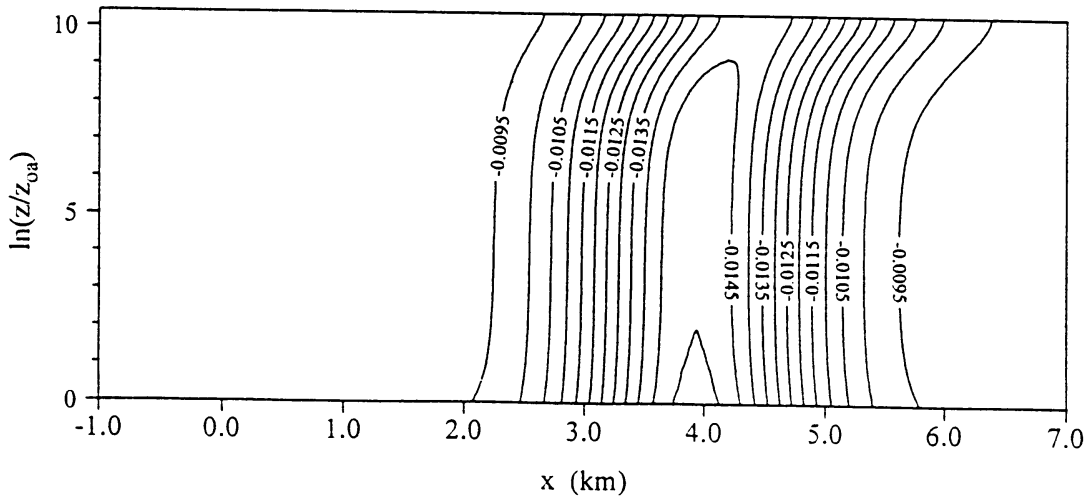

Figure 5

Session 2: How are we progressing toward our objectives?

The Effect of Long Measurement Times on Flux Measurements at Sea.

Wiebe Oost
Royal Netherlands Meteorological Institute (KNMI), de Bilt, the Netherlands

Introduction

In the KNMI eddy correlation measurements of the CO_2 flux during ASGAMAGE many correction factors have been applied (see the contribution to this report by Jacobs et al), but the resulting values for the transfer velocity k are still something like a factor two higher than e.g. the Wanninkhof curve (Wanninkhof 1992), which in itself is already some 50% higher than the other parametrization in general use, the Liss-Merlivat relation. The ASGAMAGE differential tracer results from the "Challenger", on the other hand, confirm the Liss-Merlivat curve. Both techniques, eddy correlation and differential tracer, have their weak and strong points, but both are sufficiently well founded and the experiments have been performed sufficiently carefully to expect a much better correspondence. How is this result possible?

A correction term

A difference between the two techniques that so far didn't get attention is the difference in the measurement times needed for the two types techniques. An eddy correlation measurement typically takes 20 to 45 minutes, whereas the time span for a differential tracer value is 24 hrs or longer. On the latter time scale the properties of atmosphere and sea can fluctuate significantly and it appears worthwhile to look into the effects of such fluctuations.
The transfer velocity k for CO_2 is defined as the quotient of the flux Φ and the "pressure" (better: fugacity) difference $dPCO_2$ between water and air. If we consider Φ as the sum of an average value ϕ and a fluctuating part φ and $dPCO_2$ in the same way as $\Delta PCO_2 + \delta PCO_2$ we can write, denoting averages with angular brackets,

$$k = \frac{\Phi}{dPCO_2} = \frac{\phi + \varphi}{\Delta PCO_2 + \delta PCO_2}; \quad <\varphi> = 0; \quad <\delta PCO_2> = 0 \tag{1}$$

so that, correct to second order

$$\begin{aligned} <k> &= < \frac{\phi+\varphi}{\Delta PCO_2 + \delta PCO_2} > = < \frac{\phi}{\Delta PCO_2} [\frac{1+\varphi/\phi}{1+\delta PCO_2/\Delta PCO_2}] > \\ &\approx < \frac{\phi}{\Delta PCO_2} [(1+\frac{\varphi}{\phi})(1-\frac{\delta PCO_2}{\Delta PCO_2} + \frac{\delta PCO_2^2}{\Delta PCO_2^2})] > \\ &\approx \frac{\phi}{\Delta PCO_2} [1 + \frac{<\delta PCO_2^2>}{\Delta PCO_2^2} - \frac{<\varphi\ \delta PCO_2>}{\phi\ \Delta PCO_2}] \end{aligned} \tag{2}$$

So the effective average value of k during the measurement time is not the quotient of the averages of the flux and the pressure difference, but has to be corrected for fluctuations in $dPCO_2$, with another correction term if there is a correlation between the fluctuations in the

flux and in the pressure difference.
$<\varphi\ \delta PCO_2>$ cannot be calculated directly from our ASGAMAGE data, because the flux and concentration measurements were not made simultaneously. We can, however, get at least some qualitative information in this respect. We know that k is a function of the wind speed U, which makes Φ a function of the wind speed as well. When we plot $dPCO_2$ against U (fig.1) we see that there is a positive correlation between these two quantities, so both Φ and $dPCO_2$ are correlated with U and therefore also correlated with each other. So it makes sense to try to find a value for the size of the correction term.

Estimating the size of the correction

Because it's not possible to calculate $<\varphi\ \delta PCO_2>$ directly from the ASGAMAGE data, we have to resort to a more indirect method. We start by writing out Φ again as the product of k and $dPCO_2$: $\Phi = k\ dPCO2$ with $\phi = k_0\ \Delta PCO_2$ (which defines k_0) ; therefore

$$\Phi = \phi + \varphi = k_0\ \Delta PCO_2 + k_0\ \delta PCO_2 + \delta k\ \Delta PCO_2 + \delta k\ \delta PCO_2 \quad \text{so}$$

$$\varphi = k_0\ \delta PCO_2 + \delta k\ \Delta PCO_2 + \delta k\ \delta PCO_2 \text{ and}$$

$$<k> \approx k_0\left(1+\frac{<\delta pCO_2^2>}{\Delta pCO_2^2} - k_0\frac{<\delta pCO_2^2>}{\phi\,\Delta pCO_2^2} - \frac{<\delta k\,\delta pCO_2>}{\phi} - \frac{<\delta k\,\delta p^2>}{\phi\,\Delta pCO_2} + \frac{<\varphi\,\delta pCO_2^2>}{\phi\,\Delta pCO_2^2}\right)$$

$$\approx k_0\left(1-\frac{<\delta k\,\delta pCO_2>}{\phi}\right) = k_0\left(1-\frac{<\delta k\,\delta pCO_2>}{k_0\,\Delta pCO_2}\right), \qquad (3)$$

correct again to second order.
In fig.1 we see a trend which leeds to a linear relationship between $dpCO_2$ and U_{N10}:

$$dpCO_2 = A\ U_{N10} + B = 3.6\ U_{N10} + 48.8 \qquad (4)$$

with $dpCO_2$ in µatm and U_{N10} in m/s.

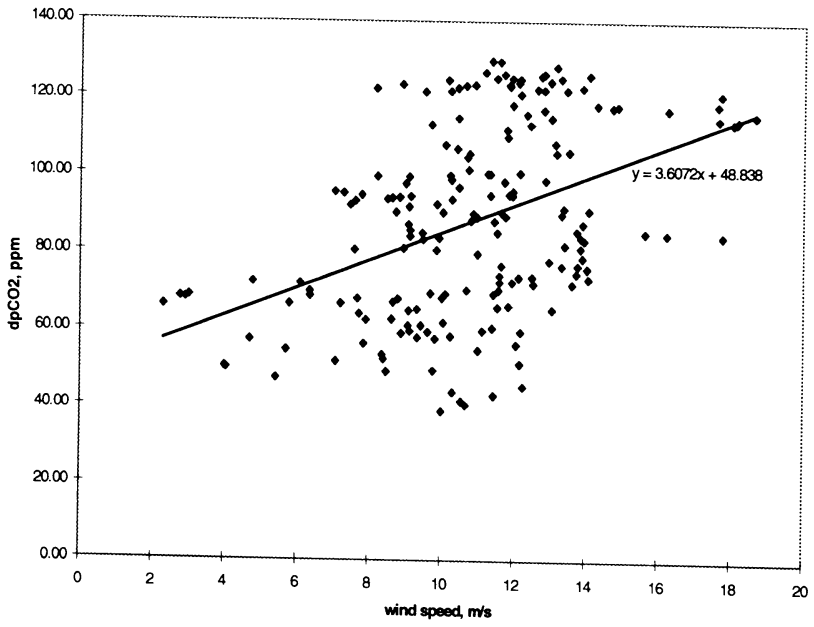

Figure 1

The analysis of the ASGAMAGE data provided an approximately quadratic relationship between k and U_{N10} (see the paper of Jacobs et al in this report):

$$k_{CO2} = C\ U_{N10}^2 = 0.53\ U_{N10}^2 \qquad (5)$$

with k in cm/hr. From the data measured during ASGAMAGE-B we find an average wind speed of 9.8 m/s, with an average spread during 24 hrs of 7.14 m/s. Distributing this variance symmetrically around the average wind speed we have a minimum wind speed U_{min} of 6.23 and a maximum U_{max} of 13.37 m/s. We will now try to calculate the correction term in (3) using (4), (5) and the wind speed values just mentioned.

δk is the difference between the actual k and k_0, where we take k_0 as the value of k when $U_{N10} = U_0 = 9.8$ m/s, to be calculated with (5). We do the same for δpCO_2 with (4) so

$$\delta k\ \delta pCO_2 = A\ C\ (U^3 - U_0U^2 - U_0^2U + U_0^3)$$

and, averaging (assuming all velocities between U_{min} and U_{max} to have equal probability):

$$<\delta k\ \delta\ pCO_2> = \frac{AC}{U_{max} - U_{min}} \int_{U_{min}}^{U_{max}} (U^3 - U_0U^2 - U_0^2U + U_0^3)\, dU$$

$$= \frac{AC}{U_{max} - U_{min}} \left[\frac{1}{4}(U_{max}^4 - U_{min}^4) - \frac{U_0}{3}(U_{max}^3 - U_{min}^3) - \frac{U_0^2}{2}(U_{max}^2 - U_{min}^2) - U_0^3(U_{max} - U_{min})\right]$$

With these values we find for the full correction term $<\delta k\ \delta pCO_2>/(k_0\ \Delta PCO_2) = 0.06$